The Global Climate 2011-2020

A decade of accelerating climate change

WEATHER CLIMATE WATER

WORLD METEOROLOGICAL ORGANIZATION

WMO-No. 1338

Cover photo: AdobeStock_618865333

WMO-No. 1338

Chair, Publications Board
World Meteorological Organization (WMO)
7 bis, avenue de la Paix
P.O. Box 2300
CH-1211 Geneva 2, Switzerland

Tel.: +41 (0) 22 730 84 03
Email: publications@wmo.int

ISBN 978-92-63-11338-2

Contents

Key messages

It was the warmest decade on record by a clear margin for both land and ocean

Each successive decade since the 1990s has been warmer than all previous decades

Atmospheric concentrations of the three major greenhouse gases continued to increase over the decade. In order to stabilize the climate and prevent further warming, emissions must be greatly and sustainably reduced

The ozone hole was smaller in the 2011-2020 period than during the two previous decades

Rates of ocean warming and acidification are increasing.

Marine heatwaves are becoming more frequent and intense. In any given year between 2011 and 2020, approximately 60% of the surface of the ocean experienced a heatwave

Global mean sea level rise is accelerating, largely because of ocean warming and the loss of land ice mass. From 2011 to 2020, sea level rose at an annual rate of 4.5mm/yr

Glaciers that were measured around the world thinned by approximately 1m per year on average between 2011 and 2020

Greenland and Antarctica lost 38% more ice between 2011 and 2020 than during the 2001-2010 period. This is consistent with an acceleration of ice sheet mass loss

Arctic sea ice extent continues a multi-decade decline: the seasonal mean minimum was 30% below average

Extreme events across the decade had devastating impacts, particularly on food security and human mobility, hindering national development and progress toward the Sustainable Development Goals (SDGs)

Virtually every attribution study carried out on an extreme heat event in the decade 2011-2020 found that the likelihood of the event increased significantly because of anthropogenic climate change

Heatwaves were responsible for the highest number of human casualties, while tropical cyclones caused the most economic damage

In order to achieve the SDGs and meet the targets of the Paris Agreement, there is need for synergistic action, whereby advancements in one can lead to improvements in the other.

Foreword

This seminal report explores critical components of the global climate between 2011 and 2020. Taking a longer-term perspective than annual reports, the Decadal Report transcends interannual variability, highlighting, for example, how each decade since the 1990s has been warmer than the previous one. It shows without a doubt that green¬house gas concentrations have increased in the atmosphere, thereby contributing to record levels of warming of the land and ocean, the melting of ice sheets and glaciers, rising sea levels, and ocean acidification.

As emissions rise and the climate changes, extreme weather and climate events are worsening. The decadal approach is unique in that it allows time for the scientific community to analyse the mechanisms behind extreme conditions and their likelihood of occurring in the pre-industrial era. These attribution studies are a key component in understanding the role of anthropogenic climate change in increasing the risk of extreme events. In particular, the risk of heat extremes has been found to have significantly increased because of anthropogenic climate change.

Extreme weather and climate events can have widespread and lasting impacts, often affecting the most vulnerable communities. Droughts, heatwaves, floods, tropical cyclones and wildfires can damage infra-structure, destroy agricultural yields, limit water supplies or cause mass displacements.

For the very first time, this report demonstrates concrete connections between extreme events and development. Working in interdisciplinary collaboration with United Nations agencies and national statistics offices, select case studies demonstrate how extreme events across the decade have impeded progress toward the Sustainable Development Goals (SDGs). As the world continues to be off-track in reaching the SDGs, continued collaboration in addressing data challenges and socio-economic impact analyses is of ever-increasing importance.

Although improved early warning systems have reduced the number of casualties from extreme events, there is still significant work to be done. The United Nations Early Warnings for All (EW4A) Initiative, spearheaded by WMO with the United Nations Office for Disaster Risk Reduction (UNDRR), the International Federation of Red Cross and Red Crescent Societies (IFRC) and the International Telecommunication Union (ITU), aims to ensure that every person on Earth is covered by early warning services by 2027. Achieving this ambitious target requires sound observations and regular updates on key climate indicators, as provided in this report.

In order to stabilize the climate and prevent further warming, emissions must be drastically and sustainably lowered. WMO is preparing a new scheme for monitoring the sinks and sources of the main greenhouse gases based on modelling and on ground-based and satellite measurements. The scheme will enable better understanding of the uncertainties related to the strength of carbon sinks and sources associated with land use, as well as those related to the sources of methane.

I take this opportunity to congratulate and thank the experts and authors who jointly compiled this report using physical data analyses and impact assessments, and to thank all the contributors, particularly WMO Member National Meteorological and Hydrological Services (NMHSs)and Regional Climate Centres (RCCs), contributing national statistics offices, and United Nations agencies, for their collaboration and input.

Petteri Taalas, Secretary General, WMO

Atmospheric composition

- Atmospheric concentrations of the three major greenhouse gases continued to increase over the decade. In order to stabilize the climate and prevent further warming, emissions must be greatly and sustainably reduced
- The ozone hole was smaller in the 2011-2020 period than during the two previous decades

GREENHOUSE GAS GROWTH RATES AND BUDGETS

Greenhouse gases allow incoming solar radiation to reach the Earth's surface while they absorb and re-emit outgoing infrared radiation, heating the lower atmosphere and surface of the planet. According to the Sixth Assessment Report of the Intergovernmental Panel on Climate Change (IPCC), the increase in the abundance of greenhouse gases since the pre-industrial period is a major reason for observed global warming. The key greenhouse gases, carbon dioxide, methane, and nitrous oxide, have both anthropogenic and natural sources, while the others, such as chlorofluorocarbons and sulfur hexafluoride, have an exclusively anthropogenic origin.

Carbon dioxide (CO_2) is the single most important anthropogenic greenhouse gas in the atmosphere, accounting for approximately 66% of the radiative forcing by the long-lived greenhouse gases (LLGHGs) over the whole industrial era. It is responsible for about 81% of the increase in radiative forcing over the past decade. For about 10,000 years before the start of the industrial era, atmospheric carbon dioxide remained almost constant at around 280 ppm (ppm=number of molecules of the gas per million molecules of dry air). Since then, the CO_2 mixing ratio[1] has increased by nearly 50% reaching 413.2 ppm in 2020, primarily due to emissions from the combustion of fossil fuels, deforestation, and changes in land-use. Global average CO_2 mixing ratio (Figure 1) during the period 1991-2000 was 361.7ppm, during the decade 2001-2010 it was 380.3 ppm, while in 2011-2020 the global average CO_2 mixing ratio rose to 402.0 ppm. During the same periods the average growth rate increased from 1.5 ppm/yr and 1.9 ppm/yr to 2.4 ppm/yr. The largest growth rate during the last decade was 3.3 ppm/yr in 2016 and the lowest growth rate was observed in 2014 at 2.0 ppm/yr. These interannual variations are driven by changes in the annual uptake of CO_2 by the terrestrial biosphere in tropical and subtropical regions.

Each of the past three decades has had successively higher fossil fuel CO_2 emissions. About 55% of the CO_2 emissions from human activity is absorbed by the ocean and by sinks on land, such as forests. This fraction has remained largely constant over the past three decades, indicating that CO_2 sinks have grown in response to increasing atmospheric CO_2, although on the global scale the land sector is still a net source. Oceans were responsible for removing 25% of total anthropogenic emissions and land, 29%, from 2010 to 2019.

1 Mixing ratio shows the ratio of different molecules in a mixture. In the case of CO2, the ratio is in parts per million, describing how many molecules of CO2 are found in each 1 million molecules of air.

Atmospheric composition

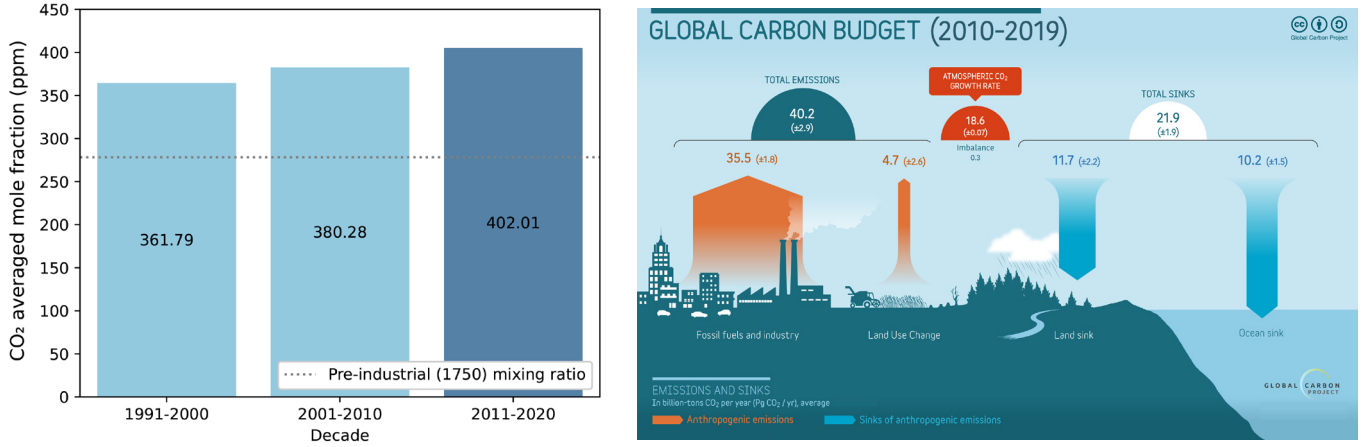

Figure 1. Left: Decadal averaged mole fraction in parts per million (ppm) of carbon dioxide (CO2), 1991-2020. Pre-industrial levels indicated by gray dotted line
Source: WMO.
Right: Global carbon budget, 2010-2019, highlighting sources of anthropogenic emissions and sinks
Source: Global Carbon Project.

Methane (CH_4) accounts for about 16% of the radiative forcing by LLGHGs. Approximately 40% of methane is emitted into the atmosphere by natural sources (such as wetlands and termites), and about 60% comes from anthropogenic sources (such as ruminants, rice agriculture, fossil fuel exploitation, landfills and biomass burning). Before the industrial era, atmospheric methane was near 730 ppb (ppb = parts per billion (109)). In recent years, the globally averaged CH_4 mixing ratio (Figure 2) from 1991 to 2000 was 1761.4 ppb, from 2001 to 2010 it was 1792.5 ppb, while from 2011 to 2020 it reached 1850.2 ppb. The growth rate of CH_4 decreased from ~13 ppb/y during the early 1980s to 5.9 ppb/y in the 1990s, then to 2.6 ppb/y in the 2000s, and increased again to 8 ppb/y in the 2010s. After a brief stabilization phase between 1999 and 2006, the methane mixing ratio started to rise again in 2007. The largest growth rate during the decade was 11 ppb/yr in 2020 and the lowest growth rate was in 2012, at 5 ppb/yr.

This decadal atmospheric growth has been driven by the growth in emissions from agriculture, waste, and fossil fuel production and use, though natural emissions from wetlands have also contributed to a lesser degree. The human disruption of the global methane budget remains dominated by CH_4 emissions from the agricultural sector and waste (61% of total).

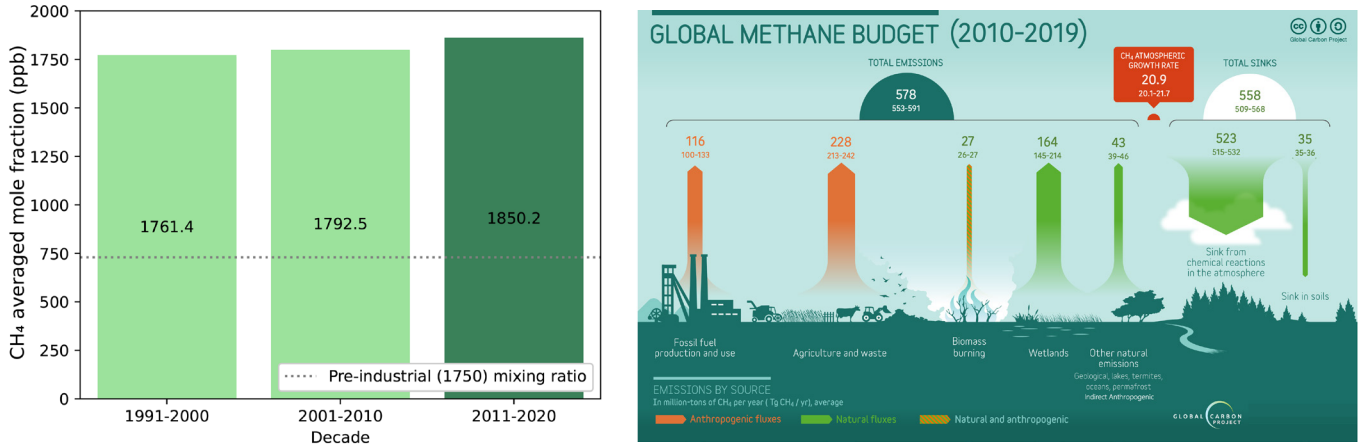

Figure 2. Left: Decadal averaged mole fraction in parts per billion (ppb) of methane (CH4), 1991-2020. Pre-industrial levels indicated by gray dotted line.
Source: WMO.
Right: Global methane budget, 2010-2019, highlighting sources of anthropogenic emissions and sinks
Source: Global Carbon Project.

Atmospheric composition

Nitrous oxide (N_2O) accounts for about 7% of radiative forcing by LLGHGs. N_2O is emitted into the atmosphere from both natural sources (approximately 64%), and anthropogenic sources (approximately 36%), including oceans, soils, biomass burning, fertilizer use, and various industrial processes. It is a potent greenhouse gas as its impact on climate, integrated over 100 years, is 298 times greater than equal quantities of CO_2 emissions. Its atmospheric abundance prior to industrialization was 270.1 ppb. In more recent times the global average mixing ratio has increased from 312.0 ppb (1991-2000) to 319.7 (2001-2010) and to 328.6 ppb (2011-2020). The near-linear global growth rate increased from 0.71 ppb/yr during the 1991-2000 decade to 0.78 ppb/yr (2001-2010) and to 0.98 ppb/yr in the most recent decade.

Growth in global N_2O concentrations is exclusively driven by emissions from human activity, particularly from the excess use of nitrogen fertilizers in agriculture. Emissions from agriculture have been rising rapidly and steadily since the mid-twentieth century. Fossil fuels and industry have also contributed, but with slower growth over the past three decades than agriculture. In addition to anthropogenic emissions, there are large emission fluxes from natural sources, including soils, and coastal and open oceans, which are taken up by chemical reactions in the atmosphere.

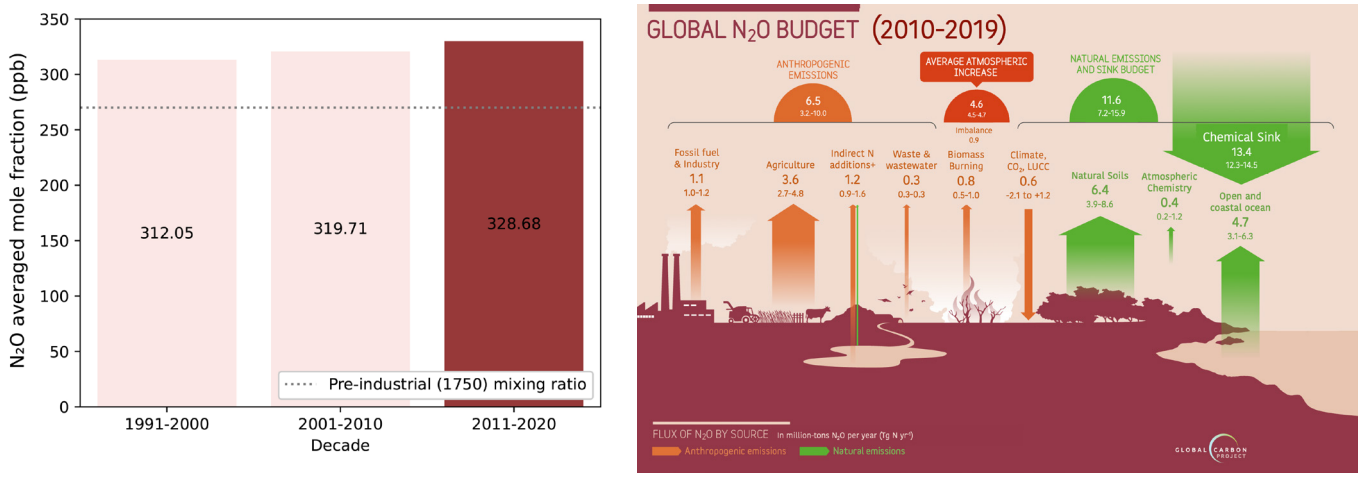

Figure 3. Left: Decadal averaged mole fraction in parts per billion (ppb) of nitrous oxide (N2O) (1991-2020). Pre-industrial levels indicated by gray dotted line.
Source: WMO.
Right: Global N2O budget (2010-2019),highlighting sources of anthropogenic/natural emissions and sinks
Source: Global Carbon Project.

Anthropogenic GHG emissions and atmospheric concentrations of all three GHGs continued to rise over the last three decades. In order to stabilize the climate and prevent further warming, CO_2 emissions from all sources must decline to a level of net-zero (i.e. any residual emissions need to be offset by direct CO_2 removals), and CH_4 and N_2O emissions must substantially and sustainably decrease. The decadal trends presented in this analysis highlight the need for more meaningful efforts to be made if we are to stabilize the climate to 1.5°C and well below 2°C, as called for in the Paris Agreement.

STRATOSPHERIC OZONE DEPLETION

Anthropogenic ozone depletion is caused by the production and emission of Ozone Depleting Substances (ODS) such as Chlorofluorocarbons (CFCs) and halons into the atmosphere. These compounds release chlorine and bromine into the stratosphere where they act as catalysts for ozone-destroying reactions. Due to the actions taken under the Montreal Protocol, the total amount of chlorine entering the stratosphere from controlled and uncontrolled ODSs declined by 11.5% from its peak value of 3660 ppt in 1993, to 3240 ppt in 2020.

Atmospheric composition

The most severe ozone depletion has been observed in the Antarctic lower stratosphere during the southern hemisphere spring. Extreme depletion affects a wide area, in a phenomenon known as the 'Antarctic Ozone Hole', discovered in 1985 through long-term ground-based observation of the total column ozone (TCO). This ozone hole has been under observation over Antarctica in late winter every year since 1979. It typically forms each year in August, grows rapidly in area and depth by early September, before reaching its maximum size between late September and early October. The long-term trend in the severity of the ozone hole is overlaid by large interannual variability depending primarily on meteorological conditions. In general, a cold and stable stratospheric polar vortex in a given year will lead to much greater ozone depletion in that season.

Figure 4 shows the average daily progression of the ozone mass deficit for the past four decades. On average, over the 2011-2020 period, the annual maximum mass deficit was lower than during the previous two decades. The average ozone mass deficit also increased more slowly as it approached the seasonal peak months of August and September between 2011 and 2020 than it did between 2000 and 2010. However, the post-peak declines each year, in October and November, occurred at fairly similar rates in the 2001-2010 and 2011-2020 periods. During the late 1980s and early 1990s, the overall trend of ozone hole metrics showed an evident worsening towards more severe ozone depletion, which then levelled off by the late 1990s. A slow recovery since the year 2000 is now detectable in some indicators, as emissions of ozone-depleting substances have been reduced.

The 2018 WMO/UNEP Scientific Assessment of Ozone Depletion was the first to state that early indications of Antarctic ozone recovery were now evident, a finding which was confirmed by the 2022 Assessment.

In the Arctic, large interannual variability has prevented the detection of a statistically significant trend to date. Ozone recovery is also now evident in the upper stratosphere - approximately above 35 km - in the tropics and the mid-latitudes of both hemispheres.

Springtime total ozone values in the Antarctic are projected to return to 1980 values by around 2065. Large ozone holes are still expected to occur for many years, particularly in years, such as 2020, in which conditions are cold in the Antarctic stratosphere. Total springtime ozone is expected to return to 1980 values in the Arctic by approximately 2045. In the years with a particularly cold winter and spring, as was the case in 2020, severe ozone depletion will continue to be observed in the Arctic.

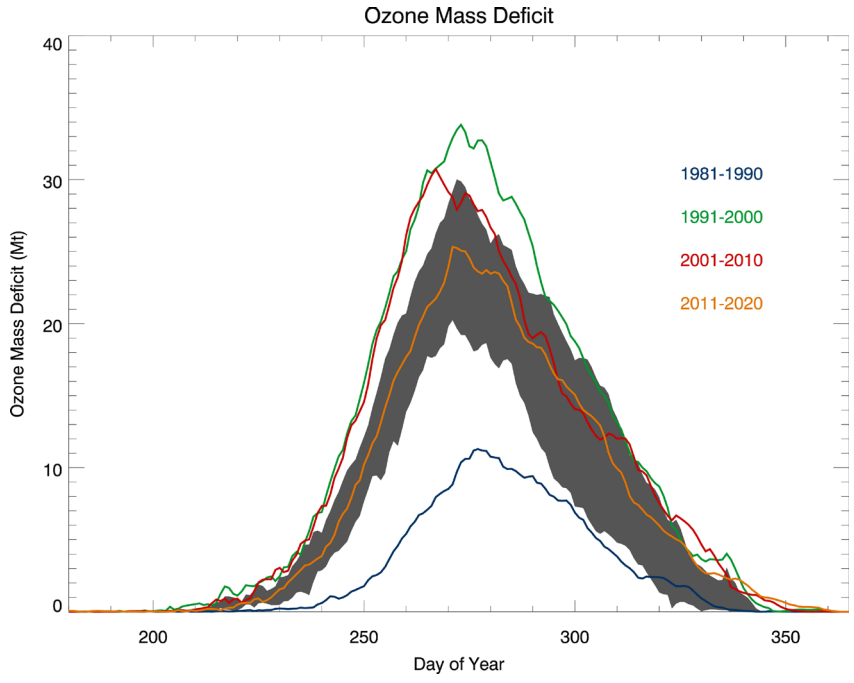

Figure 4. Decadal mean progression of daily values of the ozone mass deficit for the 1981-1990 (blue), 1991-2000 (green), 2001-2010 (red) and 2011-2020 (orange) periods. The grey band shows the daily 30th to 70th percentile range across all four decades. Data supplied by NASA Ozone Watch: (https://ozonewatch.gsfc.nasa.gov), based on data from the TOMS, OMI, and OMPS satellite instruments.

Global temperature

- By a clear margin, It was the warmest decade on record for both land and ocean.
- Each successive decade since the 1990s has been warmer than all previous decades.

GLOBAL TEMPERATURE

Global mean temperature for the period 2011-2020 was 1.10 ± 0.12 °C above the 1850-1900 average. This is based on the average of six data sets and is consistent with the value derived by the Intergovernmental Panel on Climate Change (IPCC) - 1.09 °C - using a different combination of data sets. The warmest six years on record globally were between 2015 and 2020. The actual warmest year was quite likely 2016, which followed the exceptionally powerful 2015-2016 El Niño episode. The coldest year of the decade was most likely 2011, which came after a strong La Niña occurrence in 2010 and early 2011. Regionally, temperatures were warmer than the 1981-2010 average[2] across most regions of the planet. It was the warmest decade on record for each of the WMO regional associations: Africa, Asia, South America, North America, the South-west Pacific, and Europe. Limited regions of below-average temperatures were confined to the south-east Pacific, parts of the Southern Ocean and an area of the North Atlantic to the south of Greenland. The largest positive anomalies for the decade, in places more than 2 °C above the 1981-2010 average, were located in the Arctic.

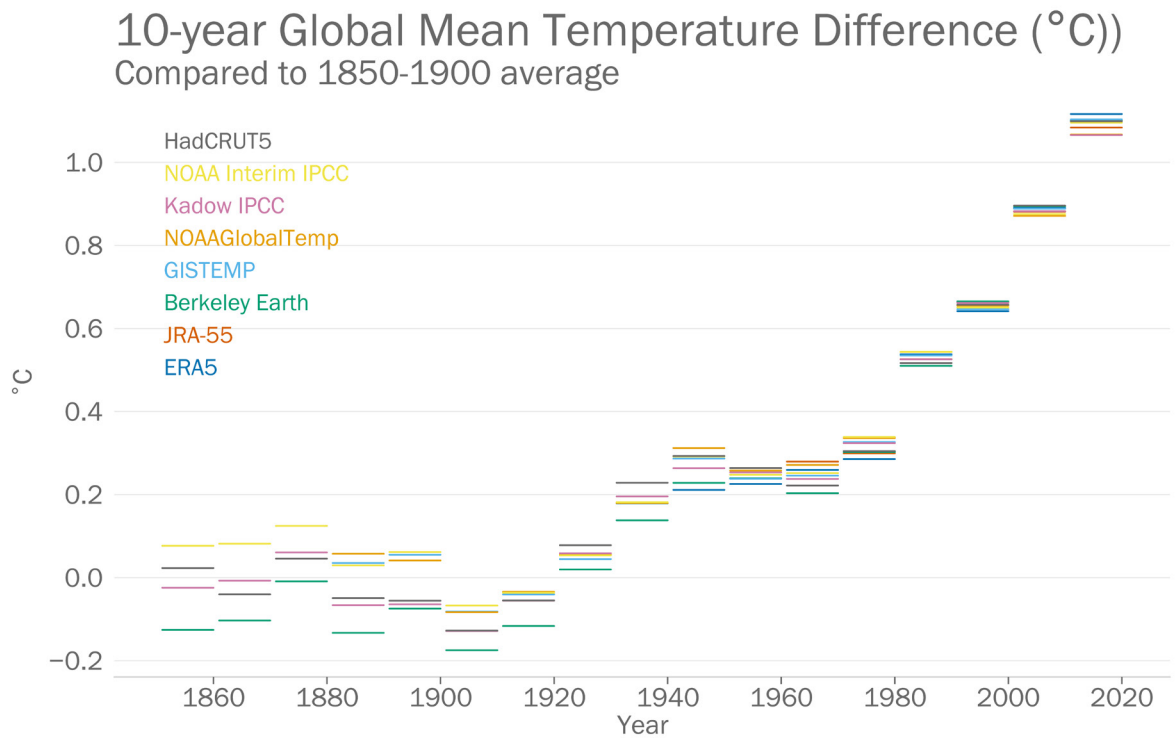

Figure 5. Decadal global average mean temperature differences from 1850 to 1900, for the periods 1851-1860 to 2011-2020. Decadal averages from eight data sets are shown as horizontal coloured lines.
Source: John Kennedy.

2 Although WMO has now moved to the more recent 1991-2020 base period for climatological reference normal, 1981-2010 is used here for consistency across the report as it was the reference period used at the time when some of the information was provided. In parts of the report different reference periods are used where relevant data are available for a limited period only.

Global temperature

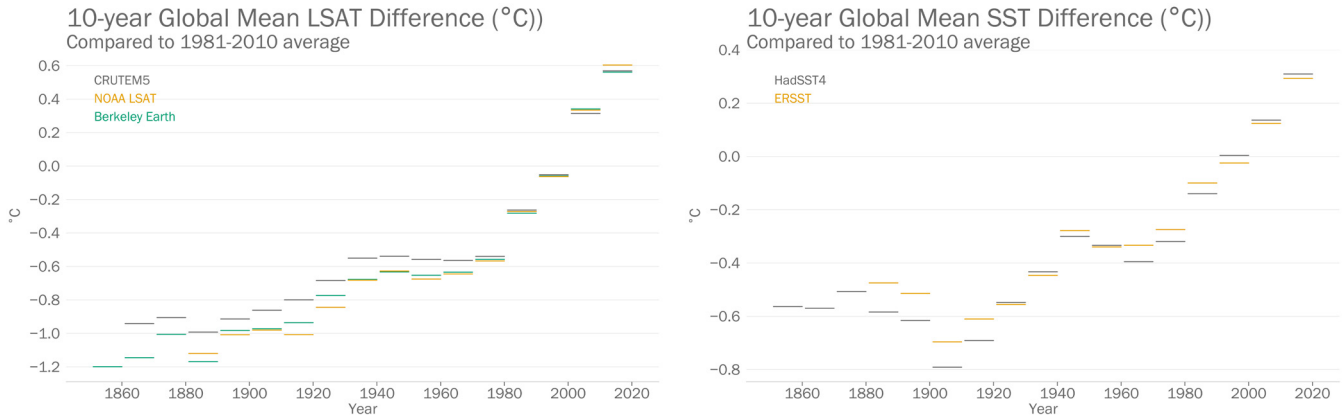

Figure 6. Decadal global average mean temperature for land (left) and sea (right) difference from 1850 to 1900, and for the periods 1851-1860 to 2011-2020. Decadal averages from three land data sets and two sea-surface temperature data sets are shown as horizontal coloured lines
Source: John Kennedy.

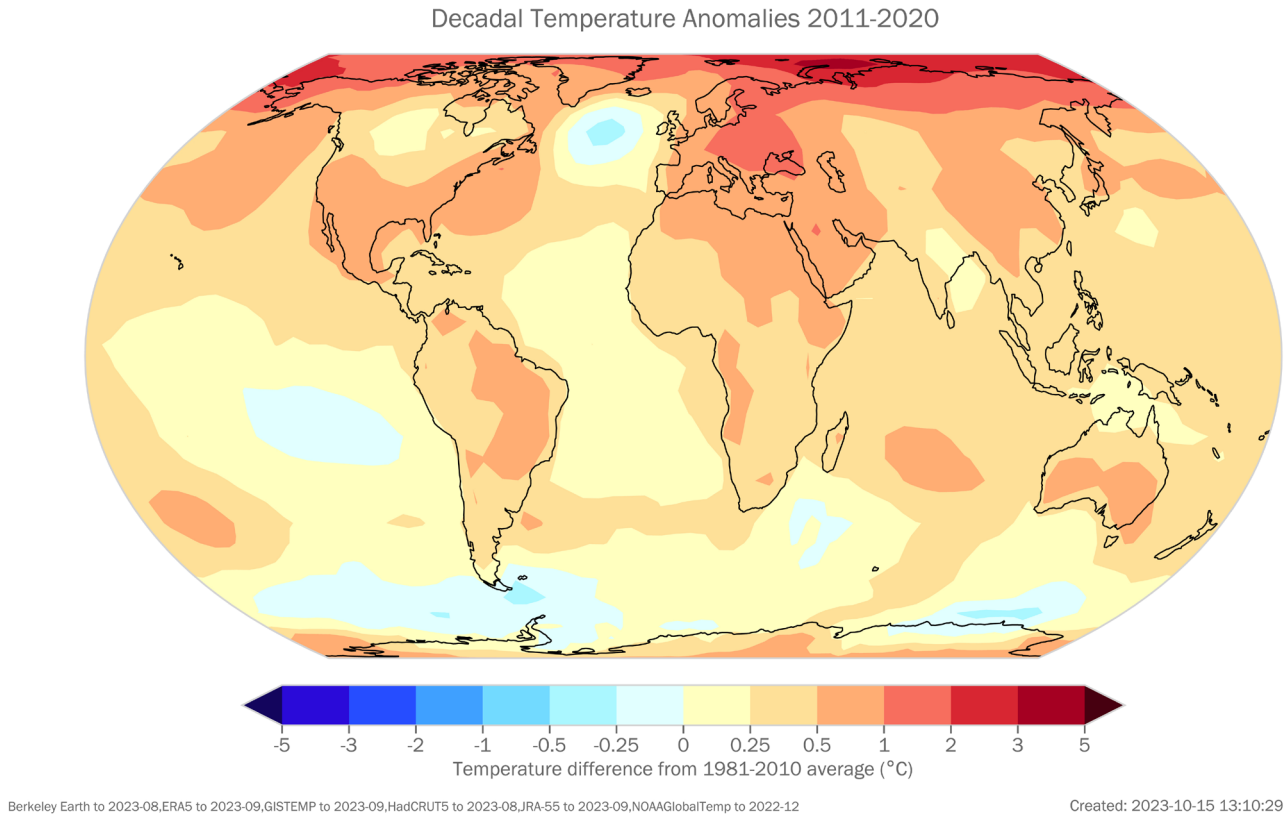

Figure 7. Ten-year average of near-surface temperature differences relative to the 1981-2010 average. Data shown is the median of six global temperature data sets: HadCRUT5, NOAAGlobalTemp, GISTEMP, Berkeley Earth, JRA-55 and ERA5
Source: John Kennedy.

Global temperature

NATIONAL REPORTS

WMO Members were requested to complete a survey on country-wide temperature anomalies, national absolute records for daily maximum temperature, daily minimum temperature and 24-hour total precipitation. Almost every reporting country had decadal mean temperatures for the 2011-2020 period that were above the 1981-2010 average. Only three of 99 reporting countries were below the 1981-2010 average.

The strongest warm anomalies occurred in central and eastern Europe and south-west Asia. Of the 32 countries that reported 2011-2020 decadal anomalies of +0.8 °C or above, 31 were from these regions, with most European countries included, except for parts of the western fringe. The largest reported decadal anomaly was +1.6 °C for Qatar, followed by + 1.26 °C for Finland, which was one of a group of 18 adjacent countries in central and eastern Europe with decadal anomalies of +1 °C or more. The only other country to reach the +1 °C threshold was Kuwait.

Most countries outside Europe and south-west Asia had decadal mean anomalies between +0.3 °C and +0.7 °C. While tropical anomalies were generally smaller than those at higher latitudes, most tropical countries were within this range, leaning towards the lower end of the range in the Americas, west Africa and southern Asia.

Although 2016 and 2020 were the years with the highest average temperatures measured over global land areas, 2019 was the year that the greatest number of countries reported as being the warmest year of the decade. In comparing 2019 with 2020, the warmer year was found to be 2020 over much of northern Eurasia, which is a large area with relatively few countries. The Russian Federation, which makes up 13% of the world's land mass, recorded its warmest year in 2020 by a margin of approximately 1 °C. In contrast, for the regions of central and eastern Europe, which is comprised of a large number of relatively small countries, 2019 was a record year in terms of high temperatures.

The occurrence of record high temperatures is an indicator of long-term changes in extreme heat. While this may be considered an imperfect indicator (as it can be affected at the national level by changes in the observing network, since stations may open or close in areas experiencing extreme heat) it still provides a general indication of changes over time. Of the 96 Members having sufficient data on their highest temperatures in each of the decades in the 1961 to 2020 period, 37 reported their highest temperatures during the 2011-20 decade, and two others reported having temperatures that were as high as in the earlier period running from 1961, a significantly greater number than in any other decade, and nearly twice as many as during the previous decade (2001-2010).

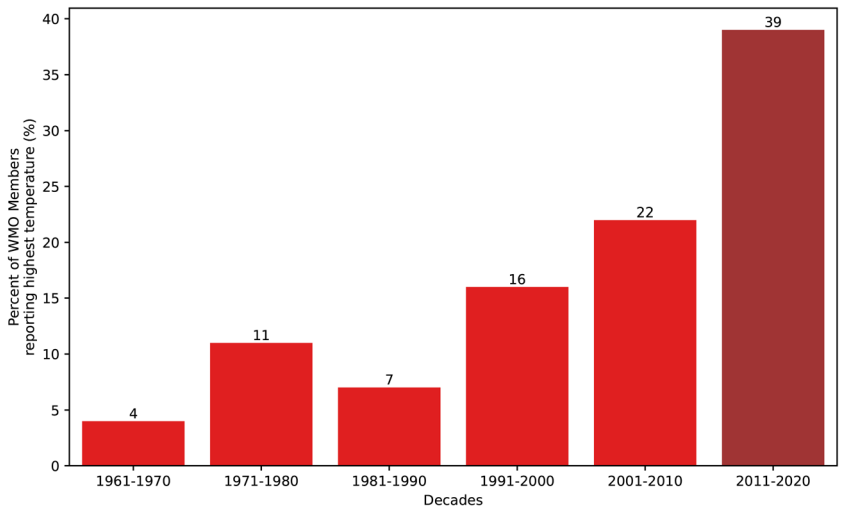

Figure 8. Percentage of reporting countries that recorded their highest temperature of the 1961-2020 period during the decade (2011-2020)

Global temperature

WHAT DOES THE 1.5 °C THRESHOLD MEAN, AND WHEN WILL IT BE CROSSED?

A global mean temperature of 1.5 °C above pre-industrial levels is a critical threshold in the policy framework around anthropogenic climate change. The Paris Agreement seeks to pursue efforts to limit human-induced warming to 1.5°C. An IPCC Special Report established that warming beyond 1.5 °C will have substantial negative impacts across a wide range of sectors.

The impacts associated with global temperatures higher than 1.5 °C above the pre-industrial level are mostly associated with long-term temperatures at that level, and "crossing" 1.5 °C is considered as such when a longer-term average of temperatures reaches that level – it does not occur simply because the temperature in a single month or year is higher than 1.5 °C above the pre-industrial level. The first months above the 1.5 °C threshold have already occurred: during the peak of the 2015-16 El Niño. The IPCC formally defines the crossing of a threshold as the midpoint of the first 20-year period with mean temperatures above that threshold. For example, the first 20-year period with mean temperatures higher than 1 °C above those of the 1850-1900 period, taken as representative of pre-industrial levels, was the period between 2002 and 2021, hence the 1 °C threshold is considered to have been crossed in 2012.

One limitation presented by the IPCC definition is that, since it covers a multi-year period, the crossing of a threshold can be definitively identified only several years after the event. An assessment of typical levels of interannual and decadal variability in global mean temperatures has found that it is very unlikely[3] that the 1.5 °C threshold has been crossed if the observed mean for the most recent 11 years has not reached 1.4 °C. While such levels have not yet been approached – the mean for the 2011-20 decade was 1.10 °C above the 1850-1900 average, and the warmest individual years 1.26 °C above that average – it is expected to do so within the next 10 to 20 years. The central estimate for the period of projected crossing of the 1.5 °C threshold ranges from the year 2018 to 2037 in high-emission scenarios, to 2025 to 2044 in low-emission scenarios, and this implies that the crossing of the threshold is expected to take place in 2028 and 2035 respectively.

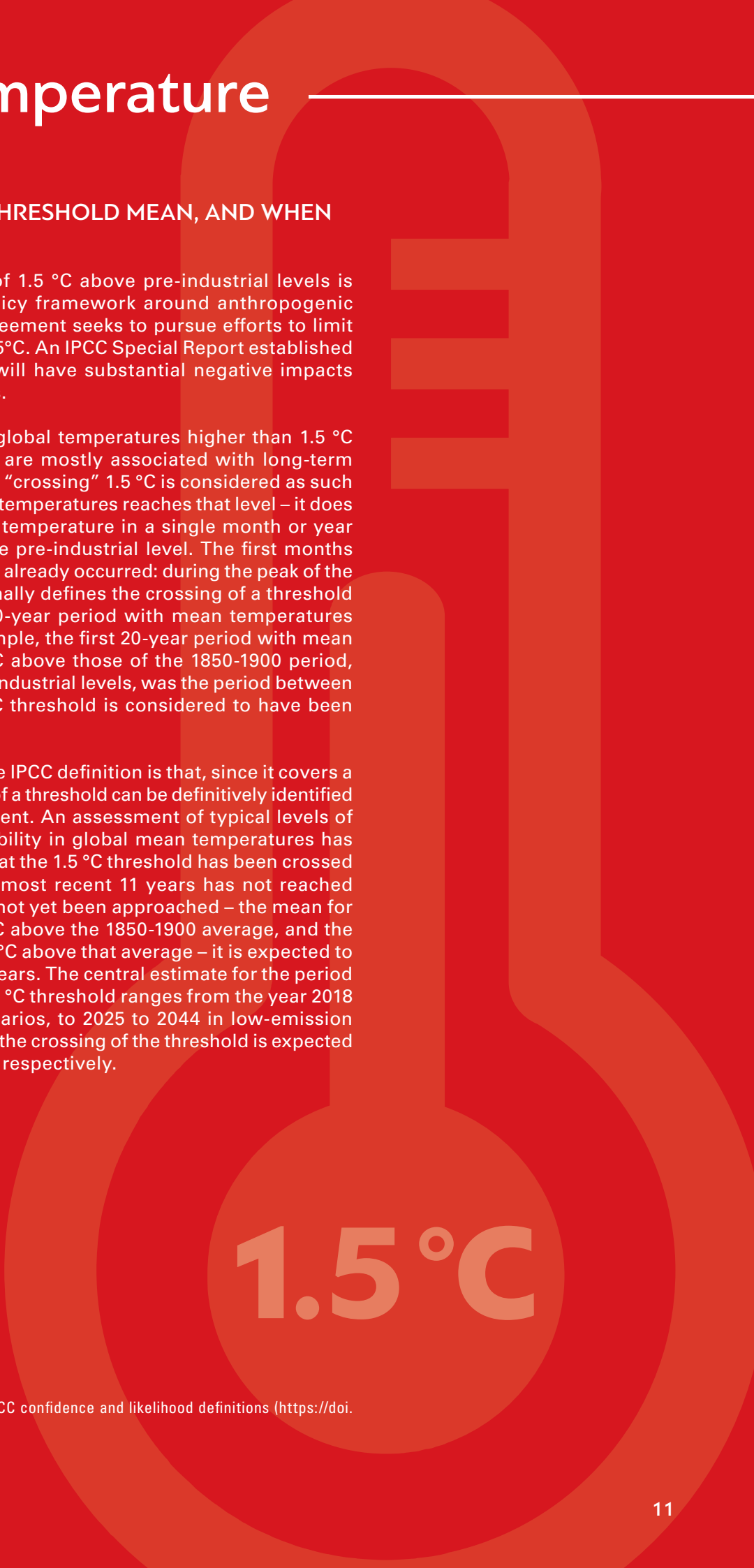

3 Less than 10% probability, as per IPCC confidence and likelihood definitions (https://doi.org/10.1029/2022JD036747).

Oceans

- Rates of ocean warming and acidification are increasing
- Marine heatwaves are becoming more frequent and intense. In any given year between 2011 and 2020, approximately 60% of the surface of the ocean experienced a heatwave.[4]
- Global mean sea level rise is accelerating, largely because of ocean warming and the loss of land ice mass. From 2011 to 2020, sea level rose at an annual rate of 4.5mm.

OCEAN HEAT CONTENT

Around 90% of the accumulated heat in the Earth system is stored in the ocean, which is measured through Ocean Heat Content (OHC). With the deployment of the Argo network of autonomous profiling floats, which first achieved near-global coverage in 2006, it is now possible to routinely measure OHC changes down to a depth of 2000m.[5,6] Earlier OHC assessments depend on ship-based measurements that were sparser in space and time, which means that uncertainty in pre-2006 OHC is much greater than in more recent data. Various research groups have developed estimates of global OHC, and all results show continued ocean warming (Figure 9). A concerted effort has been made to provide an international outlook on the global evolution of ocean warming[7,8,9] up to the year 2020.

All data sets agree that ocean warming rates show a particularly strong increase in the past two decades. Ocean warming rates for the 0-2000m depth layer reached rates of 1.0 ± 0.1 Wm^{-2} over the period 2006-2020, compared with 0.6 ± 0.1 Wm^{-2} over the full 1971-2020 period. By comparison, the values for the upper 700m depth amount were 0.6 (0.4) ± 0.1 Wm^{-2} over the period 2006-2020 (1971-2020). Below a depth of 2000m, the ocean also warmed, albeit at a lower rate of 0.07 ± 0.04 Wm^{-2} from 1991 to 2018.[10] The upper 2000m depth of the ocean continued to warm throughout the decade, reaching a record high in 2020. This continues a sequence of record years that began in 2013 in most data sets, and it is expected that this trend will continue to warm in the future.[11,12]

4 Defined by Hobday, A et al., 2016, as a prolonged discrete anomalously warm water event that can be described by its duration, intensity, rate of evolution, and spatial extent. Specifically, an anomalously warm event is considered a MHW if it lasts for five or more days, with temperatures warmer than the 90th percentile based on a 30-year historical baseline period.

5 Riser, S. C. et al. Fifteen Years of Ocean Observations with the Global Argo Array. *Nature Climate Change* **2016**, 6 (2), 145–153. https://doi.org/10.1038/nclimate2872.

6 Roemmich, D. et al. On the Future of Argo: A Global, Full-Depth, Multi-Disciplinary Array. *Frontiers in Marine Science* **2019**, 6, 439. https://www.frontiersin.org/article/10.3389/fmars.2019.00439.

7 Boyer, T. et al. Sensitivity of Global Upper-Ocean Heat Content Estimates to Mapping Methods, XBT Bias Corrections, and Baseline Climatologies. *Journal of Climate* **2016**, 29 (13), 4817–4842. https://doi.org/10.1175/JCLI-D-15-0801.1.

8 von Schuckmann, K. et al. An Imperative to Monitor Earth's Energy Imbalance. *Nature Climate Change* **2016**. https://doi.org/10.1038/nclimate2876.

9 von Schuckmann, K. et al. Heat Stored in the Earth System: Where Does the Energy Go? The GCOS Earth Heat Inventory Team. *Earth System Science Data Discussion,* **2020**, 1–45. https://doi.org/10.5194/essd-2019-255.

10 Update from Purkey, S. G., Johnson, G.C. Warming of Global Abyssal and Deep Southern Ocean Waters between the 1990s and 2000s: Contributions to Global Heat and Sea Level Rise Budgets. *Journal of Climate* **2020**, 23, 6336–6351. https://doi.org/10.1175/2010JCLI3682.1.

11 Intergovernmental Panel on Climate Change (IPCC). Summary for Policymakers. *IPCC Special Report on the Ocean and Cryosphere in a Changing Climate*; Pörtner, H. O.; Roberts, D. C.; Masson-Delmotte, V. et al., Eds.; in press. 2019

12 Intergovernmental Panel on Climate Change (IPCC). Summary for Policymakers. In *Climate Change 2021: The Physical Science Basis. Contribution of Working Group I to the Sixth Assessment Report of the Intergovernmental Panel on Climate Change.* Masson-Delmotte, V.; Zhai, P.; Pirani, A. et al., Eds.; Cambridge University Press, Cambridge, United Kingdom and New York, USA, 2021.

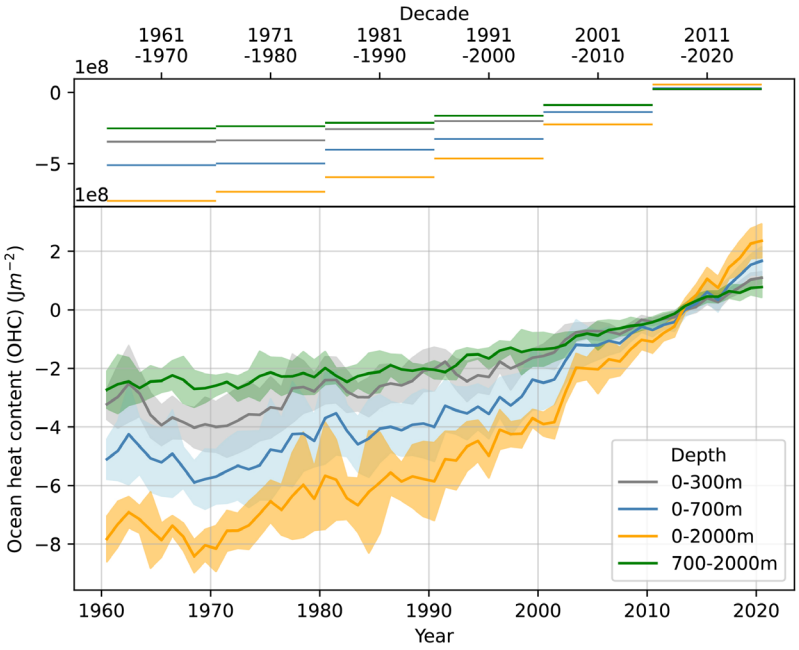

Figure 9. The 1960-2020 ensemble mean by decade (top) and time series and ensemble standard deviation (2-sigma, shaded) of global ocean heat content anomalies relative to the 2005-2017 climatology for the 0-300m (grey), 0-700m (blue), 0-2000m (yellow) and 700-2000m depth layer (green) Updated from von Schuckmann et al., 2020.

MARINE HEATWAVES

Focused study of marine heatwaves (MHWs) and marine cold-spells (MCSs)[13] became prominent in the current decade. The 2011 extreme (Category IV) Western Australia MHW can be credited as having finally clarified the need to create a globally consistent definition of the marine heatwave phenomenon. This event wreaked havoc on hundreds of kilometres of coastal kelp forests,[14] most of which have remained as a much less productive scrub turf since then.[15] The 2012 severe (Category III) north-west Atlantic MHW occurred at just the right time of year to drive the centre of the North American lobster fishery far enough north as to cross over an international border, making it the first ocean climate event on record to cause political tension between two high-income nations.[16]

Over the 2011-2020 period, an average of 60% of the surface of the ocean experienced MHWs in any given year, with the highest being 65% in 2016 (Figure 10a). In the case of marine cold spells, the present decadal average cover is 31.5%, and none of the years from this or the previous decade is ranked in the top ten. The three years having the highest average of days with MHWs were 2016 (61 days), 2020 (58 days), and 2019 (54 days) (Figure 10b). The last eight years of the decade, that is, from 2013 to 2020, were all in the top ten years in terms of the number of highest average MHW days. In general, the opposite has been observed for MCSs: only 2011 (21 days) ranked in the top ten years of highest daily averages, which otherwise would include the years going back to the beginning of the data record. The uptick in MCS days globally for this decade started in 2007 and is due to an increase in the duration, but not intensity, of MCSs in the Southern Ocean.[17]

13 Hobday, A. J.; Alexander, L. V.; Perkins, S. E. et al. A Hierarchical Approach to Defining Marine Heatwaves. *Progress in Oceanography* **2016**, 141, 227-238.

14 Wernberg, T.; Smale, D. A.; Tuya, F. et al. An Extreme Climatic Event Alters Marine Ecosystem Structure in a Global Biodiversity Hotspot. *Nature Climate Change* **2013**, 3 (1), 78-82.

15 Wernberg, T.; Bennett, S.; Babcock, R. C. et al. Climate-driven Regime Shift of a Temperate Marine Ecosystem. *Science* **2016**, 353 (6295), 169-172.

16 Mills, K. E.; Pershing, A. J.; Brown, C. J. et al. Fisheries Management in a Changing Climate: Lessons from the 2012 Ocean Heatwave in the Northwest Atlantic. *Oceanography*, **2013**, 26 (2), 191-195.

17 Schlegel, R. W.; Darmaraki, S.; Benthuysen, S. et al. Marine Cold Spells. *Progress in Oceanography*, **2021**,198, 102684.

MHWs have become relatively more intense in the most recent decade. Category II (Strong) events have become more common than those rated in Category I (Moderate), which had only occurred previously in 1998 and 2010. Category IV (Extreme) events were so uncommon in the past that they could hardly be measured on a global scale. Nowadays, Category IV MHWs occur frequently enough that, in the current decade, the ocean experienced an average of 0.5 extreme MHW days per year (25 times the rate of MCSs), with a record of 1 full day in 2016. It has been established that the occurrence of Category IV events may be able to change entire ecosystems.[18,19]

The largest MHW to have occurred since record keeping began in 1982 was a severe (Category III) 2014-2016 event. This MHW covered much of the north-eastern Pacific and persisted for more than two years, with major impacts on marine life.[20] There were few noteworthy MCSs from 2011 to 2020, except for the semi-persistent colder-than-normal region found in the North Atlantic Ocean south of Greenland. It has been posited that this may be a sign of the slowing of the Atlantic Meridional Overturning Circulation (AMOC).[21]

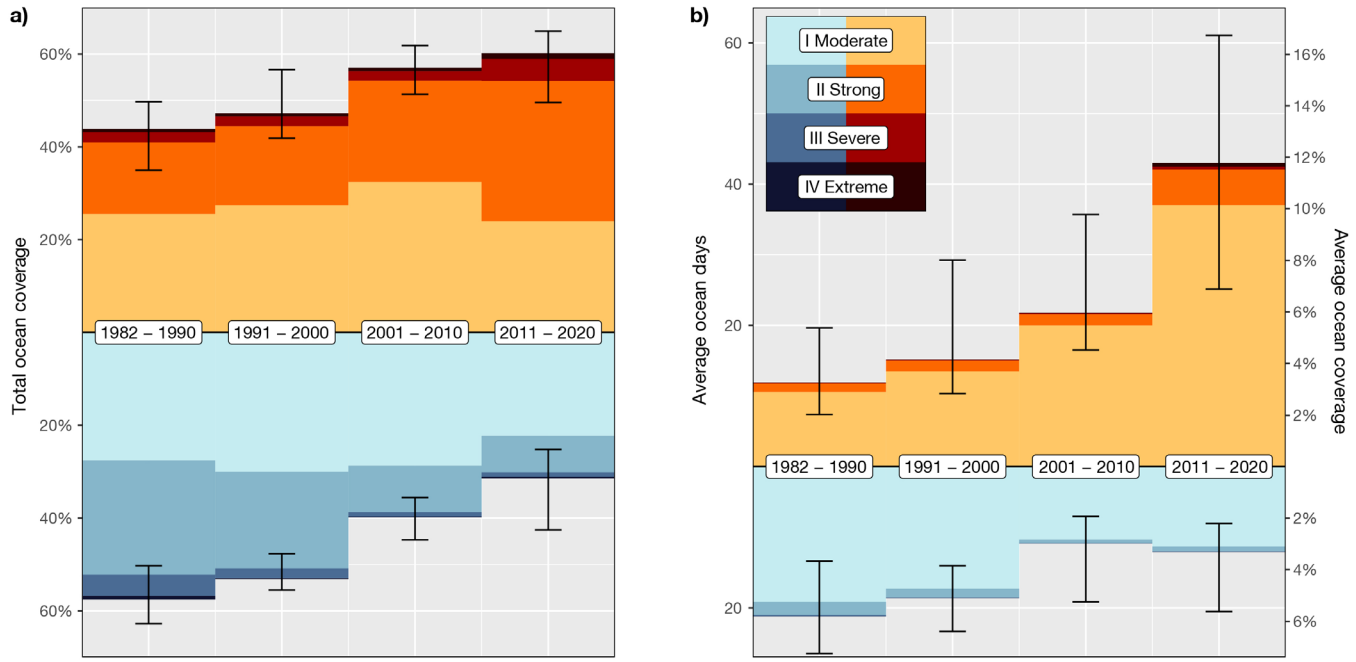

Figure 10. a) Average annual percentage of the global ocean surface that experienced at least one MHW or MCS. b) Globally averaged annual days on which the ocean experienced a MHW or MCS (left Y-axis), also expressed as the average percentage of the ocean that this could cover for the entire year (right Y-axis). All bars show the annual values averaged over the decade indicated, with whiskers showing the highest and lowest annual values. The colours in the bars show the proportion of the category of the MHW/MCS. Marine cold spell values are shown below the X-axis for ease of comparison.

18 Wernberg, T.; Bennett, S.; Babcock, R. C. et al. Climate-driven Regime Shift of a Temperate Marine Ecosystem. *Science* **2016**, 353 (6295), 169-172.

19 Smale, D. A.; Wernberg, T.; Oliver, T. et al. Marine Heatwaves threaten Global Biodiversity and the Provision of Ecosystem Services. *Nature Climate Change* **2019**, 9 (4), 306-312.

20 Cavole, L. M.; Demko, A. M.; Diner, R. E. et al. Biological Impacts of the 2013–2015 Warm-water Anomaly in the Northeast Pacific: Winners, Losers, and the Future. *Oceanography* **2016**, 29 (2), 273-285.

21 Yeager, S. G.; Kim, W. M.; Robson, J. What Caused the Atlantic Cold Blob of 2015. *US CLIVAR Variations*, **2016**, 14 (2), 24-31.

SEA LEVEL

During the 2011-2020 period sea level continued to rise, with indications of acceleration, as recorded by high-precision satellite altimeters (IPCC, 2021). While the 2001-2010 rate of global mean sea level (GMSL) rise[22] was 2.9 +/- 0.5mm/yr, it increased to 4.5 +/- 0.6 mm/yr during the period between 2011 and 2020. Since 1993, the acceleration of the GMSL rise has been estimated at 0.11 +/- 0.06 mm/yr.[23] The GMSL acceleration is mostly due to a speeding up of ice mass loss from the Greenland ice sheet, and, to a lesser extent, due to accelerated glacial melting and ocean warming. It is *very likely* that human influence was the main driver of the observed global mean thermosteric sea level change since 1970.[24]

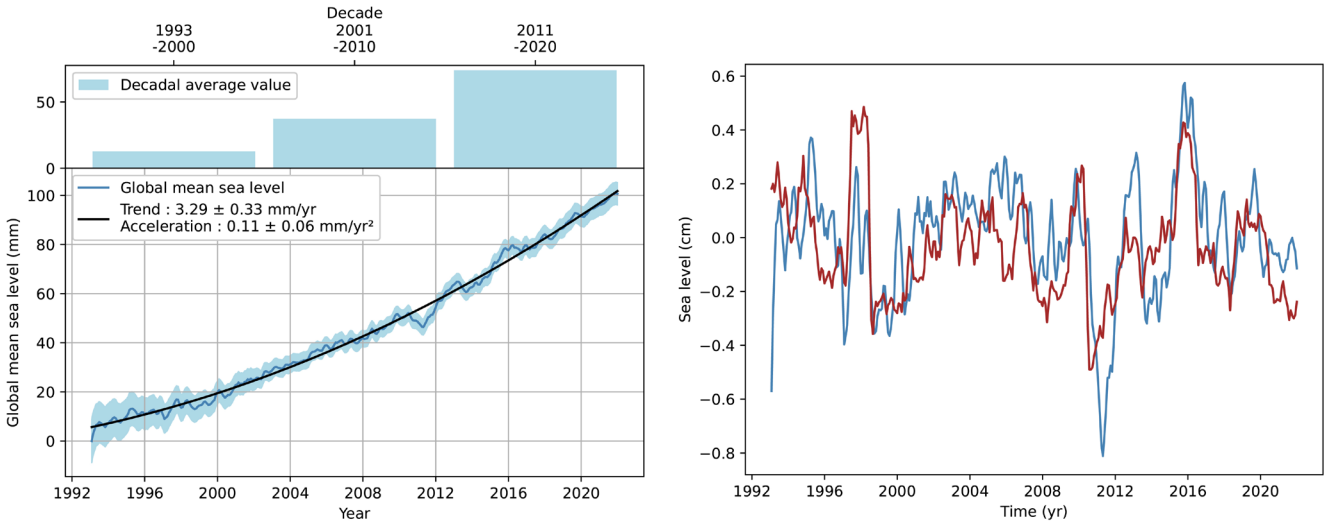

Figure 11. (Left) Evolution of the global mean sea level measured by satellite altimetry since 1993 (red curve). The shaded area represents the 90% level uncertainty, and the black line is a quadratic fit to the data. (Right) Interannual variability of the GMSL (blue curve) and multivariate ENSO index (red curve)

Recent assessments indicate that the GMSL budget is closed, within data uncertainties, over the altimetry era (since 1993).[25,26] In other words, observed sea level rise can be attributed almost entirely to known contributing factors. From the 2003-2016 period, ocean warming and total mass changes due to glacier and ice sheet melting contributed 33% and 67% to GMSL rise, respectively.[27]

---

22 The quoted errors are 90% level uncertainties estimated from error assessments affecting the whole satellite altimetry system.

23 Ablain, M., Meyssignac B., Zawadski, L., Jugler R., Ribes, A., Spada, G., Benveniste, J., Cazenave, A. and Picot, N.(2019), Uncertainty in satellite estimates of global mean sea-level changes, trend and acceleration, *Earth Syst.Sci. Data*, 11, 1189–1202.
Nerem, R.S., Beckley, B.D., Fasullo, J., Hamlington, B.D., Masters, D. and Mitchum, G.T. (2018). Climate ChangeDriven Accelerated Sea Level Rise Detected In The Altimeter Era, *Proceedings of the National Academy of Sciences*, 15, 9, 2022-2025, https://doi.org/10.1073/pnas.1717312115.

24 Eyring, V.; Gillett, N. P.; Achuta Rao, K. M. et al. Human Influence on the Climate System. In *Climate Change 2021: The Physical Science Basis. Contribution of Working Group I to the Sixth Assessment Report of the Intergovernmental Panel on Climate Change*; Masson-Delmotte, V.; Zhai, P.; Pirani, A. et al., Eds.; Cambridge University Press, Cambridge, United Kingdom and New York, USA, 2021. http://doi.org/10.1017/9781009157896.005.

25 World Climate Research Programme (WCRP). Global Sea Level Budget Group. Global Sea Level Budget, 1993-present, *Earth System Science Data*, **2018**, 10, 1551-1590. https://doi.org/10.5194/essd-10-1551-2018.

26 Horwath M., et al. Global Sea Level Budget and Ocean Mass Budget, with Focus on Advanced Data Products and Uncertainty Characterization. *Earth System Science Data* **2022**, 14, 411–447. https://doi.org/10.5194/essd-14-411-2022.

27 Horwath M., et al. Global Sea Level Budget and Ocean Mass Budget, with Focus on Advanced Data Products and Uncertainty Characterization. *Earth System Science Data* **2022**, 14, 411–447, 2022. https://doi.org/10.5194/essd-14-411-2022.

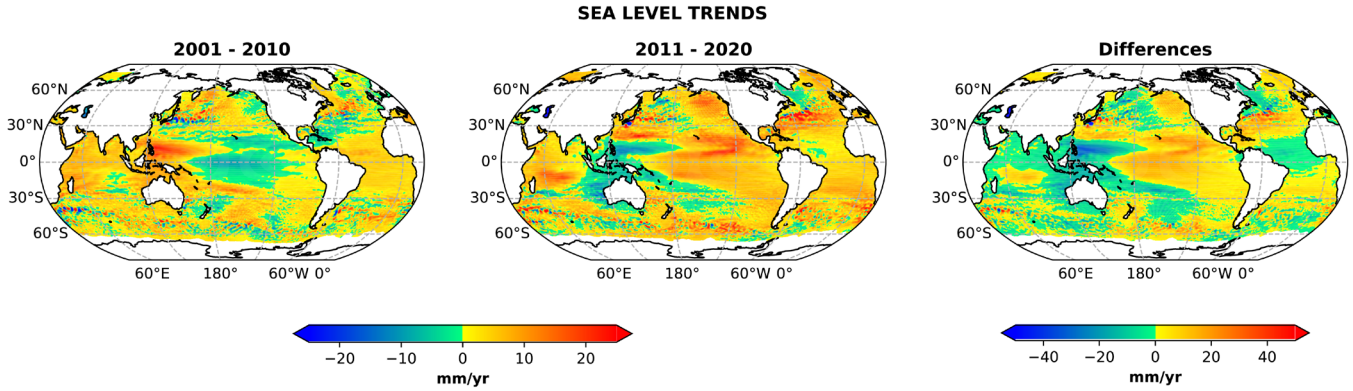

Figure 12. Regional sea level trends (mm/yr) over the 2001-201 (left panel), 2011-2020 (middle panel) periods, and difference in trends between the two periods (right panel)

The GMSL curve displays temporary (1–3-year duration) positive or negative departures from the global mean sea level rise. Most of this interannual variability is driven by ENSO events. El Niño and La Niña events give rise to positive and negative sea level anomalies of about 1-2 mm, as seen during the 1997-1998 and 2015-2016 El Niño events, and the 2011 La Niña.[28,29] These temporary fluctuations in the GMSL are mostly due to land and ocean water exchanges. During an El Niño, several tropical and subtropical river basins, such as the Amazon and the inland Australian basins, typically suffer droughts, while increased precipitation affects the eastern tropical Pacific.

Opposite effects are observed during La Niña. For example, heavy rain and floods occurred in Australia during the 2011 La Niña while rain deficits were reported over the tropical ocean.[30] This led to a temporary decrease in ocean mass, and a corresponding fall in the GMSL. A smaller but sizeable part of the interannual variation is also due to thermal expansion.[31]

Satellite altimetry continues to show that the rate of sea level change is also highly variable at the regional level, as illustrated in Figure 20, which compares regional sea level trends for the successive decades of 2001-2010 and 2011-2020. The spatial trend patterns are not stationary, particularly in the tropical and north Pacific, as well as in the tropical and north Atlantic where positive trends shift to negative trends from the first to the second decade, and vice versa. This is explained by the fact that decadal-scale spatial trend patterns in sea level so far are still mostly driven by internal climate modes such as ENSO. The few regions that show similar trends in the two decades include the Southern Ocean and the western part of the Indian Ocean. In these areas, the regional sea level trends may result from anthropogenic forcing.[32,33]

28 Cazenave, A., et al. Estimating ENSO Influence on the Global Mean Sea level, 1993–2010. *Marine Geodesy* **2012**, 35, 82–97. https://doi.org/10.1080/01490419.2012.718209.

29 Hamlington, B. D.; Cheon, S. H.; Piecuch, C. G. et al. The Dominant Global Modes of Recent Internal Sea Level Variability. *Journal of Geophysical Research: Oceans* **2019**, 124, 2750–2768. https://doi.org/10.1029/2018JC014635.

30 Fasullo, J.; Boening, C.; Landerer, F. et al. Australia's Unique Influence on Global Sea Level in 2010-2011. *Geophys. Res. Let.* **2012**, 40, 4368-4373. https://doi.org/10.1002/grl.50834.

31 Piecuch, C. G.; Quinn K. J.; Ponte, R. M. El Niño, La Niña, and the Global Sea Level Budget. *Ocean Science* **2016**, 12, 1165–1177. https://doi.org/10.5194/os-12-1165-2016.

32 Hamlington et al. Understanding Contemporary Regional Sea Level Change and the Implications for the Future. *Review of Geophysics* **2020**. https://doi.org/10.1029/2019RG000672.

33 Cazenave, A.; Moreira, L. Contemporary Sea Level Changes from Global to Local Scales: a Review. *Proc. Royal Society* **2022**, 478: 20220049. https://doi.org/10.1098/rspa.2022.0049.

OCEAN ACIDIFICATION

Over the last four decades, the ocean has taken up an average of 25% of the global anthropogenic CO_2 emissions[34,35] thereby strongly mitigating anthropogenic climate change. A consequence of the accumulation of anthropogenic CO_2 in the ocean is its acidification, namely a drop in the oceanic pH and saturation state of seawater with respect to the dissolution of mineral carbonates (Ω. Decreasing pH and W makes it more challenging for marine organisms to build and maintain their shells and skeletons.

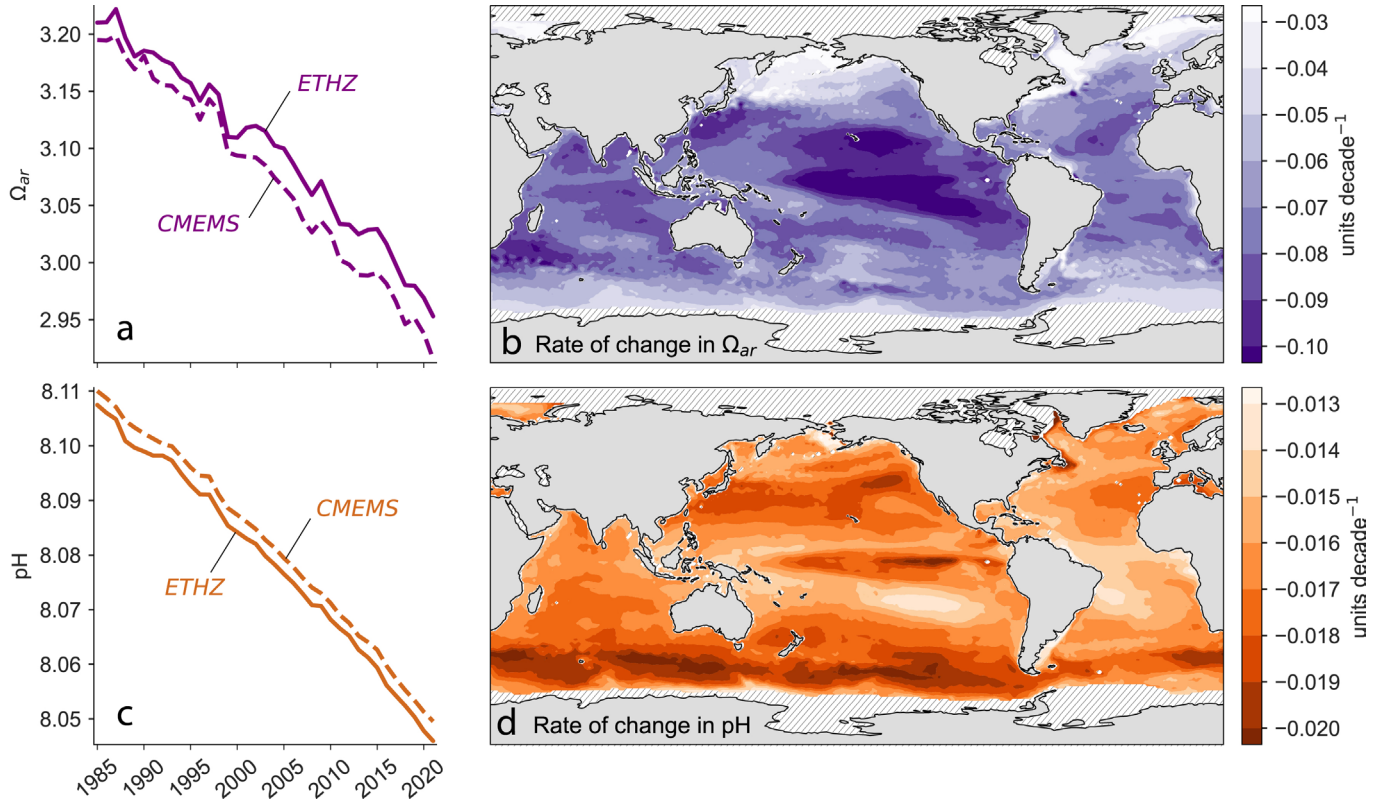

Figure 13. Long-term trends in ocean surface calcium carbonate, mineral aragonite saturation state (Ω) and pH, from 1982 to 2021
Deseasonalized Ω (a) and pH (c) trends during this period based on weighted areas. Rates of Ω (b) and pH (d) change per decade from linear regression models mapped for each location in global oceans using the mean of the two products. (Regions in the high latitudes with more than 50% sea ice coverage are hatched). Based on data from ETHZ[36] and Chau et al. (2022) CMEMS.[37,38]

The two parameters differ fundamentally with regard to the spatial pattern of the rates of change, as shown in Figure 13 (b) and (d). The highest rates of change in pH occur in the high latitudes, especially in the Southern Ocean around latitude 60°S, where the average rates of change are reaching -0.020 decade^{-1}. The rates of change in W (Ω) have the opposite spatial pattern, with the highest rates of change in the tropical Pacific.

34 Friedlingstein, P. et al. Global carbon budget 2021", *Earth Syst. Sci. Data* **2022**, 14 (4), 1917–2005. https://doi.org/10.5194/essd-14-1917-2022.

35 Gruber, N.; Bakker, D. C. E.; DeVries, T. et al. Trends and Variability in the Ocean Carbon Sink. *Nat. Rev. Earth Environ* **2022**.

36 Gregor, L.; Gruber, N. OceanSODA-ETHZ: a Global Gridded Data Set of the Surface Ocean Carbonate System for Seasonal to Decadal Studies of Ocean Acidification. *Earth Syst. Sci. Data* **2021**, 13 (2), 777–808. https://doi.org/10.5194/essd-13-777-2021.

37 Chau, T. T. T.; Gehlen, M.; Chevallier, F. A Seamless Ensemble-based Reconstruction of Surface Ocean pCO2 and Air-sea CO2 Fluxes over the Global Coastal and Open Oceans, *Biogeosciences*, **2022**, 19 (4), 1087–1109. https://doi.org/10.5194/bg-19-1087-2022.

38 The mean differences between the two products are due to differences in the reconstructions of the underlying products, that is, surface ocean pCO2 and alkalinity, and different choices in the dissociation constants used to compute Ω and pH from these underlying products.

Cryosphere

- Glaciers measured around the world thinned by an annual average of approximately 1m from 2011 to 2020. This amount of loss is unprecedented in the observed record.
- Greenland and Antarctica lost 38% more ice between 2011 and 2020 than during the 2001-2010 period, consistent with an acceleration of ice sheet mass loss.
- Arctic sea ice extent continues on a multi-decade decline: the mean seasonal minimum was 30% below average.

GLACIERS

The World Glacier Monitoring Service (WGMS)[39] collects, analyses, and disseminates data on glacier changes from around the world. The latest assessment based on 42 reference glaciers with long-term (>30 years) measurements (Figure 14, left) reveals that the period between 2011 and 2020 experienced the most negative decadal mean mass balances of any observed decade (-0.9 m water equivalent per year).[40] This implies that each year, and averaged over their entire surface, the glaciers that were measured had thinned by about 1m. The decadal mean value[41] shows large regional variability (Figure 14, right) but in nearly all regions the cumulative curves indicate a trend towards increasingly negative mass balances. As glacier areas are shrinking at the same time, this trend implies that ablation regions must reach higher and higher altitudes, consistent with a continuing rise in temperatures. Some of the mass balance reference glaciers have already melted away, as the winter snow nourishing the glacier melts completely during the summer months.

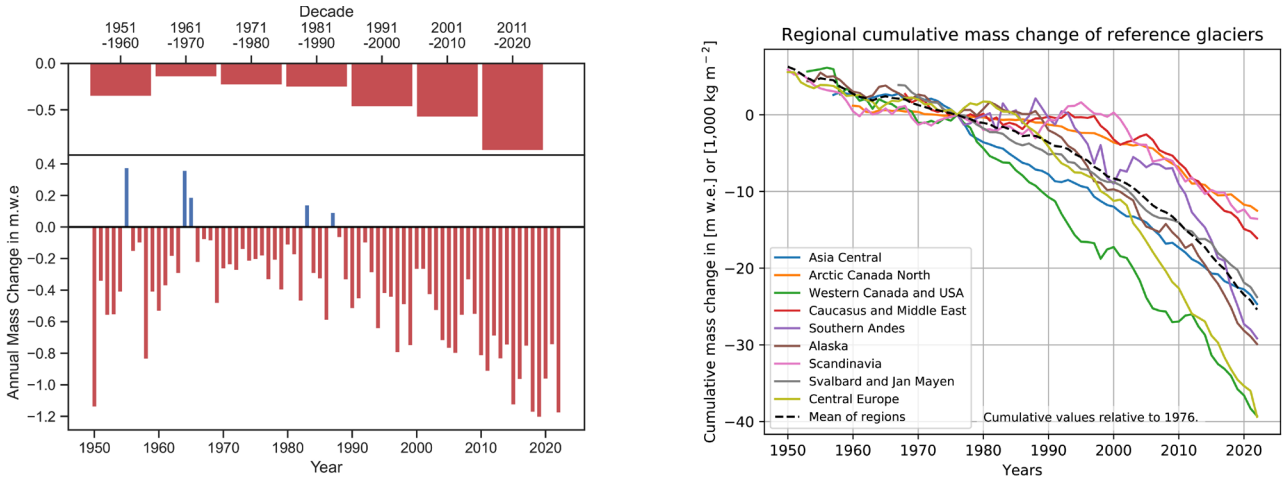

Figure 14. (Left) Annual and decadal mass changes of reference glaciers with more than 30 years of ongoing glaciological measurements. (Right) Cumulative mass change compared to 1976 for regional and global means based on data from reference glaciers. Annual mass change values are given on the y-axis in the unit metre water equivalent (mwe) that corresponds to tons per square metre (1,000 kg m^{-2}) and are calculated as arithmetic averages of regional means. *Source:* WGMS (2021 and earlier reports).

39 World Glacier Monitoring Service. Home page. https://wgms.ch.

40 World Glacier Monitoring Service. *Global Glacier Change, Bulletin No. 4* **2021**.; Zemp, M.; Nussbaumer, S. U.; Gärtner-Roer, I. et al.; Eds.; ISC(WDS)/IUGG(IACS)/UNEP/UNESCO/WMO, World Glacier Monitoring Service: Zurich, Switzerland, 2018-2019, 278 pp. Publication based on database version: https://doi:10.5904/wgms-fog-2021-05.

41 Zemp, M.; Frey, H.; Gärtner-Roer, I. et al. Historically Unprecedented Global Glacier Decline in the Early 21st Century. *Journal of Glaciology* **2015**, 61 (228), 745–762. http://dx.doi.org/10.3189/2015JoG15J017.

Cryosphere

The trend towards increasingly negative glacier mass balances has recently been confirmed by a global scale geodetic survey[42] using time series of digital elevation models derived from ASTER (Advanced Spaceborne Thermal Emission and Reflection Radiometer) stereo images. The analysis showed increasingly large negative values from 2000 to 2020 for nearly all the 19 primary glacier regions (Figure 15). This analysis, in combination with the annual field measurements of selected glaciers,[43] demonstrates that it is now possible to determine annual mass balances of nearly all 215,000 glaciers worldwide for the first time. This will vastly improve our ability to determine run-off from glaciers in regions where their meltwater is fundamentally important to sustaining human life, for example, providing water for agriculture, industry, or human consumption.

A critical impact of glacial mass loss is the collapse of entire or large sections of glaciers, killing people and livestock, destroying downstream infrastructure, and creating other possible consequences, such as damage to crops or disturbance of water sources.[44,45] Although the link to rising global temperatures is not yet fully clear, potential changes in the occurrence of such events constitute a risk that needs to be considered. The rapid growth of pro-glacial lakes,[46] and the potential hazard of a glacier lake outburst flood, poses an additional threat.[47] Water from glacial melt contributed to one of the decade's worst flooding disasters, the Uttarakhand floods of June 2013 (see Extreme Events).

The remaining glaciers near the Equator are generally in rapid decline. Glaciers close to Puncak Jaya in Papua, Indonesia have shrunk in area from 19 km^2 in 1850 to 0.34 km^2 in May 2020, and are likely to disappear altogether within the next decade. In Africa, glaciers on the Rwenzori Mountains and Mount Kenya are projected to disappear by 2030, and those on Kilimanjaro by 2040.

42 Hugonnet R.; McNabb, R.; Berthier, E. et al. Accelerated global glacier mass loss in the early twenty-first century, *Nature* **2021**, 592, 726–731. https://doi.org/10.1038/s41586-021-03436-z.

43 Zemp, M.; Huss, M.; Thibert, E. et al. Global Glacier Mass Changes and their Contributions to Sea-level Rise from 1961 to 2016", *Nature* **2019**, 568, 382–386.

44 Kääb, A.; Jacquemart, M.; Gilbert, A. et al. Sudden Large-volume Detachments of Low-angle Mountain Glaciers - More Frequent than Thought. *The Cryosphere* **2021**, *15*, 1751-1758. https://doi.org/10.5194/tc-15-1751-2021.

45 Shugar, D. H. et al. A Massive Rock and Ice Avalanche caused the 2021 Disaster at Chamoli, Indian Himalaya. *Science* **2021**, *373* (6552), 300-306. https://doi.org/10.1126/science.abh4455.

46 Shugar, D. H. et al. Rapid Worldwide Growth of Glacial Lakes since 1990. *Nature Climate Change*, **2020**, 10, 939–945.

47 Carrivick and Tweed. A Global Assessment of the Societal Impacts of Glacier Outburst Floods. *Global and Planetary Change* **2016**, 144, 1–16.

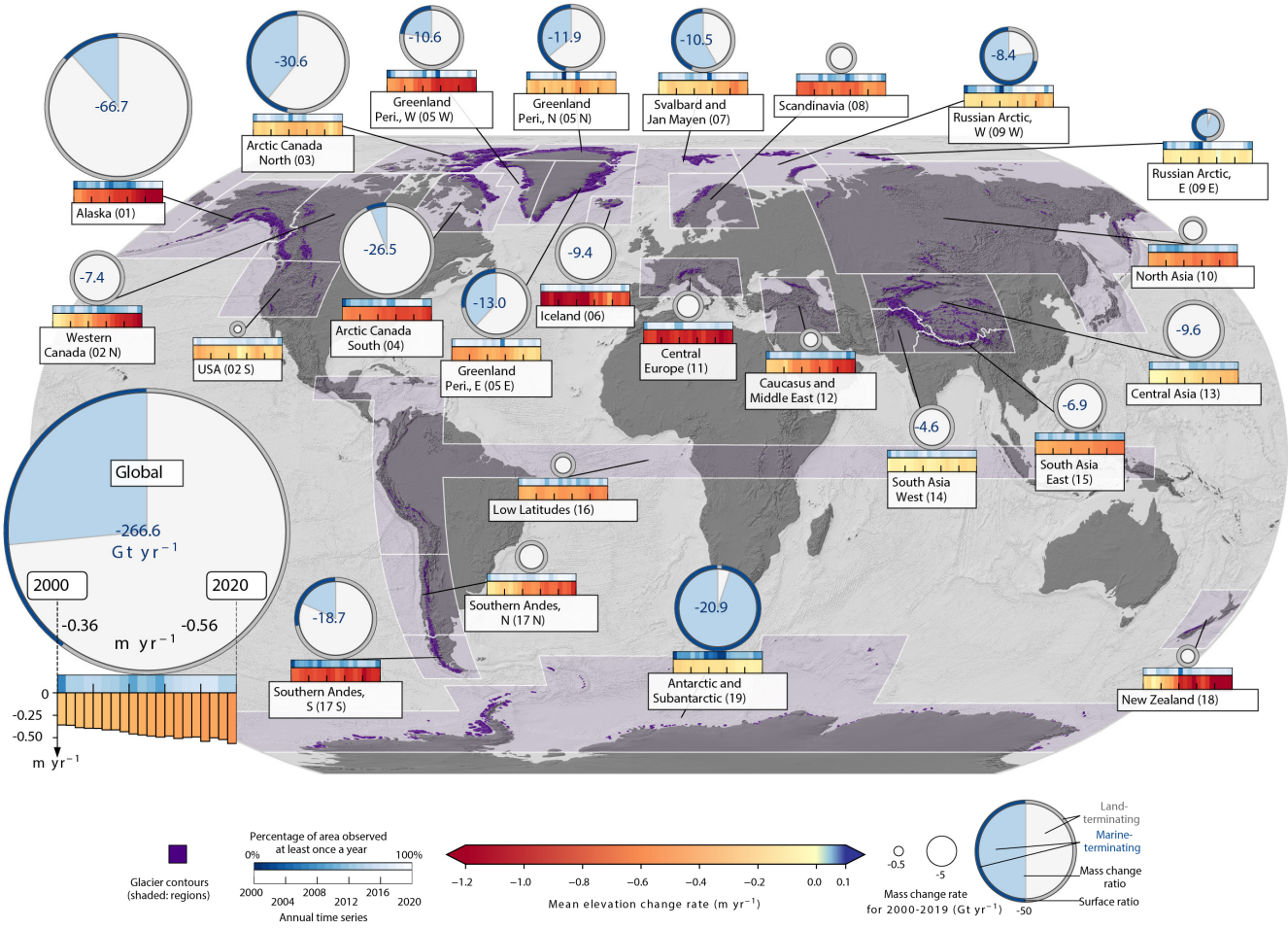

Figure 15. Regional and global glacier elevation change rates (m yr^{-1}) and mass change rates (Gt yr^{-1}) from 2000 to 2020
Source: Hugonnet, R., McNabb, R., Berthier, E. et al. Accelerated global glacier mass loss in the early twenty-first century. Nature 592, 726–731 (2021). Licensed with permission from Springer Nature.

ICE SHEETS

The Greenland and Antarctic Ice Sheets are the largest freshwater reservoirs on Earth, storing a volume of 29.5 million km^3 of frozen water. When ice sheets lose mass, they directly contribute to raising the global mean sea level and, therefore, monitoring the volume of ice they gain or lose is critical to assessing sea level change. Due to the vast area they cover and the difficulty of reaching these remote regions, only satellite observations can be used to comprehensively study their mass balance. Ice sheet mass balance can be estimated by tracking changes in ice sheet volume, mass changes via gravitational attraction, or estimated glacier flow combined with an estimate of snow accumulation. These three techniques complement each other and combining multiple ice sheet mass balance estimates leads to greater certainty in determining the changes in their mass. During the 2011-2020 decade, Greenland lost mass at an average rate of 251 Gt yr^{-1} and reached a new record mass loss of 444 Gt in 2019. Antarctica lost ice at an average rate of 143 Gt yr^{-1} during this decade, with more than three-quarters of this mass loss coming from West Antarctica. Compared to the previous decade (2001-2010), this represents an increase of 38 % in ice losses from Greenland and Antarctica combined and confirms the sustained increase of ice sheet mass loss compared to the 1990s (1992-2000), when Greenland and Antarctica ice losses amounted to only 84 Gt yr^{-1}.

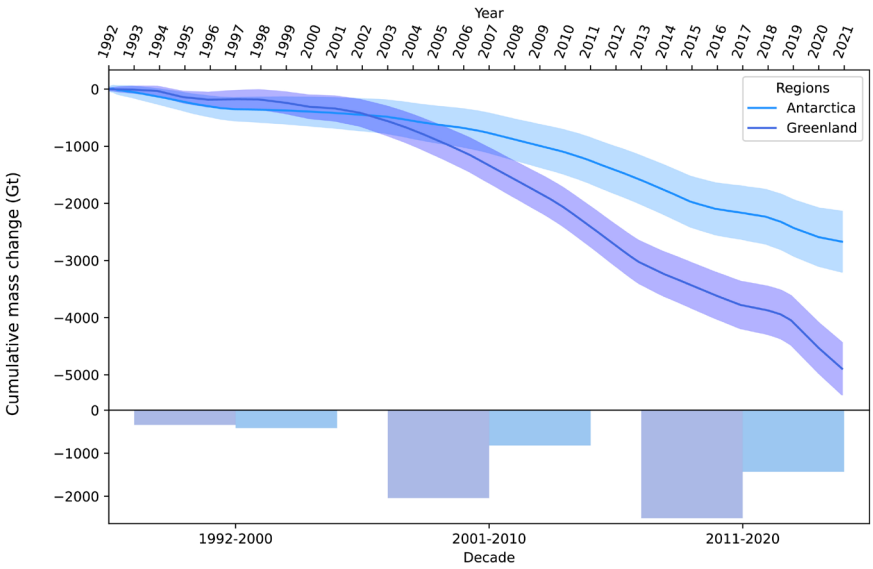

Figure 16. Cumulative annual and decadal ice sheet mass change from 1992 to 2020 for the Greenland and Antarctic Ice Sheet in Gt (gigatons), from the Ice Sheet Mass Balance Inter-Comparison Exercise (IMBIE) which combines 50 satellite-based measurements of ice sheet mass balance. The shading represents the corresponding uncertainty.

SEA ICE

Both the Arctic and Antarctic regions have substantial sea ice covers. Arctic sea ice continued to decline during the decade in question, particularly during the summer melt season. The mean seasonal minimum during the 2011-2020 period was 4.37 million km², 30% below the 1981-2010 average of 6.22 million km². The decrease was less pronounced, but still substantial, during the winter accumulation season, with an annual mean maximum during the decade of 14.78 million km², 6% below the 15.65 million km² average for the 1981-2010 period.

There was considerable interannual variability, particularly during the summer months. The year 2012 had the lowest seasonal minimum since satellite recording began in 1979 (3.39 million km²), and the Sixth Assessment report of the IPCC[48] was able to state, with a high degree of confidence, that it was the lowest seasonal minimum since 1850 at least. Seven of the ten years with the lowest ice extent occurred during the 2011-2020 decade. Each year in the decade had a seasonal minimum below the 1981-2010 average.

The years 2017 and 2018 had the lowest winter maximum extents of the years recorded by satellite technology, with a maximum extent of 14.41 million km² in 2017. As for the summer minimum, every year of the decade produced readings below the 1981-2010 average.

Reduced sea ice extent was accompanied by a decrease in thickness and volume, although data for these indicators are more limited. There has also been a marked decrease in the extent of ice which lasted for more than one year. In March 1985, old ice (four years or more) accounted for 33% of the total ice cover of the Arctic Ocean, but that figure had fallen below 10% by 2010, and in March 2020 it had dropped to 4.4%.[49] Ice of this age is now mostly confined to a narrow strip extending from north of Greenland along the north-west edge of the Canadian archipelago.

48 Fox-Kemper, B.; Hewitt, H. T.; Xiao. C. et al. Ocean, Cryosphere and Sea Level Change. In *Climate Change 2021: The Physical Science Basis. Contribution of Working Group I to the Sixth Assessment Report of the Intergovernmental Panel on Climate Change;* Masson-Delmotte, V.; Zhai, P.; Pirani , A. et al., Eds.; Cambridge University Press, Cambridge, United Kingdom and New York, USA, 2021, 1211–1362. https://doi.org/10.1017/9781009157896.

49 National Oceanic and Atmospheric Administration (NOAA). Arctic report card. 2020. https://repository.library.noaa.gov/view/noaa/27904.

Cryosphere

The most drastic reduction in summer Arctic sea ice has been observed in the Eurasian sector east of 90 °E and in the Beaufort Sea. Historically, even at the summer minimum, sea ice extended to within 300 km of the coast in most of these regions and reached the coast in the vicinity of the Taymyr Peninsula, but the summer ice edge is now much farther north in these areas. In winter, the largest declines occurred in the Barents and Greenland Seas, including the area around the Svalbard archipelago.

By contrast, Antarctic sea ice extent shows no clear long-term trend, and this is partially due to the relatively weak warming trend in much of the Southern Ocean. There was considerable variability in sea ice extent during the decade, with very high and very low values observed at different stages. Overall, mean sea ice extent for the decade was close to the average of the preceding years. The mean winter maximum extent for the 2011-2020 period was 18.93 million km^2, slightly above the 1981-2010 average of 18.71 million km^2, while the mean summer minimum extent for the decade of 2.85 million km^2 almost exactly matched the 1981-2010 average of 2.84 million km^2.

There was a period of abnormally high sea-ice extent from 2012 to 2015. In 2014, 20.16 million km^2 was measured, and this was the only time since 1979 that Antarctic sea ice extent exceeded 20 million km^2. An abrupt shift during late 2015 and 2016 reversed the trend from well above average sea ice extent to well below average, with values at record low seasonal levels for much of 2017 and 2018. The summer minimum of 2.11 million km^2 in February 2017 was the lowest ever for the 1979-2020 period; 2018 was only slightly behind, and the 2017 winter maximum of 18.10 million km^2 ranked the third lowest on record. Changes in the atmospheric circulation were a major driver of this variability, associated in part with broader climate modes of variability such as the Southern Annular Mode. Changes in near-surface ocean stratification also played a role.[50]

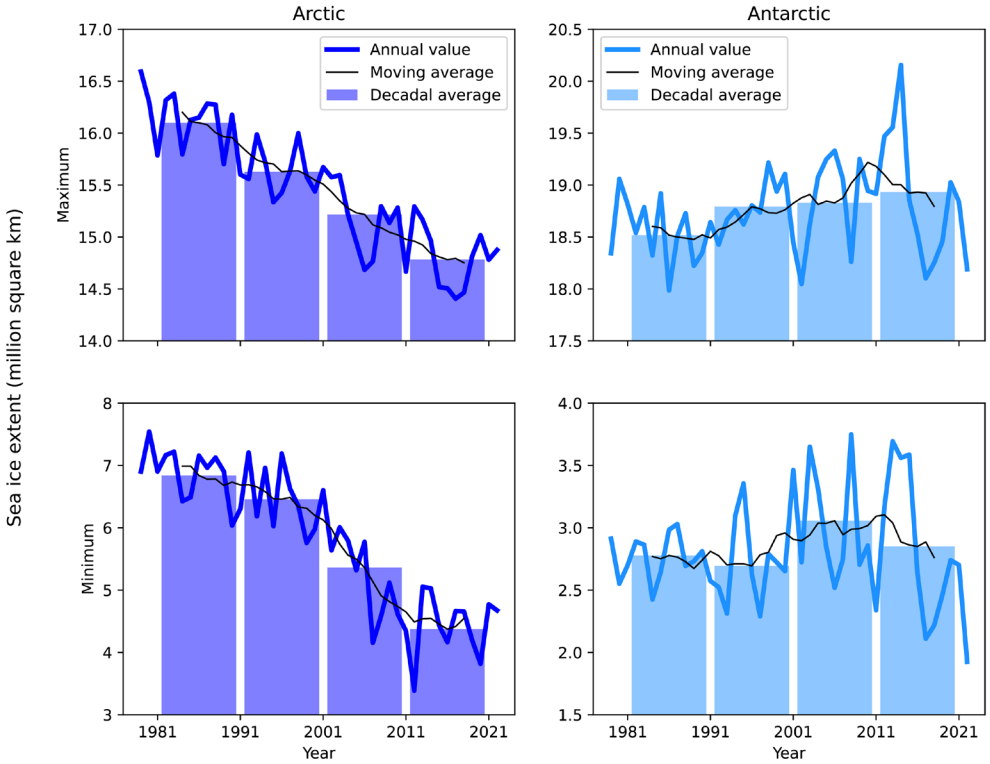

Figure 17. Seasonal maximum (top) and minimum (bottom) sea ice extent for the Arctic (left) and Antarctic (right) by decade, with annual values and a 10-year moving average overlaid.

50 Fox-Kemper, B.; Hewitt, H. T.; Xiao. C. et al. Ocean, Cryosphere and Sea Level Change.In *Climate Change 2021: The Physical Science Basis. Contribution of Working Group I to the Sixth Assessment Report of the Intergovernmental Panel on Climate Change;* Masson-Delmotte, V.; Zhai, P.; Pirani, A. et al., Eds.; Cambridge University Press, Cambridge, United Kingdom and New York, USA, 2021, 1211–1362. https://doi.org/10.1017/9781009157896.

PERMAFROST

Permafrost is ground that remains at or below 0°C for at least two consecutive years. When thawing, it can cause hazards, including ground subsidence or landslides, as well as having a noticeable influence on the global climate through emissions of greenhouse gases from microbial breakdown of previously frozen organic carbon. Two variables are broadly monitored to evaluate the state of the permafrost and to support projections: active layer thickness (ALT), the thickness of the layer which melts and refreezes, and permafrost temperature. As permafrost increases in temperature or melts altogether, ALT rises.

Decadal assessments of changes in the permafrost are difficult because of the limited number of observation sites with records of data covering the period. Permafrost observations are carried out under difficult operating conditions and at significant cost. As many observations have been made as part of research projects without long-term ongoing support, this has led to substantial observation gaps. Active layer thickness is the permafrost variable with the best spatial coverage, with little long-term permafrost temperature data available outside Alaska.

The ALT trends in the Alaskan interior (0.67±0.05 m/decade), Svalbard (0.21±0.04 m/decade) and Chukotka (0.11±0.02 m/decade) from 2011 to 2019 are increasing and are statistically significant at a level of 99% (Figure 18), and a similar trend has been detected for the northern hemisphere as a whole where ALT is also increasing (0.09±0.03 m/decade) and statistically significant at a level of 95%. Over the previous decade, ALT has increased in most sub-regions, although some of the changes are non-significant. However, ALT in Greenland and Canada has reduced slightly.

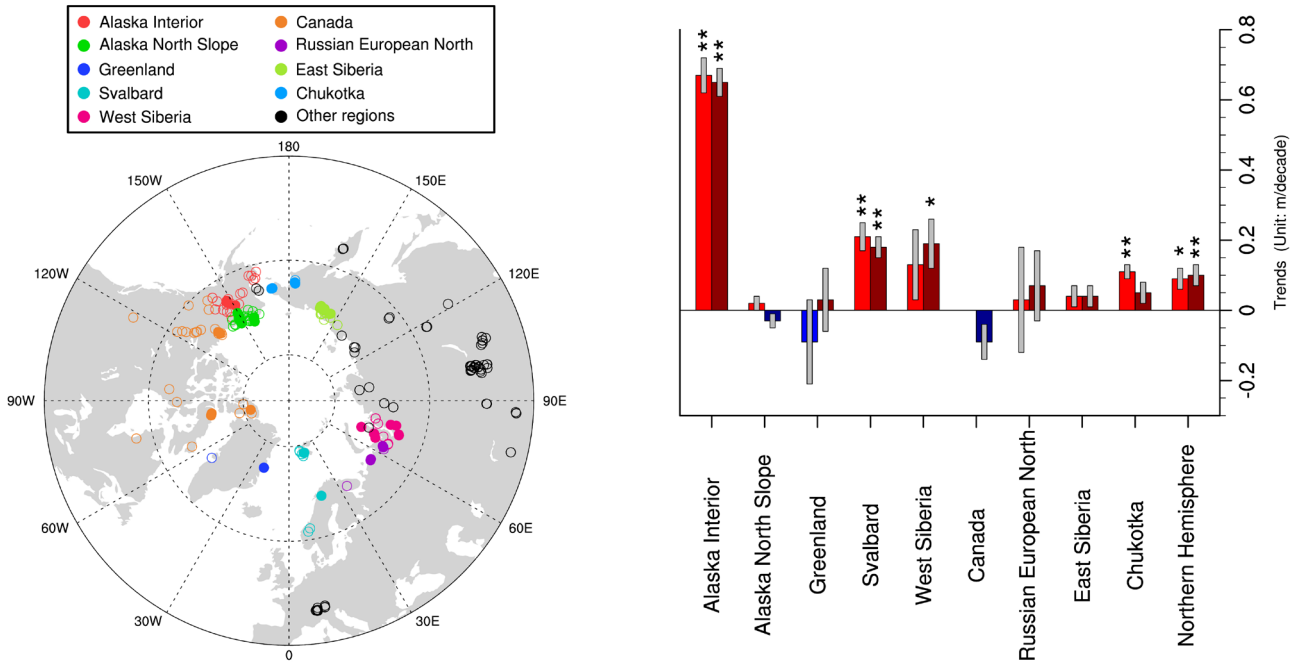

Figure 18. Left: Distribution of ALT sites from CALM data set in different regions. Solid dots indicate sites with sufficient data for assessment, circles indicate sites not used for the assessment due to excessive missing data. Right: ALT trends in different regions. Red(blue) bars indicate the trends between 2011 and 2019, while dark red (blue) bars indicate the trends for all years with ALT data after 2011 (from 2011 to 2021 the data on Svalbard/Canada was updated only up to 2020/2018). A single asterisk "*" indicates statistically significant trends at a level of 95% (student's t test), while a double asterisk "**" indicates statistically significant trends at a level of 99%.
Grey bar indicates standard deviation.

The limited data available for permafrost temperature, mostly from Alaska, suggest that it has risen during the last decade, and this increase is statistically significant at a level of 99%. A mean trend of 0.6˚C/decade was calculated from the available data at these sites.

Modes of Climate Variability

Natural modes of climate variability strongly influence how climate varies from year to year in various parts of the world. The El Niño-Southern Oscillation (ENSO), a phenomenon centred in the equatorial Pacific, is the most well-known, and it influences the climate over many parts of the world. Another key mode of tropical ocean variability, the Indian Ocean Dipole (IOD), has a strong impact on the climate around the Indian Ocean basin. In the atmosphere, the related phenomena of the Arctic Oscillation (AO) and North Atlantic Oscillation (NAO) strongly influence the climate of the northern hemisphere mid-latitudes, while the Antarctic Oscillation (AAO) - also known as the Southern Annual Mode (SAM) - does likewise in the southern hemisphere.

The decade 2011 to 2020 experienced one powerful El Niño event in the period 2015-2016, and a strong La Niña event in the period 2010-2011. The 2015-2016 El Niño episode was one of the strongest El Niño events since 1950 and was associated with significant drought conditions in several parts of the world, especially in southern Africa. The 2010-2011 La Niña event, followed by a weaker but still significant event in 2011-2012, was also among the most powerful in recent decades. It brought heavy rainfall and significant flooding to eastern Australia, south-east Asia and the Indian subcontinent, as well as drought in the Greater Horn of Africa and the southern United States. In addition to its regional climate impacts, ENSO not only has a substantial influence on global mean surface temperature, as is evident in the record warm temperatures of 2016 during the El Niño phase and relatively cool year of 2011 during La Niña, but also has the potential to change global mean sea level by as much as 5 to 10 mm.

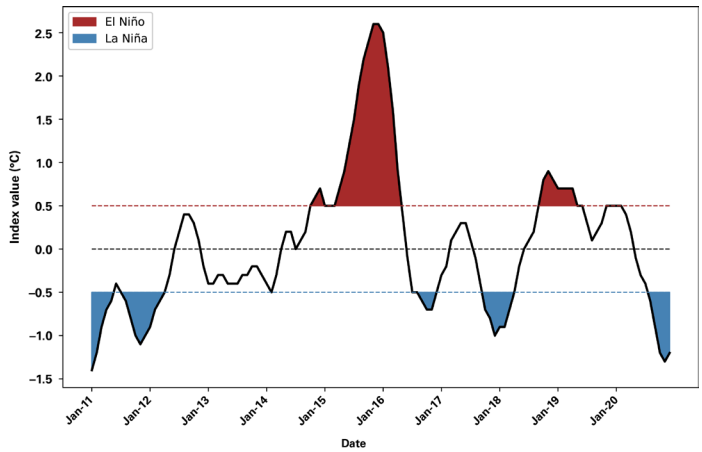

Figure 19. NOAA Oceanic Nino 3.4 Index for the 2011-2020 decade. Sustained values above 0.5 °C are indicative of El Niño events (red) and those below –0.5 °C are indicative of La Niña events (blue). *Source:* NOAA.

While its impacts cover less of the globe than those of ENSO, the IOD nonetheless has a strong influence on the climate of the Indian Ocean basin. One of the strongest positive IOD events on record (with warm waters off the east African coast and cool waters off north-western Australia) occurred in the second half of 2019. This was associated with severe drought and associated wildfires in many parts of Australia, as well as drought in parts of south-east Asia. It was also associated with high rainfall in the Greater Horn of Africa in late 2019 and early 2020. A significant negative IOD event in 2016 led to a very wet year in many parts of Australia, and drought in eastern Africa.

The AO/NAO and AAO/SAM were both predominant in their positive phase during the decade. Averaged over the January-March period, when it has its strongest influence on the climate, the AO index in 2020 was the most strongly positive on record. This was associated with the warmest winter on record in western Europe and most of the western half of the Russian Federation. The only year with a significantly negative AO was 2013, driven by the most strongly negative value on record for March, a very cold month in Europe. The NAO was even more consistently positive, with positive index values in 26 of the 30 January-March months during the decade, although the peak seasonal averages, in 2015 and 2020, fell short of the record high value that was set in 1989. The AAO/SAM was also predominantly positive, with an especially protracted period of positive values between late 2014 and mid-2016. A period of strongly negative AAO/SAM values in late 2019, driven by a rare Antarctic sudden stratospheric warming event in September 2019, and combined with the positive IOD further intensified drought in eastern Australia, thereby contributing to the exceptional wildfire season.

Precipitation

There were large regional variations in precipitation: with some regions having an abnormally wet decade and others, where it was abnormally dry during the same period, especially in the subtropics

Precipitation varies greatly from year to year and from place to place. For many other indicators, trends are relatively consistent over most parts of the world and global-scale indicators provide a good summary of the state of the climate. For precipitation, regional changes are more significant than global-scale indicators, and some of the largest impacts occur when there are large deviations from the average, either positively or negatively, over a period of multiple years.

Figure 20 shows precipitation in the 2011-2020 decade compared with the 1951-2000 reference period. Northern Eurasia was one of the largest areas of consistent above-average rainfall during the decade, extending from the Nordic countries eastwards to cover much of the Russian Federation. Precipitation over most of this area between 2011 and 2020 was 10 to 20% above the 1951-2000 average. It was also a wet decade over China, particularly in the west, Pakistan and northwest India, and the southern coast of the Arabian Peninsula. Outside Eurasia, the areas with 2011-2020 average precipitation more than 10% above the 1951-2000 average included the eastern United States, Western Australia (apart from the south-west), and parts of subtropical South America.

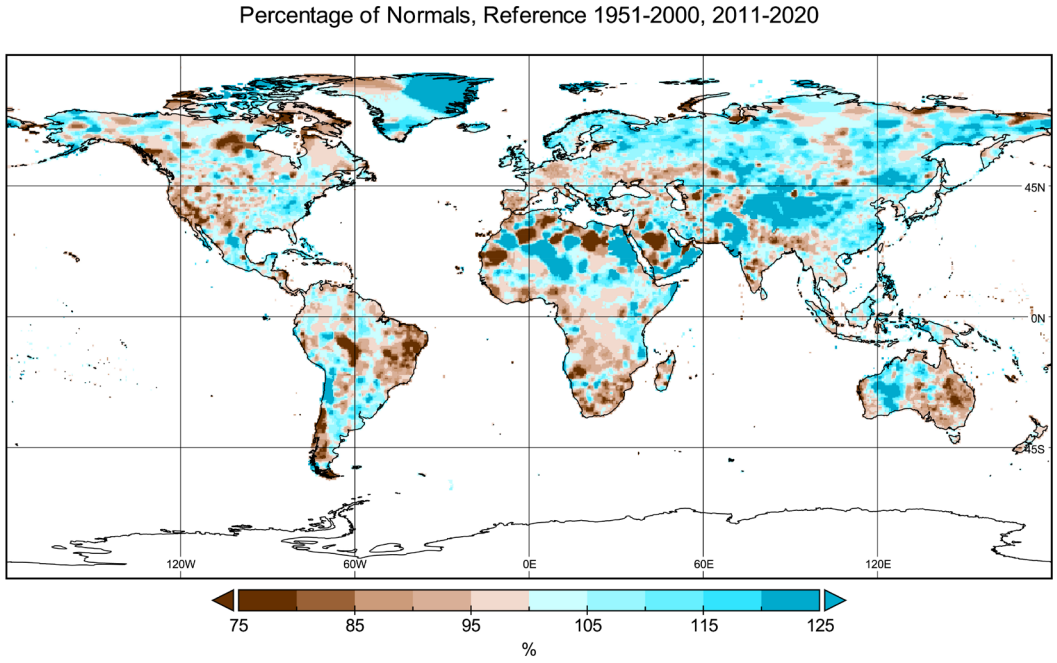

Figure 20. Mean annual precipitation over the decade 2011-2020, expressed as a percentage of the mean for the 1951-2000 reference period.

Long-term drought was predominant in many subtropical regions of the world, resulting in decadal average rainfall more than 10% below that of the 1951-2000 reference period. These regions include the south-western United States, the western Mediterranean, eastern Australia south of the tropics, southern Africa, and central Chile. In Chile, where rainfall in some places was below the long-term average in every year of the decade, dry conditions also extended to higher latitudes. In the tropics, north-east Brazil was notably an area of persistently low rainfall, while at higher latitudes, one area of central Europe, centred on Germany, also experienced a dry decade.

On the other hand, the decade shows above average to extreme wet conditions across most of Asia. The year 2020 was exceptionally wet in parts of China, particularly over the Yangtze catchment, which had its wettest year of the post-1961 period, contributing to substantial flooding. Rainfall in Pakistan was more than 50% above average in both 2019 and 2020. In contrast, 2019 and 2020 were both dry years over Indochina, with rainfall in the peak rainy season, May-September, more than 10% below average in both years and significant drought over the Mekong basin. Indochina's wettest year was in 2011, when May-September

Precipitation

rainfall rose to 22% above average and there was major flooding, especially in Thailand. India was dry in 2014 and 2015. This represented only the fourth instance since 1900 of consecutive years in which the south-west monsoon (June-September) rainfall was more than 10% below average. In contrast, 2019 and 2020 were the second and third wettest south-west monsoon seasons on record.

The decade saw some extremely wet years in the eastern and central United States. The years 2011, 2018 and 2019 in the Ohio Valley region were the three wettest years on record during the decade. Indeed, 2019 was also the wettest year on record for the regions of the Upper Midwest, Northern Rockies and Great Plains, while 2011 was the wettest year in the Northeast. In contrast, 2013 and 2020 were the two driest years on record for the West, and 2011 to 2015 was the driest four-year period[51] on record for the state of California. 2020 was also the second driest year for the Southwest.

Large parts of Australia experienced severe drought from 2017 to 2019, when the three-year rainfall in many parts of the eastern interior was the lowest on record. The driest year on record nationally, 2019, was especially extreme, with some parts of northern inland New South Wales receiving annual rainfall more than 70% below average, and 50% below previous record lows. The 2010-2011 and 2011-2012 summers, particularly the former, had widespread heavy rainfall associated with La Niña events, while 2016 was also a wet year due to a strong negative Indian Ocean Dipole. On the opposite end of the spectrum, 2019 and 2020 were particularly dry in much of the North Island of New Zealand with several locations recording their driest year ever in one of those years.

The strong El Niño episode of 2015-2016 resulted in strong precipitation anomalies in various parts of the world. Rainfall in much of southern Africa was well below average from mid-2014 to mid-2016. From May to October 2015 the Maritime Continent registered rainfall that was 32% below average, which contributed to the outbreak of major wildfires that year. Meanwhile, the Amazon basin was also significantly drier than average in both 2015 and 2016. In these years El Niño also created very dry conditions in parts of the Pacific, including much of Micronesia, Vanuatu and the Solomon Islands. Subtropical South America, east of the Andes, was wet in the first half of the decade, particularly in 2014 and 2015, but was dry from 2018 onwards, and especially so in 2020.

The latter part of the decade was wet in the northern hemisphere section of the African monsoon region,[52] with 2018, 2019 and 2020 all about 10% above average. Significant flooding ensued, particularly in 2020. The Greater Horn of Africa saw very large anomalies in both directions. The 12-month period ending in June 2011 was extremely dry, contributing to significant famine later in 2011 and 2012, and also had severe drought in the 2016 -2017 and the 2018-2019 periods. However, in late 2019, and, to a lesser extent, early 2020, conditions became extremely wet. Severe localized drought from 2015 to early 2018 in the winter-dominant rainfall zone of south-western South Africa contributed to severe water shortages in Cape Town and its surrounding areas.

Many countries reported significant precipitation extremes during the decade. Twenty out of 97 reporting countries, encompassing all regions except South America and the south-west Pacific, experienced their highest or equal-highest daily precipitation of the 1961-2020 period during the decade, slightly above the long-term average (although lower than in the period between 2001 and 2010). Long-term trends in this indicator are difficult to assess from national reports, as some countries have had substantial changes in their observing network over time, including the opening or closing of stations in particularly wet areas.

51 Water years measuring 2011-12, 2012-13, 2013-14, and 2014-15. A water year is defined as extending from October of one year to September of the next.

52 Defined here as 8-18 °N, 10 °W-35 °E.

High-Impact and Extreme Events

- Extreme events across the decade had devastating impacts, particularly on food security and human mobility, hindering national development and progress toward the Sustainable Development Goals (SDGs).
- For many extreme events, the likelihood of an event of that magnitude has been altered, often greatly, because of anthropogenic climate change. Virtually every attribution study carried out on an extreme heat event in the 2011-2020 period found that the likelihood of the event increased significantly because of anthropogenic climate change.
- Heatwaves were responsible for the highest number of casualties, while tropical cyclones caused the most economic damage. The number of casualties from extreme events has declined, associated with improved early warning systems, but economic losses have increased.

The years 2011 to 2020 saw a large number of extreme events, many of which had significant impacts. The impacts of extreme events are a function of the hazard itself, exposure to the hazard, and the vulnerability of the affected population.

The number of casualties from extreme weather and climate events has gone down substantially over time. A major contributor to this decrease has been improved early warning systems, driven by improvements in forecasting, coupled with improved disaster management. The 2011-2020 decade was the first since 1950 when there was not a single short-term event with 10,000 deaths or more.[53] However, economic losses from extreme weather and climate events have continued to increase. While Hurricane *Katrina* in 2005 remains the world's most costly weather disaster, the next four most costly events were all hurricanes that occurred in the 2011-2020 decade, and whose greatest impacts were in the United States and/or its territories.

There was great contrast between events causing large numbers of casualties and those incurring great economic losses, both in terms of the type of event and their geographic distribution. Of the 13 known events resulting in more than 1000 deaths,[53] six were heatwaves; four were monsoonal flooding or landslides associated with such flooding, and three were tropical cyclones. Eight of the events occurred in Asia; four, all heatwaves, in Europe, and one in Africa. On the other hand, of the 27 events with known economic losses exceeding 10 billion US dollars (USD), in 2022 dollars, 16 occurred within the United States and eight in East Asia; 13 of the 27 events were tropical cyclones, eight floods and three wildfires. Only two events, Typhoon *Haiyan* in the Philippines in 2013, and monsoon season flooding in India in 2019, appear on both lists. Although the thorough collection and analysis of data on impact is improving, the assessment of the economic impact of extreme events continues to bear a high degree of uncertainty. Since only a small number of countries systematically assess excess deaths from heatwaves, and those that do, have not all done so for the entire decade, it is likely that many events are missing from the assessment process.

53 Data from the EM-DAT disaster database are used in this assessment. EM-DAT lists events by country, so some events will be missed (for example, Cyclone *Idai* in southern Africa in 2019, where there were more than 1000 deaths in total but not in any single country), and in some instances there will be multiple entries for the same event (heatwaves in 2020 are shown as separate events for the United Kingdom, France and Belgium). EM-DAT also does not typically capture long-term events such as drought and associated famine.

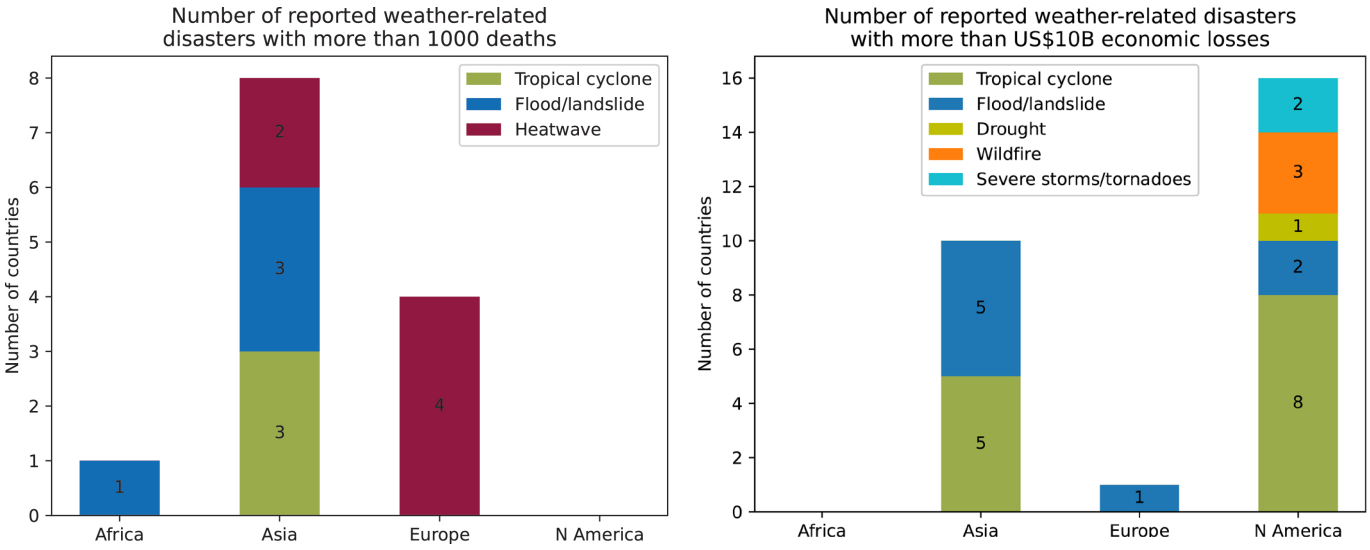

Figure 21. Left: Number of reported weather-related disasters with more than 1000 deaths by disaster type and region. Right: Number of reported disasters with more than USD 10B in economic losses (2022 dollars) by disaster type and region
Source: EM-DAT.

ATTRIBUTION

The science of determining the extent to which anthropogenic climate change contributed to the risk of an extreme event developed greatly during the decade 2011-2020. At the start of the decade, such assessments were in their infancy, and those that were carried out were not published for months or years after the event. However, analysis capabilities have rapidly improved, and there are now numerous groups, involving collaboration between NMHSs and other research institutions, which are carrying out event attribution for certain types of events within days or weeks of the event. The spatial and temporal scales on which attribution is being done are also decreasing, although results are still typically stronger at larger scales (for example, a seasonal average for a country or large region) than at smaller scales, (such as a daily extreme at a specific point). There are, so far, few events where it can be said that anthropogenic climate change "caused" the event in the sense that it would have been impossible in a pre-industrial climate. However, for many extreme events, the risk of an event of that magnitude has been altered, often greatly, because of anthropogenic climate change.

Most of the events in this section are described in greater detail in annual WMO *State of the Climate* reports. Impact data from the WMO pilot project on the impacts of extreme events with national statistics offices (Box 2) as well as from United Nations agencies including the Food and Agriculture Organization (FAO), International Organization for Migration (IOM), and the Internal Displacement Monitoring Centre (IDMC) can be found throughout the descriptions of various extreme events in the text below.

MEASURING EXTREME EVENT IMPACTS ON THE SUSTAINABLE DEVELOPMENT GOALS

It is becoming increasingly clear that climate extremes are affecting the ability of populations to develop sustainably. To help put the various components of climate change and development together, WMO, in partnership with various United Nations agencies and national statistics offices (NSOs), has piloted a project exploring the impact of extreme events on national progress toward the Sustainable Development Goals (SDGs).

The SDGs were chosen because they represent a globally-agreed set of goals and indicator frameworks that enable an understanding of impacts beyond mortality and economic losses, to encompass additional areas such as water, energy, food, and biodiversity. The IPCC has shown that there is a narrowing window of opportunity for climate-resilient development that includes achievement of the SDGs,[54] thereby necessitating better understanding of how progress is hindered by extreme events. Demonstrating the impact of extreme events on national development requires both sound knowledge of national progress toward the SDGs and access to official data on disaster statistics—which has historically been difficult to obtain.[55] National statistics offices were therefore designated to evaluate extreme event impact as the principal entity responsible for providing official statistics to inform the SDG process. This role uniquely positions them to evaluate the impact of any given event.

METHODOLOGY

Select NSOs were provided with a survey developed by a WMO-led expert group to evaluate the impact of a pre-selected event on the SDGs. Although there are 17 SDGs in total, to lessen the burden on NSOs, the survey requested data on only SDGs 1 – No Poverty, 2—Zero Hunger, 3—Good Health and Wellbeing, 6—Clean Water and Sanitation, 7—Affordable and Clean Energy, 10—Reduced Inequalities, 11—Sustainable Cities, and 15—Life on Land. These Goals were determined to be the most likely to be affected by an extreme event.[56] The survey consisted of 8 questions for NSOs to rank the impact of the event on progress toward each of the SDGs according to a scale of "no impact", "insignificant", "significant" and "major". Given differences in how events could have an impact on national development, there were no specific definitions for each level of impact. It was up to the discretion of the NSOs to define the level of impact based on available data. Boxes following each question allowed for the NSO to provide data or comments on each SDG where available and appropriate.

The analysis provided herein was not meant to achieve a comprehensive assessment, but, rather, to focus on a few countries in order to understand the role of selected extreme events on development issues. This exercise will help to guide future assessments at global and regional scales. It is hoped that as data become increasingly accessible and adequate for quantitative assessment, regular reporting could be done through the WMO *State of the Climate* reports at the global and regional scales.

RESULTS

Input received from six NSOs across Africa, Europe, South America, and the Caribbean demonstrates the cross-cutting impacts of diverse extreme events in various domains of development and also highlights disparities in how these impacts inhibit national progress toward development goals (Figure 22). For example, Hurricane *Irma* was a category 5 hurricane that crossed Antigua and Barbuda in the Caribbean at near-peak intensity, resulting in catastrophic impacts. A joint recovery needs assessment from the World Bank and European Union found the combined value of destroyed assets and production disruptions amounted to approximately 9% of Antigua and Barbuda's Gross Domestic Product (GDP). The overall impact on GDP growth in 2017 was assessed at –1.1% (SDG 1: No Poverty). The most affected sector was

54 IPCC Sixth Assessment Report.

55 https://www.nature.com/articles/s41597-022-01667-x.

56 *Climate Indicators and Sustainable Development: Demonstrating the Interconnections (WMO-No. 1271).*

housing (USD 79.6 million), with 95% of the houses on Barbuda damaged, 45% made uninhabitable and 28% required complete replacement. Tourism (USD 69.7 million) and transport (USD 29.1 million) were sectors that were also gravely compromised, hindering progress toward SDG 11 (Sustainable Cities). While the assessment contained several gaps, including the impact on biodiversity, it clearly illustrated the high level of vulnerability of Small Island Developing States (SIDS) to such disasters and the diverse impacts extreme events can have on development.

Overall, progress toward SDG 1 and SDG 7: Clean Energy were the most frequently reported as being hampered by extreme events. Impacts to SDG 15: Life on Land had the least responses, with several NSOs noting the difficulty in evaluating the impact of extreme events on areas such as biodiversity or ecosystem services. Values in the Figure below may therefore be more representative of data availability rather than true impact.

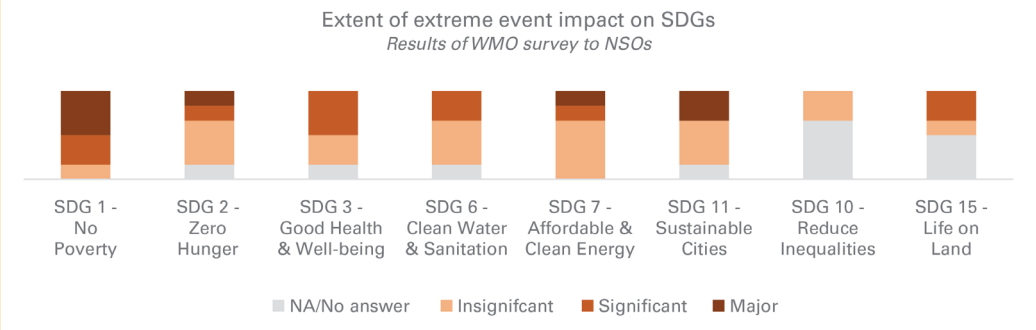

Figure 22. Results of WMO survey of NSOs on the extent of impact of select extreme events on the SDGs, with grey representing no impact or no answer, and colors increasing in shade based on levels from insignificant, significant to major.

DATA GAPS:

Unfortunately, multi-sectoral quantitative and qualitative analysis is not consistently done after every disaster, making it difficult to obtain a clear image of the overall impact to development. Several key data gaps and recommended areas for improved reporting therefore emerged from this project. First of all, for many NSOs, disaster data are often reported annually and not disaggregated by event, thereby presenting a challenge in attributing impacts to a single specific event. Additionally, it was found that in many cases the diverse components of the SDGs meant that different agencies across state, national and regional levels are responsible for housing different types of impact data, therefore requiring a collaborative effort between agencies to combine the data. Overall, the project found a need for high-quality, accessible, timely and reliable disaggregated impact data, and for strengthened international collaboration between NSOs and United Nations agencies.

Understanding how extreme events are impacting sustainable development is critical not only to support adaptation efforts, but also to serve as a basis for stronger climate action to mitigate worsening events in the future. WMO is committed to continuing efforts to improve understanding of the connections between climate and development, and will explore how future partnerships could guide the statistical community to standardize extreme event impact data as it relates to the SDGs.

In the subsequent sections on extreme events, data received from the case studies will be displayed in the following format: SDGs will be separated into categories of insignificant, significant, or major impact.

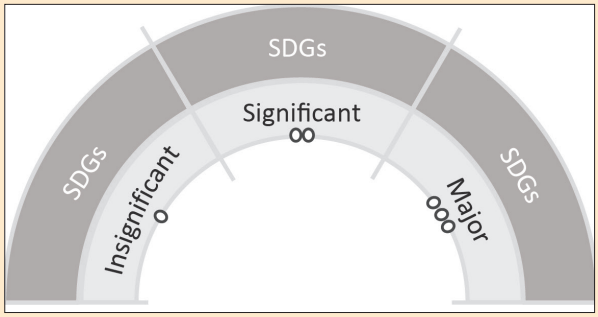

Figure 23. Example display of national survey on responses on the extent of extreme events on progress toward the SDGs.

EXTREME EVENTS: EXTREME HEAT

Extreme heat has been rising in almost all parts of the world, both by day and night.

Every year of the 2011-2020 decade had a frequency of extreme warm days and nights[57] well above the Global Historical Climatology Network Daily Dataset Extremes (GHCNDEX) 1961-1990 average of 10%. The occurrence of extreme warm days in the 2011-2020 period was approximately twice the 1961-1990 average in most of Europe, southern Africa, Mexico, parts of eastern Australia, and parts of south-east Asia.

Virtually every attribution study carried out on an extreme heat event in 2011-2020 found that the risk of the event increased significantly because of anthropogenic climate change. In a small number of cases, it was found that the event would have been virtually impossible in the absence of anthropogenic climate change.

Asia

India and Pakistan: Temperatures of up to 47 °C were observed in late May 2015 in eastern India and southern Pakistan, in coastal areas where such temperatures are rare, and were accompanied by high humidity. Over 4000 deaths were attributed to the extreme heat, mostly in the eastern Indian states of Andhra Pradesh and Telangana, and in and around Karachi. Very high temperatures were also registered on numerous occasions further west, with the Asian record of 54.0 °C being equalled twice during the decade: at Mitribah (Kuwait) on 21 July 2016 and Turbat (Pakistan) on 28 May 2017.

Europe

Western and Central Europe: A heatwave in late June 2019 set a French national record of 46.0 °C at Vérargues. The second, in the third week of July 2019, was more widespread, setting national records for Germany, the Netherlands, Belgium, Luxembourg and the United Kingdom. Paris-Montsouris (42.6 °C) and Uccle, near Brussels (39.7 °C) broke their previous records by 2.2 °C and 3.1 °C respectively. Northern and **Central Europe:** July 2015 saw extreme heat conditions in central Europe, with several records set, and (many subsequently broken in 2019). The year 2018 had another exceptionally hot summer, particularly in Scandinavia.

South-West Pacific

Australia: Extreme heat occurred on numerous occasions during the decade, most significantly during 2019. January and December 2019 were each the hottest on record. Australia's hottest area-averaged day on record was 18 December 2019, and 18 of the 22 days on which the Australian area-averaged maximum temperature has exceeded 40 °C since 1910 occurred in late 2018 or 2019.

Africa

South Africa: Repeated extreme heat in southern Africa during the summer of 2015-16, in the latter part of a severe drought associated with El Niño, culminated in a heatwave in early January 2016, which saw Pretoria (42.7 °C) and Johannesburg (38.9 °C) both surpass their pre-2015 records by more than 3 °C.

South America

South America: Numerous records were broken in Chile and parts of Argentina in the 2016-2017 and 2018-2019 summers. Santiago had its highest recorded temperature (38.3 °C) on 27 January 2019, breaking a record set in 2017, while on 4 February 2019, Rio Grande, Argentina (53.8 °S), became the world's southernmost location known to have had a temperature over 30 °C, with a reading of 30.8 °C.

57 Defined here as maximum/minimum temperatures above the 90th percentile for the time of year. Extreme cold days and nights are those with maximum/minimum temperatures below the 10th percentile.

Belgium, the United Kingdom, and the Netherlands were surveyed in order to understand the impact of heatwaves on national development. NSOs from the three countries reported differentiated impacts. Belgium identified a major impact to the economy (SDG 1), particularly due to heat-related mortality, with approximately 400 more deaths than average (SDG 3), a loss of crop production (SDG 2) and a significant drop in inland waterway transport. The United Kingdom identified a significant impact on SDG 1, citing 863 excess deaths in England over the summer 2018 period.[1] Finally, the Netherlands identified a significant impact on SDGs 3, 6, 7 and 15, citing known issues of heat-related mortality, water availability and disrupted ecosytem services during the heatwave.

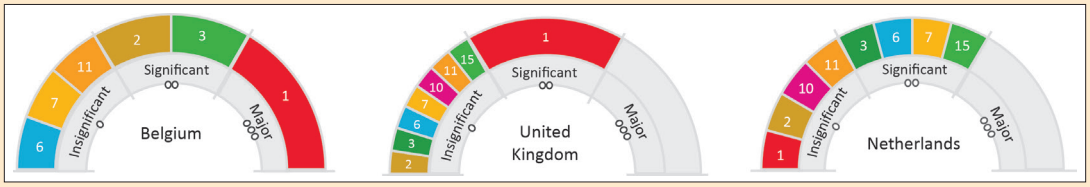

EXTREME EVENTS: EXTREME COLD AND SNOW

Extreme cold has become less frequent with warming global temperatures.

The frequency of extreme cold days and nights in the 2011-2020 period was about 40% below the 1961-1990 average, although this was only a modest reduction from 2001-2010. The year 2020 had the lowest frequency of extreme cold days on record, and 2016 had the lowest frequency of cold nights.

Attribution studies have mostly found that cold events would have been more likely in a pre-industrial climate than they were in the climate of the 2011-2020 decade.

North America

Central and eastern North America had notably colder winters in 2013-2014 and 2014-2015. February 2015 was plagued by an especially persistent cold spell, with temperatures that did not rise above freezing point during the month at locations such as Toronto, Montreal and Syracuse. There was also heavy snowfall in coastal areas. Boston had its heaviest seasonal snowfall total on record in 2014-2015. A severe snowstorm in January 2016 brought record snowfall totals for a single storm to several sites in the New York City area, including 77 cm at John F. Kennedy Airport. February 2019 was very cold in parts of western North America, with Vancouver experiencing its coldest February on record.

Asia

Abnormal levels of cold and snow affected many parts of **east Asia** in January 2016. Cold air penetrated as far south as Thailand, and snow occurred even in the southernmost parts of China, with Guangzhou experiencing its first snowfall since 1967. The temperature fell to 3.1 °C at the Hong Kong Observatory, its lowest temperature since 1957.

Europe

Over many parts of the **European continent**, a severe cold spell in the first half of February 2012 was the most significant cold spell since either 1985 or 1987, and, in some areas, since 1956, with temperatures over much of central Europe remaining continuously below freezing for two weeks or more. There was also heavy snowfall, particularly near the east coast of Italy where exceptionally cold air passed over the relatively warm waters of the Adriatic. Over 650 deaths across the continent were attributed to the cold weather. March 2013 was another rather cold month for the continent, and a major easterly outbreak of cold weather at the end of February 2018 brought extreme amounts of snow to the east coast of Ireland.

Figure 25. Ice build-up on the Lake Geneva shoreline during the February 2012 cold spell.
Source: WMO.

South America

One of the most extreme cold events of the decade occurred in **Argentina** in July 2017, when the temperature at Bariloche fell to –25.4 °C, 4.3 °C below its previous record.

South-West Pacific

A major cold outbreak in **south-eastern Australia** in August 2020 resulted in a temperature of –14.2 °C at Liawenee, a state record for Tasmania, and snow settled in central Launceston for the first time since 1921. A cold spell in **New Zealand** in June 2015 saw temperatures fall below –20 °C in parts of the interior South Island.

EXTREME EVENTS: TROPICAL CYCLONES

Tropical cyclones are still ranked among the most significant natural hazards, accounting for a large share of the decade's high-impact events both in terms of casualties and of economic losses.

The North Atlantic and North-east Pacific basins both had above average (1991-2020) tropical cyclone activity during 2011-2020, with a record number of named storms (30) in the North Atlantic in 2020. The north-west Pacific, the world's most active tropical cyclone region, was close to average. The southern hemisphere basins experienced reduced tropical cyclone activity in 2011-2020 compared to the average. The northern Indian Ocean was also close to average, despite a very active period in 2018-2020 with at least 4 cyclones of hurricane intensity per year.

No attribution study to date has found any climate change signal in the risk of occurrence or intensity of any given tropical cyclone. However, climate change signals have been found in rainfall associated with tropical cyclones, with studies of Hurricane *Harvey* (2017) and Hurricane *Dorian* (2019) in the North Atlantic, each finding that rainfall totals in those cyclones were higher because of anthropogenic climate change. Climate change has also been found to contribute to the risk of coastal inundation from storm surges, as in Hurricane *Sandy* that hit the north-eastern United States in 2012.

During the decade the Philippines experienced three out of four tropical cyclones, with over 1000 deaths: *Haiyan (Yolanda)* in 2013; *Washi (Sendong)* in 2011, and *Bopha (Pablo)* in 2012. *Haiyan (Yolanda)*, which was one of the most intense landfalls recorded anywhere in the world with 10-minute mean winds of 230 km/h and had the most devastating humanitarian impact of any tropical cyclone during the decade. More than 7,800 deaths were attributed to *Haiyan (Yolanda)*. *Washi (Sendong)* and *Bopha (Pablo)* both caused catastrophic damage from flooding.

Typhoon *Haiyan* affected hundreds of thousands of farmers, leading to an approximate 900,000-ton shortfall in rice production.[58] Heavy rainfall conditions harshly affected five cereal-producing regions where crop losses accounted for one-third of the total rice production in 2012. This left farmers in areas hit by the typhoon at severe levels of food insecurity.

Some 4.3 million people were internally displaced.[59] Six months on, more than 2 million people were still displaced.[60]

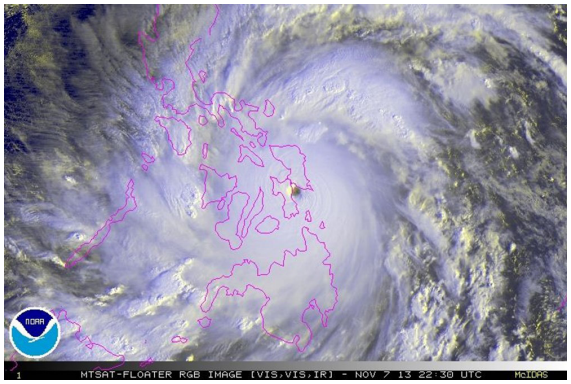

Figure 26. Satellite image of Typhoon Haiyan (Yolanda) as it made landfall near Tacloban, Philippines, at 22.30 UTC on 7 November 2013
Image: NOAA Office of Satellite and Product Operations.

58 Food and Agriculture Organization of the United Nations (FAO), 2013b. Farmers hit by Typhoon Haiyan need urgent assistance; FAO: Rome, 2013. Available at: https://www.fao.org/newsroom/detail/Farmers-hit-by-Typhoon-Haiyan-need-urgent-assistance/en

59 Philippines Disaster Response Operations Monitoring and Information Center (DROMIC).

60 Internal Displacement Monitoring Centre (IDMC), 2014. https://www.internal-displacement.org/sites/default/files/publications/documents/The-Evolving-Picture-of-Displacement-in-the-Wake-of-Typhoon-Haiyan.pdf.

Japan's most significant event of the decade was Typhoon *Hagibis* in October 2019. The adverse effects were due primarily to flooding from extreme rainfall, which included a daily total of 922.5 mm at Hakone in the foothills of Mount Fuji, a Japanese record. Ninety-six deaths were reported along with estimated economic losses of USD 18 billion,[61] the largest on record for a tropical cyclone outside the United States. There were also numerous devastating landfalls in China and on the Korean Peninsula during the decade.

Asia

India & Bangladesh suffered great damage by Cyclone *Amphan*, which made landfall in May 2020 and was the costliest tropical cyclone on record in the region, with reported losses of more than USD 14 billion. However, improvements in early warning systems and emergency preparedness meant that no cyclone in the region during the decade caused loss of life on the scale that had occurred on numerous occasions along the Bay of Bengal coast up until the 2000s.

Amphan damaged crops and affected household incomes. Impacts on non-rice crop losses were estimated to continue well into the following 5 to 7 years due to increased soil salinity from the tidal saline water inundations.[62] Overall, the cyclone disrupted the lives of 2.6 million people in Bangladesh and damaged more than 18,000 water points, 32,000ha of cropland, and about 18,000ha of aquaculture areas,[63] as well as causing terrible consequences in adjacent areas of India.

Some 2.4 million people were displaced in India and another 2.5 million in Bangladesh, mostly through pre-emptive evacuations. The displaced persons took refuge nearby, where they were dangerously exposed to future potential hazards.

South-West Pacific

Harold (2020) affected an estimated 65% of Vanuatu's population and caused significant damage in Fiji, Tonga and the Solomon Islands. *Winston* (2016) was the strongest cyclone on record to affect Fiji and caused major damage, especially along the northern coast of the island of Viti Levu, as well as in Tonga. *Yasi* (2011) was the most powerful tropical cyclone known in the Australian state of Queensland since 1918.

North America

The United States & Caribbean experienced a succession of severe tropical cyclones in 2017, of which the most significant were *Harvey, Irma,* and *Maria*. *Irma* and *Maria* reached Category 5 intensity, and *Harvey* reached Category 4. All of them caused at least USD 50 billion in economic losses in the United States. *Irma* damaged more than 90% of the buildings on Barbuda (see Box 2). *Harvey's* major impact was catastrophic flooding from heavy rainfall in coastal Texas, with total rainfall measurements of between 900 and 1200 mm in much of metropolitan Houston. *Maria* caused massive damage to Puerto Rico's infrastructure, leaving nearly half the island's population without power for three months or more, and almost 3,000 deaths indirectly attributed to the storm.

Damages from *Irma* and *Maria* in the Dominican Republic included the loss of over 7,500ha of rice crops. They also caused devastation to 5,000ha of banana farms and related irrigation systems,[64] and, in their aftermath, food shortages were prevalent in Antigua and Barbuda, Dominica, the British Virgin Islands, and Saint Maarten. In Dominica, *Irma* caused severe crop losses, and, in parts, entirely wiped out cultivations, destroyed forests, killed livestock, and disrupted traffic, which then impeded access to crop fields and markets. The agriculture sector alone suffered losses amounting to USD 380 million.[65] In total, losses in Dominica represented more than 200% of its GDP.

61 EM-DAT – The International Database

62 Kabir, M. et al. *Impact of Super Cyclone Amphan on Agriculture and Farmers' Adaptation Strategies in the Coastal Region of Bangladesh*, 2020.

63 IRFC, 2021. *Final Report Bangladesh: Cyclone Amphan*. Available at: https://reliefweb.int/report/bangladesh/bangladesh-cyclone-amphan-final-report-n-mdrbd024

64 Inter-American Institute for Cooperation on Agriculture (IICA), 2017. *Impacts of Hurricanes Irma and Maria in the Dominican Agricultural Sector.* Available at: https://iica.int/en/node/17467

65 United Nations Development Programme (UNDP), 2017. *Regional Overview: Impacts of Hurricanes Irma and Maria.* Conference Supporting document. Available at: https://www.undp.org/latin-america/publications/regional-overview-impact-hurricanes-irma-and-maria

Harvey, Irma and *Maria* displaced over 3 million people in the space of a month, mainly in the United States and a number of Caribbean islands, including Cuba, Dominica and Puerto Rico.

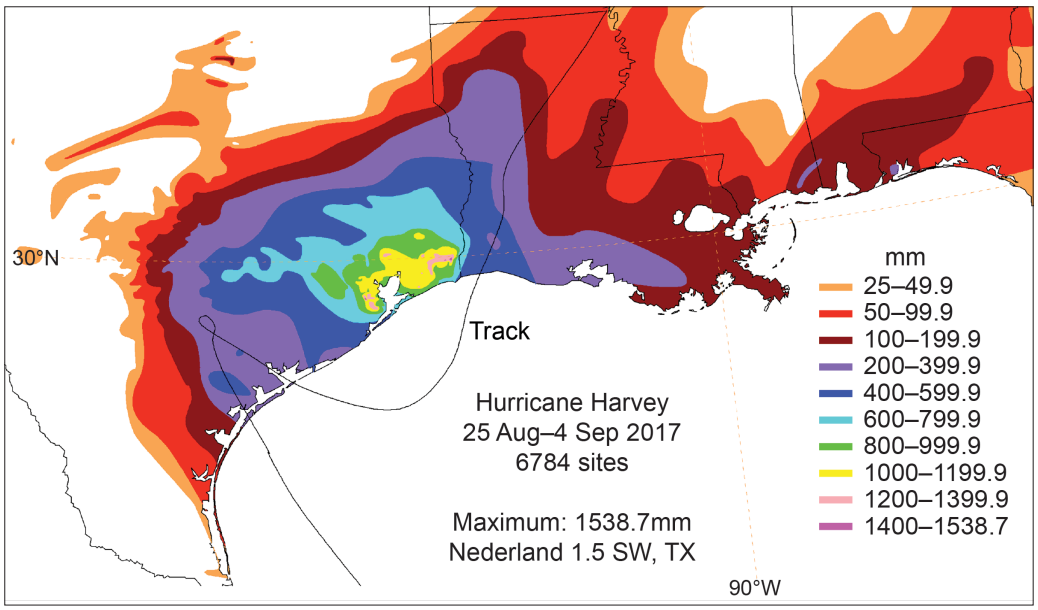

Figure 27. Hurricane *Harvey* associated rainfall.
Source: BAMS State of the Climate, 2017.

Outside the 2017 season, Hurricane *Sandy* caused severe storm surge flooding in and around New York City in 2012, with over 200 deaths reported in the **United States and the Caribbean**, and USD 85 billion in economic losses. Hurricane *Matthew* in 2016 was directly responsible for over 500 deaths in western Haiti, and exacerbated the pre-existing food security and disease issues there. In 2019 Hurricane *Dorian* brought widespread destruction to the Bahamas with reported economic losses totalling more than USD 3 billion.

North America

In 2020, Hurricanes *Eta* and *Iota*, which reached Categories 4 and 5, respectively, ravaged the entire territory of Nicaragua, affecting 3 million people and costing more than USD 738 million, an amount equivalent to 6.2% of the country's GDP.[66] Honduras also suffered significant damage.

The continuous torrential rains and strong winds triggered landslides that resulted in further crop damage and losses, severe damage to harvesters and production infrastructure, including processing facilities and drying patios.

Africa

Mozambique and Zimbabwe: The tropical cyclone causing the most impact in the South Indian Ocean region during the decade was Cyclone *Idai*, which made landfall in March 2019 with sustained winds of 105 kt, one of the most intense cyclones ever to make landfall on the east coast of Africa. Winds and storm surges caused major destruction in the landfall area, while heavy rain resulted in extensive flooding.

66 Ministerio del Ambiente y los Recursos Naturales (MARN). *Contribución Nacionalmente Determinada de Nicaragua*, 2020. Available at: https://unfccc.int/sites/default/files/NDC/2022-06/Contribuciones_Nacionales_Determinadas_Nicaragua.pdf

Idai and *Kenneth* were the strongest recorded storms in their respective landfall areas and triggered 640,000 and 45,000 displacements respectively.[67] *Idai* resulted in approximately 478,000 displacements in Mozambique and left millions in need of humanitarian assistance. More than 93,500 people were still displaced by the end of 2019.[68,69] At least 1,236 deaths were attributed to Cyclone *Idai*, making it the deadliest cyclone in the southern hemisphere for at least 100 years. Cyclone *Kenneth* struck just six weeks later, the first time on record that two cyclones had struck the region in such close succession.

IMPACT OF HURRICANE IRMA ON DEVELOPMENT:

Hurricane *Irma* had a devastating impact on the Caribbean. Antigua and Barbuda was among the worst hit and was therefore chosen as a case study for understanding the development impact of tropical cyclones. One of the major impacts cited was economic, given the fact that Hurricane *Irma* led to an approximate 1.1% loss of GDP (SDG 1). The tourism and infrastructure sectors suffered the gravest impact, and this hindered the country's progress toward SDG 11. According to a joint assessment[70] conducted by the Government of Antigua and Barbuda, the EU and the World Bank, the combined damage and loss estimate for the infrastructure sector was approximately USD 21 million. The housing sector was also significantly affected, with 95% of houses damaged on Barbuda, and 45% left uninhabitable (SDG 10). Minor damage was also reported to the agriculture, health, and water sectors (SDGs 2, 3, and 6).

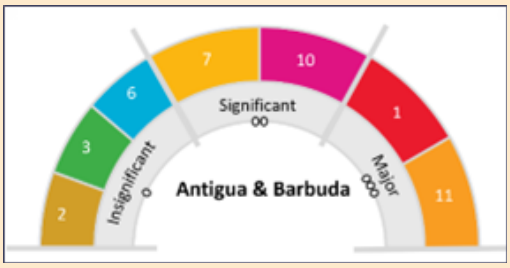

Figure 28. Extent of impact of Hurricane *Irma* on SDG progress in Antigua & Barbuda

67 Internal Displacement Monitoring Centre (IDMC), *GRID* 2020.

68 International Organization for Migration (IOM)- Internal Displacement Monitoring Centre (IDMC), 2019. Eight months after Idai.

69 UNHCR, 2019. UNHCR Response in Mozambique, Malawi and Zimbabwe. https://reporting.unhcr.org/sites/default/files/UNHCR%20Tropical%20Cyclone%20Idai%20Response%20Update%20-%20June%202019.PDF.

70 Antigua and Barbuda Executive Summary (gfdrr.org)

EXTREME EVENTS: EXTREME RAINFALL AND FLOODS

Extreme rainfall and flooding created a significant natural hazard at a range of timescales, causing billions of dollars worth of damage, thousands of deaths and the displacement of millions of persons in the decade 2011-2020.

The relationship between extreme rainfall and anthropogenic climate change is complex. Warmer air can hold more moisture than cooler air, at a rate of approximately 7% per °C of warming. However, anthropogenic climate change can also influence the occurrence of weather systems favourable to heavy rainfall, making them more likely in some parts of the world and less likely in others. Combining these influences, extreme rainfall has become more likely over time in many parts of the world, particularly in middle and higher latitudes of the continents of the northern hemisphere, but in some other parts of the world no significant change has yet become evident in observations.

The results of attribution studies for extreme rainfall events reflect this complexity. Nonetheless, an increasing number of studies are finding a climate change influence on particular extreme rainfall events, reflecting both the emergence of climate signals over time and the improved capability of climate models to represent events occurring over small areas. Some events still show no significant climate change signals, and in a few cases, such as the 2020 Yangtze River floods, studies have found that the weather patterns driving the floods have less, rather than more, likely due toanthropogenic climate change.

Thailand, Cambodia, and the Lao People's Democratic Republic experienced widespread inundation following major flooding in the Mekong and Chao Phraya basins in late 2011, driven by persistent above-average rainfall throughout the monsoon season. Large areas of Bangkok were inundated from October until early December. Economic losses were estimated to exceed USD 40 billion, and over 1000 deaths were reported across the three countries.

Asia

China experienced significant monsoon season flooding on numerous occasions, with the Yangtze River and its tributaries particularly affected in 2016 and 2020.

Throughout 2016, the Chinese Ministry of Civil Affairs reported that 23 million people were affected by the heavy rains, and that there were close to 3.8 million evacuations.

In October and November 2020, eight tropical cyclones or depressions in five weeks brought severe flooding to **Vietnam**, with Hué receiving 2615 mm rainfall for the month of October, including over 1800 mm in a single week. **India** had the worst single flooding episode in a monsoon season in June 2013, when heavy rains, mountain snowmelt and glacial lake outbursts led to extreme flooding and landslides in Uttarakhand—killing more than 5800 persons. Kerala was badly affected by floods in 2018, and in 2019 and 2020, India's two wettest monsoon seasons in the previous 25 years saw intense and widespread flooding. Over 2000 flood-related deaths were reported in India and neighbouring countries. **Pakistan** experienced significant flooding in 2011 and 2012.

Africa

In **the Sahel**, the year 2020 was marked by severe flooding, with an especially active monsoon season. The early months of 2020 were particularly wet in much of East Africa. Record levels of precipitation were observed in Lake Victoria, the Niger River at Niamey (Niger) and the Blue Nile at Khartoum (Sudan). Two hundred and eighty-nine deaths were reported in Kenya and 156 in Sudan.

High precipitation and abnormal vegetation growth created favorable conditions for the feeding, breeding and proliferation of desert locusts and, consequently, the worst swarm infestation in

70 years, in Kenya, and the previous 25 years in Ethiopia and Somalia.[71] Efforts to mitigate the devastating impacts on agriculture did not prevent up to 2.5 million people from being affected in 2020.[72]

Intense flooding in Somalia affected 540,000 people, 370,000 of whom were displaced,[73] and in South Sudan flooding affected approximately 200,000 people, including refugees and host populations.[74] Overall, floods triggered around 2.5 million internal displacements across sub-Saharan Africa in 2019.

Yemen's humanitarian crisis was aggravated by devastating floods and storms during two intense rainy seasons between February and September 2020.

Disasters resulted in 223,000 new displacements in 2020, the highest figure on record for Yemen. Floods caused widespread destruction, killed hundreds of people, and forced thousands of internally displaced persons (IDPs) to again flee, which highlights the impacts of overlapping disaster and conflict.[75] The vast majority of Yemen's IDPs live in makeshift settlements, putting them at high risk of secondary displacement when disasters strike.[76]

The Sahel experienced a number of other significant monsoon seasons during the decade with associated flooding in the Niger River and its tributaries, particularly in 2012, following a period of severe drought, 2016 and 2018. Extreme rainfall in **Sierra Leone** in August 2017, when Freetown received 1459 mm of rain in the first two weeks of the month, contributed to a landslide on 14 August in which more than 500 lives were lost.

South America

In **Brazil**, over 900 people were killed in a landslide associated with heavy rains north of Rio de Janeiro in January 2011. Major flooding in the Paraná basin in mid-2014 resulted in significant population displacement, particularly in Paraguay.

Storms, the second most destructive disaster that affects agriculture in the Latin American and Caribbean region, just behind drought, have increased in frequency, thereby inflicting loss and damage to agriculture and livestock production to the tune of USD 6 billion between 2008 and 2018.[77]

South-West Pacific

Eastern Australia experienced frequent and extensive flooding associated with La Niña in 2011 and early 2012, with Brisbane having its highest flood levels since 1974 in January 2011.

Europe

Switzerland, Austria, and Germany had upper catchment rainfalls locally in excess of 400 mm between 29 May and 3 June 2013, resulting in major flooding in the Danube and Elbe catchments leading to severe economic impacts.

---

71 World Meterological Organization (WMO). *State of the Climate in Africa 2021*; WMO: Geneva, 2021. Available at: https://library.wmo.int/records/item/58070-state-of-the-climate-in-africa-2021

72 Food and Agriculture Organization of the United Nations (FAO). Desert Locust Upsurge. *Progress report on the response in the Greater Horn of Africa and Yemen.* FAO: Rome, January-April 2021. Available at: https://www.fao.org/documents/card/en/c/cb7161en

73 Reliefweb, https://reliefweb.int/sites/reliefweb.int/files/resources/Situation%20Report%20-%20Somalia%20%20-%2017%20Nov%202019.pdf

74 United Nations High Commissioner for Refugees (UNHCR). https://www.unhcr.org/news/briefing/2019/10/5da977fe4/.

75 International Organization for Migration (IOM). *Yemen Covid-19 response update (26 July- 8 August).* 14 August 2020; Shelter Cluster, Second Flash Update: Flooding in Yemen. 10 August 2020; Al Jazeera News: *At least 172 killed in Yemen flash floods this month.* 12 August 2020; International Committee of the Red Cross (ICRC). Yemen: Torrential floods. Available at: https://www.icrc.org/en/document/yemen-torrential-floods-wreak-havoc-war-stricken-country. Accessed: 13 April 2021.

76 Shelter Cluster. *Impact Monitoring Report for the Shelter Cluster Programs, Yemen 2019.* July 2019; IOM. Shelter NFI Winterization Activities, December 2019-February 2020. 13 April 2020; Shelter Cluster. *Yemen Shelter Typologies.* October 2020.

77 FAO. *The impact of disasters and crises on agriculture and food security.* FAO: Rome, 2021. Available at: https://www.fao.org/3/cb3673en/cb3673en.pdf

EXTREME EVENTS: DROUGHT

Droughts during the 2011-2020 decade had major socioeconomic and humanitarian impacts.

Droughts occur on longer timescales than most of the other extreme events considered in this report. According to the self-calibrating Palmer Drought Severity Index,[78] which incorporates both precipitation and temperature indicators, over most of the decade, about 10% of the world's land surface was assessed as being under severe or extreme drought conditions, similar to the 2001-2010 decade, but higher than typical pre-2000 values.

Attribution studies of droughts have shown mixed and index-dependent results, with stronger attribution found for evapotranspiration-based indices than for precipitation-based indices. A significant climate change signal has also been found for some droughts where mountain snowpack, and the lack thereof, is a relevant component. In the Greater Horn of Africa, studies of several droughts, notably in 2017, found that anthropogenic climate change had contributed to sea surface temperature patterns, particularly warming in the western Pacific, which increase the risk of drought in the region.

The Greater Horn of Africa region was severely affected by droughts during the decade. Drought beginning in the second half of 2010 and extending into mid-2012 contributed to one of the most significant humanitarian crises of the decade in Somalia.

The prolonged dry period between late 2010 and early 2012 resulted in the poorest harvest since the 1992-1993 famine.[79] This situation led to 8 million people suffering from high levels of acute malnutrition in Djibouti, Kenya, Ethiopia, and Somalia.[80] Livestock deaths and sky-rocketing food prices made it increasingly difficult for poor households to feed themselves. Estimates suggest that 258,000 Somalis died due to severe food insecurity and famine.

Soaring food prices and interlocking regional conflict exacerbated vulnerabilities while restricting human mobility and humanitarian access. Some 13 million people were affected, and hundreds of thousands were displaced across southern Ethiopia, south-central Somalia and northern Kenya. Reliable displacement numbers do not exist as no proper drought displacement monitoring was in place in 2012.

The region was again significantly affected by drought between 2016 and 2017.

In Somalia, more than 850,000 displacements were recorded in 2017, following the 2016-2017 drought that brought the country to the brink of famine. The scarcity of safe drinking water led to outbreaks of Acute Watery Diarrhea /Cholera resulting in around 800 fatalities.[81,82] Significant displacement also occurred in 2018.

In 2015 **Ethiopia** experienced its worst drought in decades, which was marked by a strong El Niño phenomenon affecting about 10 million Ethiopians.

78 Bulletin of the American Meterological Society (BAMS). *State of the Climate.*

79 FAO. *Mortality among populations of southern and central Somalia affected by severe food insecurity and famine during 2010-2012;* FAO: Rome, 2013. Available at: https://www.fao.org/publications/card/fr/c/be225a03-c4e6-4b65-90aa-d6386c27997a/

80 FAO. *Drought in the Horn of Africa threatens millions*; FAO: Rome, 2011. Available at: https://www.fao.org/news/story/en/item/80157/icode/

81 Global Facility for Disaster Reduction and Recovery (GFRDD). 2018. https://www.gfdrr.org/en/somalia-drought-impact-and-needs-assessment-and-resilient-recovery-framework.

82 Internal Displacement Monitoring Centre (IDMC). *Global Report on Internal Displacement – 18 (GRID18)*

The impacts were particularly important during the *Kiremt* season, extending from June to September, which is the peak rainy season in large parts of Ethiopia. In the most affected areas of the country up to 75% of crop production was reported lost, one million livestock were reported dead, and about 435,000 people were estimated as suffering from severe acute malnutrition.

Africa

Southern Africa was badly affected by drought following poor rainy seasons in the 2014-2015 and the 2015-2016 periods due to the El Niño phenomenon, while three successive dry years from 2015 to 2017 in the Cape Province of South Africa resulted in critical water shortages during the first half of 2018 in Cape Town and surrounding areas. The driest calendar year on record as an average for South Africa was 2015.

The 2015-2016 agricultural season in Southern Africa was the driest in 35 years, and this affected a region in which the livelihood of 70% of the population was reliant on agriculture. The two and, in some cases, three consecutive years of meteorological drought, intensified by El Niño, left about 40 million people in a precarious position in terms of food security; a 9.3 million-ton shortfall in regional crop production; more than 643,000 livestock deaths, all of which necessitated a USD 109 million emergency response running up to mid-2017.[83]

South & Central America

Droughts associated with the 2015-2016 El Niño episode were significant in many other tropical and subtropical areas, including Indonesia; the Amazon Basin and north-east Brazil; Central America, north-west South America and the Caribbean, and parts of India. In **India** itself, drought was declared in 11 of its 28 states, leading to severe food and water insecurity; the situation was exacerbated by inequalities in water availability and access to its supply.

Due to substantial crop failures (between 10% and 100% in the districts surveyed) the drought increased the reliance of households on India's Public Distribution System (PDS) for access to staple food grains. During this drought event, 82% of households in affected areas were at risk of food insecurity.[84]

Central Chile experienced below-average rainfall every year of the decade. The year 2019, when Santiago received only 82 mm rainfall (less than 25% of the average), was the country's worst single year. Later in the decade, drought also extended to subtropical South America east of the Andes, particularly in the 2017-2018 summer season and in 2020. A two-year drought that struck Haiti in 2016 caused a 60% drop in agricultural production, compared to 2013.

The compounded effect of drought, political, and economic instability caused a spike in food prices, forcing millions of Haitians into food insecurity. According to the United Nations Office for the Coordination of Humanitarian Affairs (OCHA,) in mid-2016, 600,000 farmers were affected by drought and up to 1.5 million people were severely plagued by food insecurity.[85]

North America

While La Niña contributed to heavy rainfall in some parts of the world, it was a major driver for drought in the south-central **United States** in 2011 and 2012. Texas experienced its second-driest year on record in 2011, with record low annual rainfalls also observed in some northern Mexican states. Over the longer term, California had its driest four-year period on record from October 2011 to September 2015 with rainfall 30% below the 20th century average.

South-West Pacific

Drought extended from **southern Australia** to cover large parts of the continent between 2017 and 2019, particularly in 2019 which was Australia's driest year on record. In parts of northern inland New South Wales, annual rainfall in 2019 was more than 70% below the 1961-1990 average and more than 40% below previous record lows. Dry conditions were particularly severe in the second half of the year and contributed

83 FAO. *Southern Africa. Situation report – September 2016*; FAO: Rome, 2016. Available at: https://www.fao.org/3/br082e/br082e.pdf

84 United Nations Children's Fund (UNICEF). *When Coping Crumbles. Drought in India 2015-16. A Rapid Assessment of the Impact of Drought on Children and Women in India.* 2016.

85 United Nations Office for the Coordination of Humanitarian Affairs (OCHA). 2016. *Haiti: Drought Snapshot.* July 2016. Available at: https://reliefweb.int/report/haiti/haiti-drought-snapshot-july-2016.

to extensive wildfire activity, while water storage levels in the northern Murray-Darling Basin dropped to below 6% of capacity at their lowest point in early 2020.

Northern and central Europe experienced significant drought on several occasions during the decade. Among st the most significant drought years was 2018. Latvia had its driest year on record, Stockholm (Sweden) its driest since 1892, and Czechia and Uccle (Belgium) their second driest. Conditions were especially dry between April and September, leading to major agricultural losses and significant disruptions to river transport and industry as major rivers, particularly the Rhine, fell to critically low levels.

Frequent hot and dry weather conditions from 2018 to 2020 had significant agricultural impacts, with drought losses at EUR 9 billion annually. As rain-fed agriculture still plays a dominant role in Europe, irrigation systems had negligible effect and between 39% (boreal region) and 60% (Mediterranean region) of the drought-related losses concerned agriculture. As a result, sharp decline in crop productivity for major yields such as wheat, grain, maize, and barley were reported during the 2018-2020 dry summer and heatwave events.[1]

IMPACT OF DROUGHT ON DEVELOPMENT IN SOMALIA AND COLOMBIA

According to the Somali National Bureau of Statistics, the 2010-2012 drought led to "devastating and repeated loss of lives, livestock and crops", and therefore had a major impact on progress toward SDGs 1 and 2. The drought coincided with a drop in humanitarian assistance and a spike in food prices, leading to a famine that claimed the lives of 258,000 people between October 2010 and April 2012, including 133,000 children under the age of 5.[86] Additionally, despite copious investments in the water and sanitation sector, access to safe and adequate water supplies in Somalia remains a challenge. Pre-existing water shortages were exacerbated by the drought, which consequently increased water contamination, and therefore had a significant impact on health, water resources and ecosystems (SDGs 3, 6, & 15).

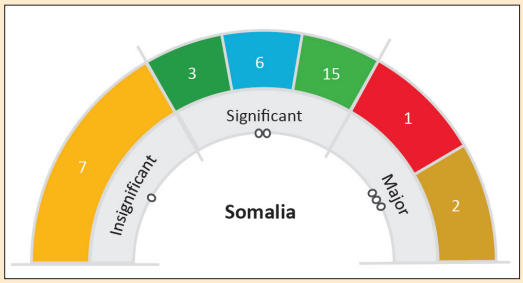

Figure 29. Extent of impact of drought on SDG progress in Somalia.

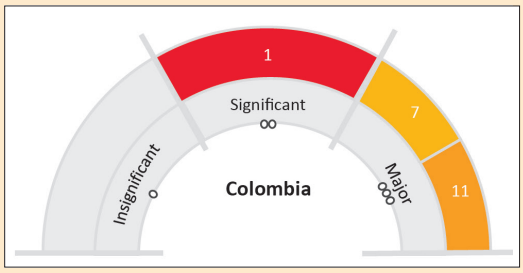

Figure 30. Extent of impact of drought on SDG progress in Colombia.

Colombia experienced a record-breaking mega-drought from 2015 to 2016. Given that over 70 % of Colombia's power mix at that time came from hydropower plants,[87] the drying up of rivers during the drought had a major impact on energy provision and infrastructure, particularly of aqueducts (SDGs 7 & 11). More than 300,000 people were affected by the drought, significantly impacting progress toward SDG 1. Additionally, in 2018, the percentage of people without access to clean water rose to nearly 8%, due at least in part to the direct and indirect effects of the drought (SDG 6). However, individuals were not the only ones affected—glacial mass loss was also higher than average from 2015 to 2017.

86 Mortality among populations of southern and central Somalia affected by severe food insecurity and famine during 2010-2012.

87 Landscape matters: Insights from the impact of mega-droughts on Colombia's energy transition - ScienceDirect.

EXTREME EVENTS: WILDFIRES

While not strictly a weather or climate phenomenon, wildfires are strongly influenced by atmospheric conditions and had devastating impacts throughout the decade on infrastructure, health, and ecosystems.

The principal impact of anthropogenic climate change on dangerous fire weather (involving a combination of some or all of low humidity, strong winds, low antecedent moisture and high temperatures) has occurred in the mid-latitudes, where increased temperatures and, in some places, reduced rainfall, has widely contributed to an increase in the number of days with dangerous fire weather, and a prolongation of the fire season. In some higher-latitude regions, such as Alaska, increased vegetation growth in a warmer climate has also led to the increased availability of fuel. Climate change influences are less clear on fire occurrence in the tropics, where non-climatic influences, such as fires lit in association with land-clearing, are also important.

Most published attribution studies for extreme fire weather events have found that anthropogenic climate change has increased the risk of these events, although in some cases no significant signal was found. Most studies have considered fire weather indices as an integrated variable. More detailed studies were carried out on fires in eastern Australia in 2018 and in the 2019-2020 period. Both found a climate change influence on the temperature component of fire weather, which was sufficient to generate a detectable influence on fire weather indices, but no significant signal for wind speed or antecedent drought.

North America

Western **North America** experienced numerous severe wildfire seasons during the decade, particularly in the latter half, as long-term drought in many areas contributed to the drying of fuels. The most destructive single event was the Camp Fire in California in November 2018, which largely destroyed the town of Paradise with a loss of 85 lives, the largest casualties in a wildfire in North America for over 100 years. Total losses for the 2018 **United States** wildfire season were estimated at USD 24 billion, the most on record for any season, while in western **Canada**, 2018 and 2017 were the two most active wildfire seasons on record, in terms of area burned, in British Columbia. 2020 was also a severe wildfire season in western North America. In 2016, fires destroyed large areas of the city Fort McMurray in Alberta, with insured losses of USD 3 billion, the costliest natural disaster on record in Canada. In eastern North America, a region rarely affected by destructive wildfires in modern times, a flash drought in the autumn of 2016 contributed to a fire in Gatlinburg, Tennessee, with 14 deaths and over 2500 buildings destroyed.

South-West Pacific

Eastern **Australia** experienced an exceptional fire season in 2019-2020, in the latter months of a severe drought. There were major fires throughout the period from early September 2019 to mid-February 2020, with some individual fires burning for two months or more; the worst losses occurred in the final days of December when there was widespread destruction in coastal towns in southern New South Wales and far eastern Victoria. At one point fire was raging almost continuously, with one small gap, from Bundanoon (New South Wales) to Bairnsdale (Victoria), over 500 kilometres, and a total of over 70,000 square kilometres of forest was burned. Thirty-four deaths were attributed directly to the fires with over 3,500 buildings destroyed, while over 400 deaths were attributed to persistent smoke pollution which badly affected centres including Canberra and Sydney for several weeks. There were also major ecological impacts.

The unprecedented bushfire season in Australia triggered 65,000 displacements, almost three-quarters of them in the first two months of 2020. Most of these displacements were in the form of pre-emptive evacuations, whereby the population was alerted through various early warning systems.[88]

88 ABC News. *SMS alerts urge north-east Victoria residents to evacuate.* 2 January 2020; Government of Australia, *National Emergency Alert Warning System.* Available at: https://www.emergencyalert.gov.au/. Accessed: 19 April 2021.

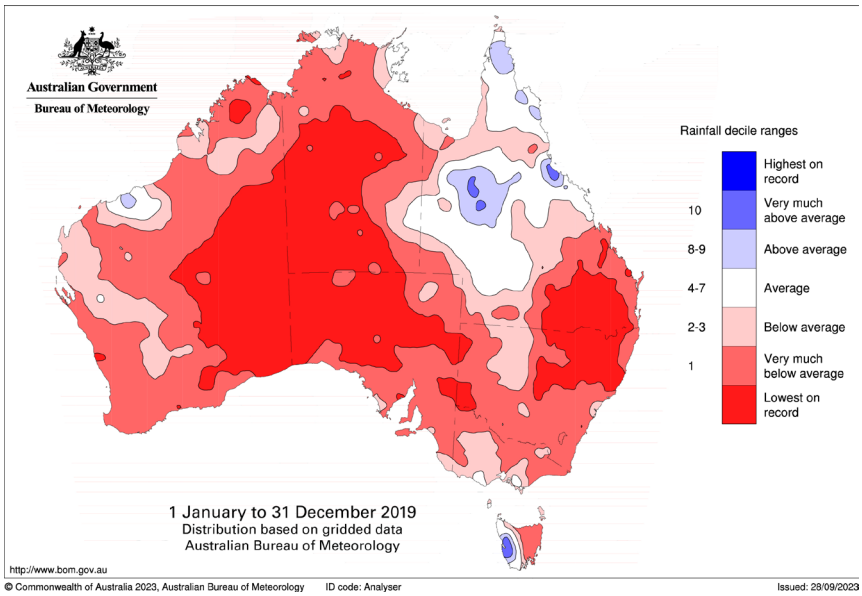

Figure 31. Rainfall map of Australia for 2019 showing record low rainfalls in many areas.
Source: Australia Bureau of Meteorology.

There were extensive wildfires, to which drought associated with El Niño was a major contributor, on the islands of Sumatra and Borneo during the second half of 2015. The area of land ravaged by fires within **Indonesia** extended to 6,000 square kilometres.

South-West Pacific

The damage and loss of agriculture and forest lands during the 2015 agricultural and land-clearing fires in **Indonesia**, exacerbated by an El Niño event due to extreme dry conditions,[89] were estimated between USD 8.7 to 9.4 billion,[90] and these losses were compounded by increased carbon emissions, smoke pollution, and related deaths from decreased air quality.[91]

Smoke pollution had health impacts and other disruptive effects throughout the region, particularly in **Indonesia, Malaysia,** and **Singapore**. Over 500,000 smoke-associated respiratory conditions were reported in Indonesia between July and October 2015, and subsequent studies found an excessive mortality rate from such illnesses in the region.

South America

Chile had an exceptional wildfire season in 2016-2017, after an April 2014 fire had already caused major losses in parts of the city of Valparaiso. The 2015 season was also serious for the Amazon basin with a record number of fires in Amazonas state, **Brazil** – although, ultimately, overall fire activity in the Amazon region for the decade was lower than in the period running from 2001 to 2010. Further south however the severe 2020 drought contributed to extensive fires in the Pantanal wetlands.

Europe

Southern Europe was badly affected by wildfires in several years during the decade. The year 2017 was especially severe, marked by the burning of over 10,000 square kilometres throughout the European Union, the mos since annual records began in 2006. Over 100 deaths were reported in two separate outbreaks of fire in **Portugal** and north-western **Spain** in June and October. The October fires were driven by strong winds associated with Hurricane *Ophelia* that passed to the west. Severe winds also contributed to the rapid spread of a fire near Athens, **Greece** in July 2018, in which 99 lives were lost, the highest number of direct casualties from a wildfire globally during the decade. Elsewhere, at higher latitudes there were reports of extensive fires in parts of Siberia in 2019 and most notably, in 2020. These occurred during periods of abnormal heat, rising to the exceptional temperature of 38.0 °C at Verhojansk, Russian Federation, the highest ever recorded north of the Arctic Circle.

89 Koplitz, S.N. et al. Public Health Impacts of the Severe Haze in Equatorial Asia in September–October 2015: Demonstration of a New Framework for Informing Fire Management Strategies to Reduce Downwind Smoke Exposure. *Environmental Research Letters* **2016**, 11.

90 Kiely, L. et al. Assessing Costs of Indonesian Fires and the Benefits of Restoring Peatland. *Nature Communications* **2021**, 12 (1), 7044.

91 Field, R. D.; Van Der Werf, G. R.; Fanin, T. et al. Indonesian Fire Activity and Smoke Pollution in 2015 show Persistent Nonlinear Sensitivity to El Niño-induced Drought. *Proceedings of the National Academy of Sciences* **2016**, 113 (33), 9204-9209.

EXTREME EVENTS: EXTRATROPICAL AND LOCAL SEVERE STORMS

Extratropical windstorms and severe thunderstorms have major impacts at the local level, causing billions of dollars in damage between 2011-2020.

Storms can lead to flash floods, hailstorms, severe winds, and tornadoes. Hailstorms alone can cause particularly heavy economic losses, as was the case when several events during the decade affected relatively small areas, but which still resulted in damage close to, or exceeding, USD 1 billion.

In general, there is no clear evidence of an observed climate change signal in these events, and no study of any specific event of this type has found a significant change in its risk level with anthropogenic climate change.

North America

The 2011 **United States** tornado season was one of the most active on record, including six Category 5 tornadoes on the Enhanced Fujita (EF) scale, the most in a single year since 1974. One hundred and fifty-seven lives were lost in Joplin, Missouri in May, the greatest loss of human lives by a single tornado in the United States since 1947, and 551 persons in total, the most since at least 1950. Over USD 28 billion in damage was attributed to tornadoes during the season. However, most other years during the decade, except for 2017 and 2019, had tornado statistics below the 1991-2020 average. Another notable severe weather event in the United States occurred in August 2020, when a *derecho* (a fast-moving line of severe winds) extended over more than 1000 km from Iowa to Ohio, with wind gusts exceeding 160 km/h over a wide area. There was widespread wind damage, particularly to mature crops, with a total estimated loss, mainly agricultural, of USD 12.5 billion.

Asia

In **China**, a tornado in Yancheng, Jiangsu province, in June 2016 caused the deaths of at least 99 persons, and proved to be one of the most destructive tornadoes on record in China.

Europe

Several windstorms affected northern and western Europe during the decade, although no single storm was as significant or destructive as some of the largest ones of the previous decades. The 2013-2014 winter season was especially active, with a sequence of major storms that brought the **United Kingdom** its wettest winter on record, significant wind damage and coastal erosion in places. Storm *Alex* in October 2020 had wind gusts of up to 186 km/h in western **France** and resulted in the wettest area-averaged day on record for the United Kingdom. It also contributed to extreme rainfall near the French-Italian border, with 24-hour rainfall totals exceeding 600 mm in **Italy**; 500 mm in France, and 400 mm in southern **Switzerland**, resulting in flash flooding in all three countries. In late October 2018, an intense low-pressure system created wind gusts exceeding 160 km/h in Italy and **Slovenia**; three days of rainfall exceeding 400 mm in Italy, Slovenia, **Austria**, and southern Switzerland, and damaging winds that extended as far north as **Poland**. Thirty deaths in Italy were directly attributed to the storm. Mediterranean storms, *medicanes*, with tropical-cyclone properties occurred on several occasions: two systems, in September 2018 and September 2020, respectively, caused significant wind damage on landfall in western Greece after initially bringing heavy rains and flooding to **Tunisia** and **Libya**.

Africa

Figure 32. Aerial image of the path of damage caused by the Joplin tornado in May 2011. Image source: NOAA.

Impacts on Human Systems

- Many of today's crises are shaped by a complex mix of climate and environmental change, disaster risk, conflict, and displacement.
- Weather-related events were responsible for nearly 94% of all disaster displacement recorded over the last decade.

FOOD SECURITY: REACHING SDG 2 "ZERO HUNGER"

The distance towards many of the SDG 2 targets grows wider each year, even though the time remaining for reaching the 2030 target date for the SGDs is narrowing.[92] The hurdles to addressing SDG 2 are reflected in the increasing prevalence and number of undernourished populations over the past two decades. While the new millennium began with a significant decline in the prevalence of undernourished persons at the global level, from 13.1% to 8.6% between 2001 and 2010, this trend remained stagnant over the following decade (2011-2020) and increased to 9.3% by 2020. The Sub-Saharan Africa and southern and central Asia regions witnessed the increase of undernourishment rates to 22.7 and 15.4%, respectively, by 2020.[93]

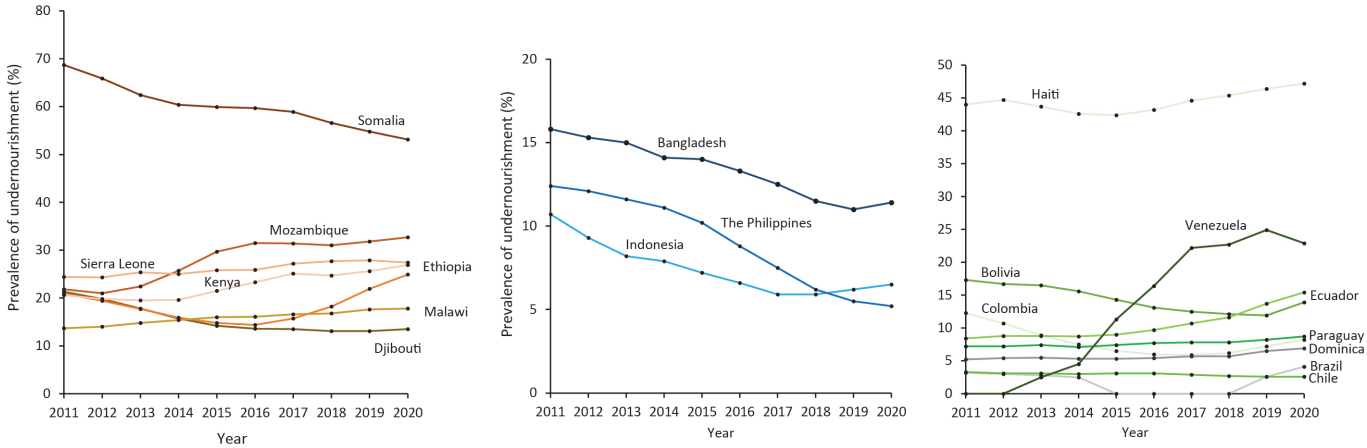

Figure 33. Prevalence of undernourishment rates (as %) in countries studied in Africa (left), Asia (center) and Latin and Central America, and the Caribbean (right) between 2011 and 2020
Source: FAO (2022).

These figures underscore a backward trend in the progress of global efforts to end hunger, food insecurity, and malnutrition. The achievement of SDG 2 is tightly linked to climate risk management, particularly along the agri-food value chain. For example, heat-stress conditions could result in food losses at the production stage and weather-related hazards such as landslides caused by heavy rains may affect road infrastructure, hindering transportation and access to markets, which then results in food spoilage and waste. Thereby, all four pillars of food security (access, availability, utilization, and stability) have been threatened by intensified extreme weather hazards over the 2011-2020 period, and will subsequently affect the achievement of SDG 2 targets by 2030.

92 FAO, IFAD, UNICEF, WFP and WHO. *The State of Food Security and Nutrition in the World 2022. Repurposing food and agricultural policies to make healthy diets more affordable;* FAO: Rome, 2022.

93 FAO. *Sustainable Development Goals. Indicator 2.1.1-Prevalence of undernourishment;* FAO: Rome, 2022. Available at https://www.fao.org/sustainable-development-goals-data-portal/data/indicators/2.1.1-prevalence-of-undernourishment/en

Impacts on Human Systems

DISPLACEMENT AND MIGRATION: COMPOUNDING RISKS TO SDGS

Weather-related events were responsible for nearly 94% of all disaster displacements recorded over the last decade[94] with an annual average of 22.1 million internal displacements triggered by weather-related hazards between 2011 and 2020.[95] Flooding was the major cause of internal displacements from such hazards, with 123 million displacements, followed by storms as the second contributor, at 86 million.[96]

Many of the largest scale displacement events took place in Asia, including countries with high population densities such as China, India, and the Philippines.[97] Millions more have been forced from their homes by drought, coastal erosion, rising sea levels, desertification, and other slow-onset events. It is essential to gather better data and to deepen our understanding on displacement in these contexts, on the interaction of sudden- and slow-onset hazards and the interplay with conflict and fragile situations. We also lack comprehensive data on cross-border displacement, which is often due to multiple factors and occurs in complex situations involving other drivers, notably, but not limited to, conflict or violence.

Resilience to climate-related disasters, environmental degradation and displacement is often lowest in places affected by conflict. Many of the current crises are shaped by a complex mix of climate and environmental change, disaster risk, conflict and displacement. Adding to the multiple risks already faced by displaced people, the impacts of hazardous weather-events and changing climatic conditions are disproportionately experienced by people in vulnerable situations, including refugees, internally displaced persons, returnees and stateless persons. Settlements of refugee and internally displaced persons (IDP) are often located in areas prone to climate-related hazards, while access to life-saving information and support that would strengthen their resilience and preparedness for further shocks is often limited.[98] When disasters strike, camps and informal urban settlements, IDPs, and refugees are often forced into secondary displacement, potentially trapping them in a downward spiral of vulnerability and risk.[99]

Combined with other drivers, the impacts of disasters and anthropogenic climate change have jeopardised development gains and the attainment of most Sustainable Development Goals. In particular, persons displaced by anthropogenic climate change and disasters, and their host communities, are often vulnerable to certain risk, as follows: loss of livelihoods, which entrenches poverty (SDG 1) and hunger (SDG 2); direct threats to their lives and well-being (SDG 3); widened inequality gaps (SDG 10), and limited access to quality education (SDG 4), water and sanitation (SDG 6), as well as clean energy (SDG 7). Due to pre-existing gender and socio-economic inequalities compounding their vulnerabilities, women and girls are among the worst affected (SDG 5).[100] With the acceleration of adverse effects due to anthropogenic climate change, it is therefore increasingly important to secure the protection, human rights and humanitarian needs of those who are displaced. Improving preparedness for climate and weather-related disasters will prevent and minimize the negative impacts of displacement and ensure that "no one is left behind".

94 Data sourced from the Internal Displacement Monitoring Centre's Global Internal Displacement Database (GIDD).

95 Ibid.

96 Data sourced from the Internal Displacement Monitoring Centre's Global Internal Displacement Database (GIDD).

97 Ibid. It is important to note that IDMC figures on disaster displacements also cover pre-emptive evacuations. Thus, the increasing trend in displacement numbers may also partially mirror an enhancement in evacuations due to improvements in terms of early warnings, disaster preparedness and response. These improvements have in the meantime led to a reduction in loss of life in single-hazard scenarios over the past decade.

98 IPCC. *Sixth Assessment report*. Available here: https://www.ipcc.ch/report/sixth-assessment-report-working-group-ii/.

99 IDMC. *Multidimensional impacts of internal displacement, The ripple effect: economic impacts of internal displacement.* October 2018.

100 UNHCR. *Gender, Displacement, and Climate Change.* July 2020. https://www.unhcr.org/protection/environment/5f21565b4/gender-displacement-and-climate-change.html.

Impacts on Human Systems

CLIMATE AND HEALTH

Urban populations are growing and are particularly vulnerable to the increasing health risks from extreme heat and air pollution, which threaten the achievement of SDGs 3 and 11.

Fifty-five per cent of the world's population live in urban settings, and this proportion is expected to increase to 68% by 2050. Urban areas exacerbate existing vulnerabilities and widen inequalities, including pre-existing health conditions (e.g. cardiovascular conditions); socioeconomic dimensions (e.g. precarious housing); demographic factors (e.g. age and gender); geographic aspects (e.g. water-stressed zones); and socio-political factors (e.g. political instability). Most of the 4.4 billion people living in cities are particularly threatened by extreme heat exposure, air pollution that exceeds WHO guidelines, as well as other urban health risks.

In combination, these impacts undermine progress toward the following SDG targets: 3.9.1, which calls for a substantial reduction in deaths and illnesses from air pollution; 11.6.2, which seeks to mitigate the environmental impact of cities by improving air quality; and 11.5.1, which aims at reducing the number of deaths, missing persons, and persons directly affected by disasters. The IPCC states that climate change is projected to significantly increase exposure to heatwaves (*very high confidence*) and heat-related morbidity and mortality (high confidence).Exposure to extreme heat results in a range of health conditions, including heat stress and heat stroke, heart disease, and acute kidney injury. Urban heat islands further aggravate health risks during periods of extreme heat.

(b) Global distribution of population exposed to potentially deadly conditions from extreme temperatures and relative humidity.

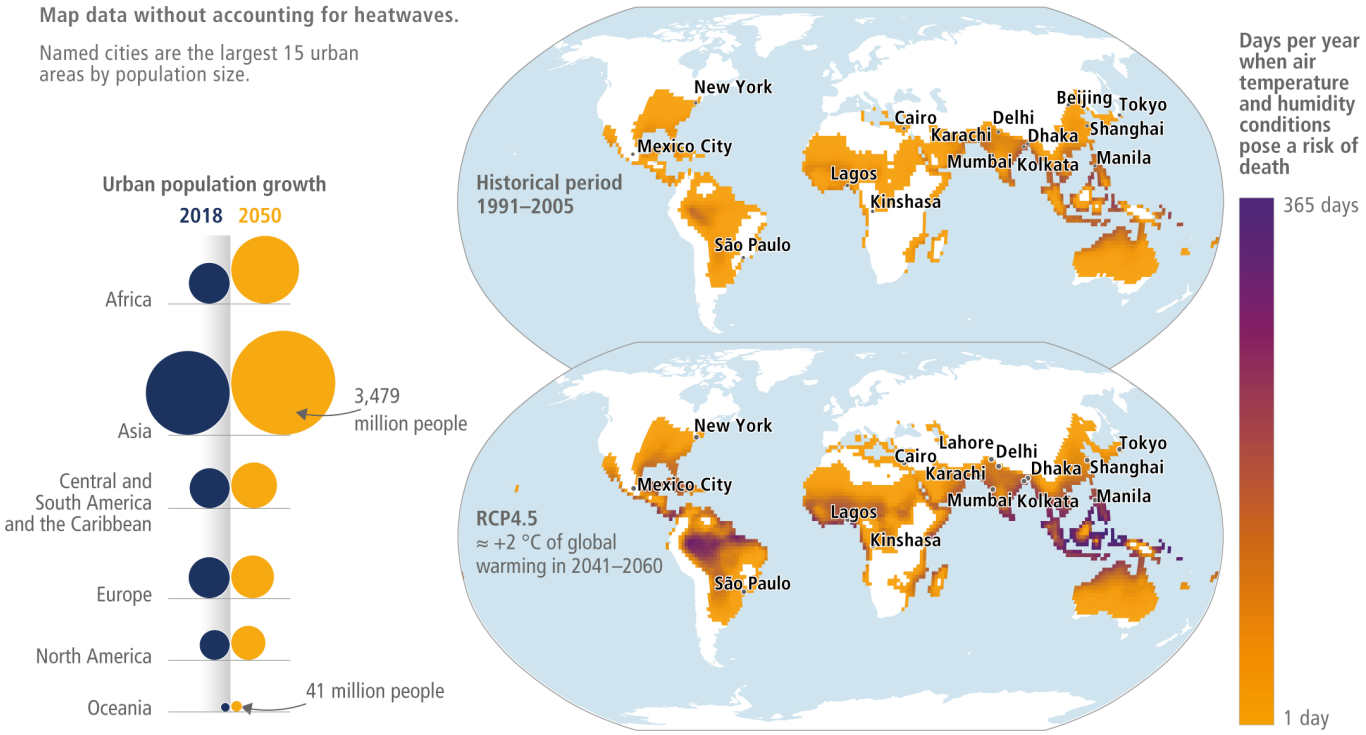

Figure 34. Global distribution of population exposed to potentially deadly conditions from extreme temperatures and relative humidity.
Note: the data does not consider heatwaves, which are also projected to increase and can cause thousands of deaths in higher latitudes.
Source: IPCC Sixth Assessment Report, WG2 2021.

Impacts on Human Systems

Besides exposure to extreme heat, over 99% of the global population breathes air that does not concur with WHO air quality standards.Air pollution is responsible for several million premature deaths every year. It has been associated with three of the leading causes of death worldwide including stroke, ischemic heart disease, and primary cancer of the trachea, bronchus, and lung.

Humans are becoming more susceptible to infectious disease as the suitability of dengue and malaria transmission is increasing with changes to the global climate.

Humans are increasingly susceptible to infectious disease transmission due to underlying factors such as global connectivity, climate change and landscape change. Vectorial capacity has increased for dengue fever, malaria and other vector-borne diseases, and higher global average temperatures are expanding the geographic areas that are conducive to transmission.

For instance, the climatic suitability for the transmission of dengue increased by around 12.0% from the 1951-1960 to 2012–2021 periods, causing febrile illnesses and, in severe cases, organ failure and death. Children under the age of five were particularly at risk. The length of the transmission season for malaria, leading from absent or very mild symptoms to severe disease and even death, increased by 31.3% and 13.8% in the highlands of the Americas and Africa, respectively, between the 1951–1960 and 2012–2021 decades.This increased transmission of infectious disease from climate change therefore threatens progress toward SDG 3.3, whose aim is to put an end to epidemics of communicable diseases.

How diseases move from the wild into human populations

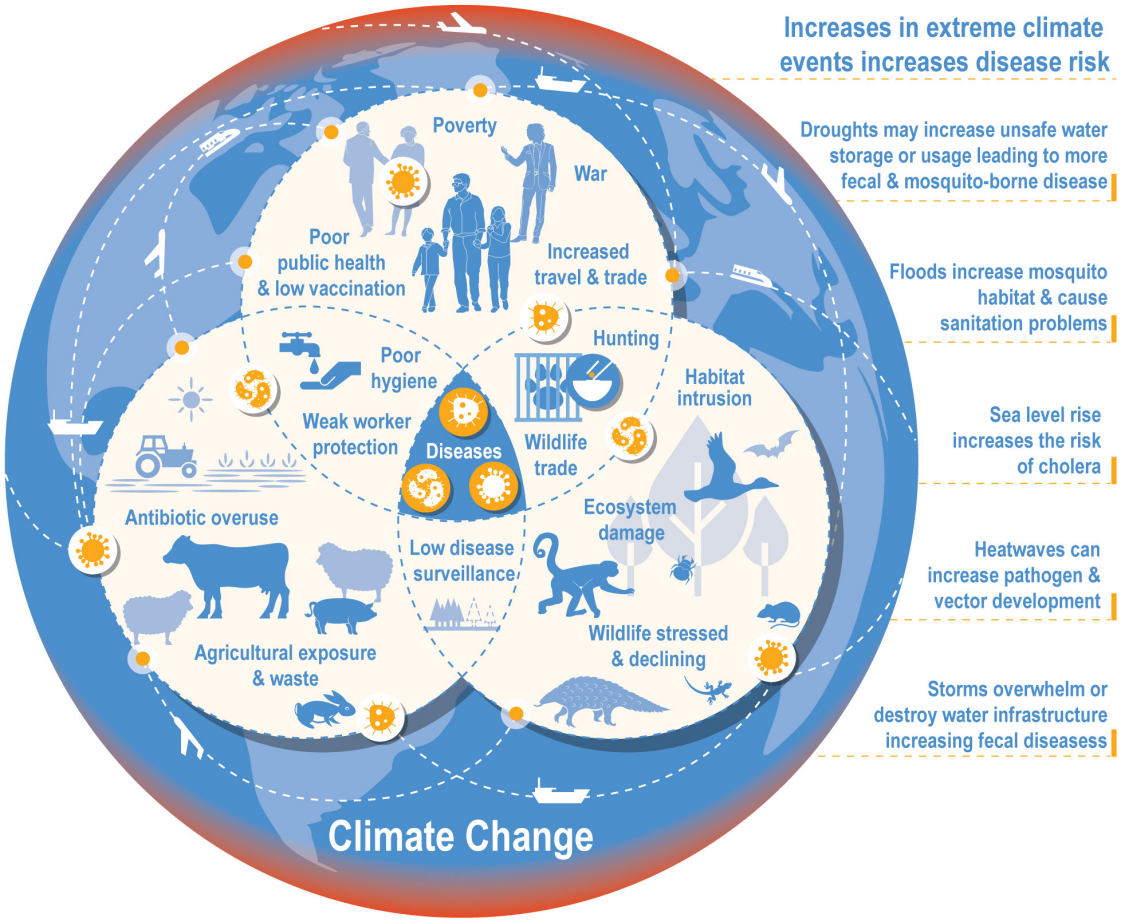

Figure 35. How disease moves from the wild into human populations. *Source:* IPCC AR6 Frequently Asked Questions.

Moving Forward: Synergistic Climate and SDG Policy

This report has underscored the fact that global temperature in 2011-2020 was already 1.1°C above pre-industrial levels and catastrophic, intensifying, and widespread extreme events have become far more frequent, affecting millions. This trend has consequently driven the prevalence of food insecurity; contributed to mass migration; and impaired health at a cost of billions of dollars in loss and damage. Meanwhile, the recent Sustainable Development Goals Report 2023: Special Edition paints a sobering picture of progress towards achieving the SDGs by 2030, stating: "Halfway to the deadline for the 2030 Agenda, we are leaving more than half the world behind. Progress on more than 50% of SDG targets is weak and insufficient; on 30% it has stalled or gone into reverse. These include key targets on poverty, hunger, and climate. Unless we act now, the 2030 Agenda could become an epitaph for a world that might have been".

The recent *Synergy Solutions for a World in Crisis* report, developed by the Expert Group on Climate and SDG Synergies (co-convened by UNDESA and UNFCCC Secretariat), reaffirms that addressing climate change and achieving the SDGs are inextricably intertwined, and that pursuing the 2030 Agenda in concert with the Paris Agreement could significantly and efficiently advance both agendas, maximize co-benefits and outweigh limit trade-offs. The report provides evidence of strong synergies between climate action and the SDGs, whereby advancements in one can lead to improvements in the other.[101] Evaluating the climate and sustainable development co-benefits is key to increasing the cost-effectiveness of interventions and to ensuring a just and equitable transition.

In order to accelerate synergistic action, the Synergy Solutions for a World in Crisis report provides a vast array of examples which showcase mitigation and adaptation climate policies that offer development co-benefits: improved health outcomes; reduced air pollution and agricultural emissions; and improved food and water security by reduced exposure to climate risks. For example, one study demonstrates how the energy system transition, pledged under the Paris Agreement, can significantly reduce global air pollution and, in so doing, prevent more than 100,000 premature deaths across Accra, Cairo, Johannesburg, and Lagos between 2023 and 2040, depending on the stringency of air pollution control measures implemented, or by as much as 350,000 annually in 2030 under a more ambitious 2°C compliant pathway.[102]

There has been much progress in moving away from siloed approaches and towards integrated planning, implementation, and reporting, but this needs to be vastly accelerated. Despite the abundance of data, tools, and methodologies addressing potential climate and SDGs synergies, there is dire need for a holistic approach that is accessible to policymakers. Most of the existing information is 'hidden' in academic literature, research institutions, government departments, or NGOs. That which is available lacks direct relevance to policy makers or cannot be used due to its format. The Synergy Solutions for a World in Crisis report highlights the importance of developing a 'framework for action' that is of practical value and enables policymakers at all levels to systemically identify, review, and evaluate complex synergistic action, and, importantly, to assess their transformative potential. Further details on a practical and step by step 'framework for action' will be developed in the next edition of the report, which is expected to be launched in 2024.

101 https://www.ipcc.ch/report/ar6/syr/longer-report.

102 Clean Air Fund. *From pollution to solution in Africa's cities,* (2022a).

Moving Forward: Synergistic Climate and SDG Policy

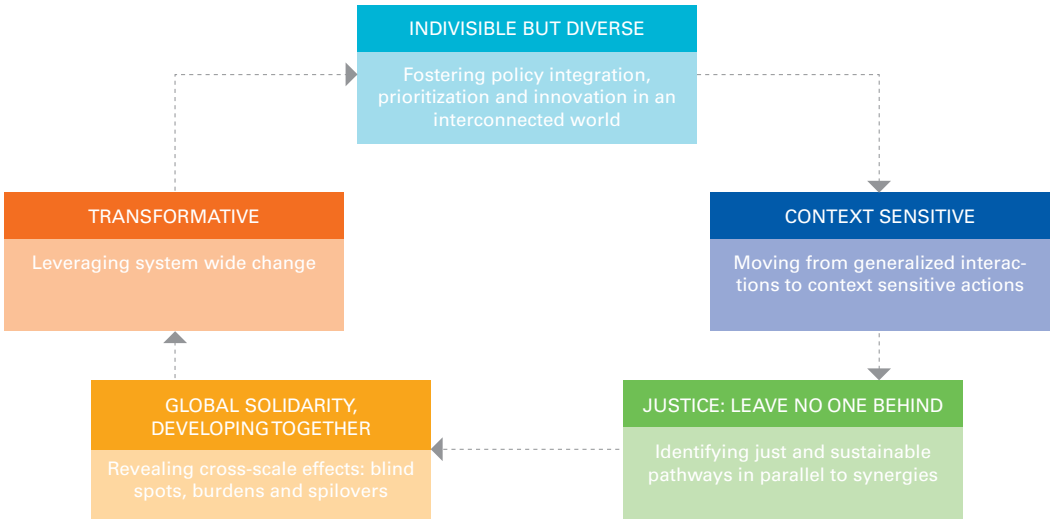

Figure 36. The five principles of the 'Framework for action' to foster systemic change *Source:* UNDESA Synergy Solutions for a World in Crisis (2023).

Central to the successful development and implementation of synergistic action on climate and development is an understanding that both agendas are context specific. Far too often, climate and development policies are enacted in a top-down, one size fits all approach — by their very nature both agendas are global in outlook. However, implementation takes place at more local levels. There are significant differences between and within the countries of the global North and global South. For example, the interconnections between SDGs and climate action are more pronounced for low-income and lower-middle-income countries as SDG progress and financing gaps are far more pressing for these countries than mitigating the impacts of climate change. In contrast, having attained considerable progress towards the SDGs, the primary focus for high-income countries is meeting their pledged targets under the Paris Agreement. The report builds on the key findings along the various sections above, and on the international community's call for action on climate. In fact, as the United Nations Secretary-General António Guterres said, "Climate action is the 21st century's greatest opportunity to drive forward all the Sustainable Development Goals." Acting aggressively on climate and development in an integrated and synergistic way creates an important opportunity to achieve the course correction he has called for. We must solve the climate emergency and sustainable development challenges together, or we will not solve them at all.

A list of recommendations for mainstreaming action on climate and development goals are listed below:

1. **Enhancing collective resilience** against current and future global crises through collaboration and cooperation with international organizations and their partners
2. **Strengthening science-policy-society interaction** to advance synergistic action
3. **Promoting institutional capacity-building** and cross-sectoral and international collaboration at national, institutional, and individual levels, especially for the global South
4. **Ensuring policy coherence and coordination** among policymakers across sectors and departments for enhancing climate and development synergies at the national, sub-national, and multi-national levels
5. **Developing a 'framework for action'** that can help decision-makers in public, private, and civil society sectors identify synergistic action for systems change and ensure a just transition
6. **Addressing the large investment gaps** in the climate and development agendas to enhance the necessary synergies and lead to the effective allocation of national budgets
7. **Prioritizing the role of synergies in the work of the United Nations** and international financial institutions, including an improved system for sharing information to help countries in their reporting responsibilities, enhanced cross-sectoral engagement in the intergovernmental and capacity-building efforts of the United Nations. Focused attention on climate and development synergies as well as climate resilient development pathways in the IPCC AR 7 are also called for
8. **Treating cities as opportunities for focusing on climate and development synergies** as sites of major population growth and expansion of economic activities

Contributors

CONTRIBUTORS

INDIVIDUAL CONTRIBUTORS:

Blair Trewin, Victoria Alexeeva, Jorge Alvar-Beltran, Vicente Anzellini, Abdishakur Awil Hassan, Hamza Benlarabi, Jana Birner, Pep Canadell, Anny Cazenave, Trang Chau, Kim Currie, Yannice Faugere, Feng Xie, Marion Gehlen, Arianna Gialletti, Luke Gregor, Nicolas Gruber, Tracelyn Joseph, Timika Joseph-Burke, John Kennedy, Yang Kong, Lancelot Leclercq, Fadumo Mumin, Michael Nairn, Rodica Nitu, Lindis Norlund, Ines Otosaka, Frank Paul, Sylvain Ponserre, Carlos Arturo Ramirez Hernandez, Claire Ransom, Yousuke Sawa, Andrew Shepherd, Robert Schlegel, Karina von Schuckmann, Bahareh Seyedi, Joy Shumake-Guillemot, Yaryna Shura, Minoru Takada, Oksana Tarasova, Matt Tully, Karen Daniela Vargas Cortes, Alex Vermeulen, Rosa Von Borries, Michael Zemp, Markus Ziese.

WMO Coordination: Claire Ransom, Omar Baddour, Atsushi Goto, Peer Hechler, Climate Monitoring and Policy, Services Division.

INSTITUTIONS:

Antigua and Barbuda Statistics Division, Commonwealth Scientific and Industrial Research Organisation (CSIRO), Departamento Administrativo Nacional de Estadística Colombia, ETH Zurich, Institut de la Mer de Villefranche (IMEV), Institut Pierre-Simon Laplace, Laboratoire d'Etudes en Géophysique et Océanographie Spatiales (LEGOS), Mercator Ocean International, National Institute of Water and Atmospheric Research (NIWA), Northumbria University, Somalia National Bureau of Statistics, Statistics Belgium, Statistics Netherlands, UK Office for National Statistics, Université Toulouse III-Paul Sabatier, University of Leeds, World Glacier Monitoring Service (WGMS).

UN AGENCIES:

Food and Agriculture Organization of the United Nations (FAO), International Organization for Migration (IOM), Internal Displacement Monitoring Centre (IDMC), The United Nations High Commissioner for Refugees (UNHCR), United Nations Department of Economic and Social Affairs (UNDESA) Climate and SDG Synergy Secretariat, World Health Organization (WHO) and World Meteorological Organization (WMO) Joint Office.

WMO MEMBERS:

Algeria, Argentina, Armenia, Azerbaijan, Bahrain, Bangladesh, Barbados, Belgium, Belize, Benin, Bosnia and Herzegovina, Botswana, Brazil, British Caribbean Territories, Bulgaria, Burkina Faso, Cameroon, Canada, Chile, China, Colombia, Costa Rica, Côte d'Ivoire, Croatia, Cuba, Cyprus, Czech Republic, Djibouti, Egypt, El Salvador, Estonia, Finland, France, Gambia, Georgia, Germany, Guatemala, Guinea, Guyana, Hong Kong, China, Hungary, Iceland, India, Indonesia, Ireland, Israel, Italy, Jamaica, Japan, Jordan, Kazakhstan, Kenya, Kuwait, Latvia, Lesotho, Libya (State of), Luxembourg, Macao, China, Madagascar, Maldives, Mali, Malta, Mauritius, Mexico, Moldova, Republic of, Mongolia, Montenegro, Morocco, Myanmar, Netherlands, New Zealand, Nigeria, North Macedonia, Paraguay, Peru, Philippines, Poland, Qatar, Republic of Korea, Russian Federation, Saudi Arabia, Serbia, Seychelles, Slovakia, Slovenia, South Africa, Spain, Sri Lanka, Sweden, Switzerland, Syrian Arab Republic, Thailand, Trinidad and Tobago, Tunisia, Turkey, Uganda, Ukraine, United Republic of Tanzania, United States of America, Vanuatu, Venezuela, Bolivarian Republic of, Viet Nam, Zambia.

Special thanks to others involved in the review process: Jose Alvaro Mendes Pimpao Alves Silva, Jessica Blunden, Awatif Ebrahim, Chris Hewitt, Renata Libonati, Atsushi Minami, Henry Reges, Johan Stander, Serhat Sensoy, José Luis Stella.

References and Data Sources

Data sources covered by specific citations within the text are generally not listed separately here.

GREENHOUSE GASES

Material in this section draws on the annual WMO Greenhouse Gas Bulletins (https://public.wmo.int/en/greenhouse-gas-bulletin). Data are available from the World Data Centre for Greenhouse Gases (https://gaw.kishou.go.jp).

GLOBAL CARBON BUDGET

Friedlingstein et al. Global Carbon Budget 2022. *Earth System Science Data* **2022**, 14, 4811–4900.

Saunois et al. Global methane budget 2000-2017. *Earth System Science Data* **2020.**, 12, 1561-1623.

Tian et al. Global nitrous oxide budget 1980-2020. *Earth System Science Data* **2023.** In review. https://doi.org/10.5194/essd-2023-401.

OZONE

Ozone data are taken from the NASA Ozone watch website (https://ozonewatch.gsfc.nasa.gov).

TEMPERATURE

The method for calculating anomalies of global mean temperature relative to an 1850-1900 baseline has been updated since the report on the *State of the Global Climate in 2020*. The method was updated for the *State of the Global Climate in 2021* to take advantage of the assessment of long-term change and its uncertainty made by the IPCC Sixth Assessment Report (AR6) Working Group I (WG1), as well as making use of a wider range of shorter data sets that are routinely updated to provide an authoritative assessment of recent temperature changes.

In the 2020 and earlier reports, changes relative to the 1850-1900 baseline were based on the HadCRUT4 data set which was the only data set that extended back to 1850. Other data sets were offset to match the average of HadCRUT4 over the period 1880-1900 (NASA GISTEMP and NOAA GlobalTemp) or 1981-2010 (ERA5, JRA-55).

In 2021, IPCC AR6 WG1 assessed change from 1850-1900 to other periods based on an average of four data sets – HadCRUT5, Berkeley Earth, NOAA Interim and Kadow et al. – which all date back to 1850. They assessed uncertainty by considering the range from the four estimates, taken from the lower bound of the uncertainty range of the coolest data set, to the upper bound of the uncertainty range of the warmest. By making use of four data sets that extend back to 1850, WG1 was able to make a more comprehensive estimate of uncertainty.

As two of the four IPCC data sets are not regularly updated, we use the estimate made by the IPCC for the temperature change between 1850-1900 and 1981-2010, and combine this with estimated changes between 1981-2010 and the current year from six data sets in order to get anomalies for 2021 relative to 1850-1900.

There is much, though not complete, agreement between the six data sets on changes from the 1981-2010 period to the present as this is a period with good observational coverage. The additional modest uncertainty from the spread of the six data sets is combined with that of the estimate made by IPCC on the uncertainty in the change from 1850-1900 to 1981-2010.

References and Data Sources

More precisely, six data sets (cited below) are used in the calculation of global temperature. Global mean temperature anomalies are calculated relative to an 1850 to 1900 baseline using the following steps:

1. Starting with a time series of global annual mean temperatures for each data set as provided by the data providers, these anomalies are presented on different baselines

2. For each data set, anomalies are calculated relative to the 1981-2010 average by subtracting the average for the period 1981-2010

3. The temperature reading of 0.69 °C was added to each series, based on the estimated difference between 1850-1900 and 1981-2010 calculated using the method from IPCC AR6 WG1. The number is provided in the caption for Figure 1.12

4. The mean and standard deviation of the estimates were calculated

5. The uncertainty in the IPCC estimate was combined with the standard deviation assuming the two are independent and assuming the IPCC uncertainty range of 0.54 to 0.79 °C is representative of a 90% confidence range (1.645 standard deviations).

TEMPERATURE MAPS

The method for calculating the map of annual temperature anomalies was also updated. In the State of the Global Climate 2020 report, a map showing anomalies relative to 1981-2010 from a single data set (ERA5) was used. While the map was based on a single data set, the accompanying assessment was based on all available data sets.

For the map of temperature anomalies used here, a median value of six data sets was used – HadCRUT5, ERA5, JRA-55, Berkeley Earth, NOAAGlobalTemp, and GISTEMP – regridded to the spatial grid of the lowest resolution data sets: NOAAGlobalTemp and HadCRUT5 data sets, which are presented on a 5° latitude by 5° longitude grid. A median is used in preference to the mean to minimise the effect of potential outliers. The half-range of the data sets provides an indication of the uncertainty. The spread between the data sets is largest at high latitudes and in central Africa, both regions having sparse data coverage.

The following six data sets were used:

1. HadCRUT.5.0.1.0 —Morice, C.P. et al. An Updated Assessment of Near-Surface Temperature Change from 1850: The HadCRUT5 Data set. *Journal of Geophysical Research: Atmospheres* **2021**, 126 (3): e2019JD032361. https://doi.org/10.1029/2019JD032361. HadCRUT.5.0.1.0 data were obtained from http://www.metoffice.gov.uk/hadobs/hadcrut5 on 24 October 2021 and are © British Crown Copyright, Met Office 2021, provided under an Open Government License. http://www.nationalarchives.gov.uk/doc/open-government-licence/version/3/.

2. NOAAGlobalTemp v5 — Zhang, H.-M., et al. *NOAA Global Surface Temperature Data set (NOAAGlobalTemp)*, Version 5.0. NOAA National Centers for Environmental Information. doi:10.7289/V5FN144H, https://www.ncei.noaa.gov/access/metadata/landing-page/bin/ iso?id=gov.noaa.ncdc:C00934. Huang, B. et al. Uncertainty Estimates for Sea Surface Temperature and Land Surface Air Temperature in NOAAGlobalTemp Version 5. *Journal of Climate* **2020**, 33 (4): 1351–1379. https://journals.ametsoc.org/view/journals/clim/33/4/jcli-d-19-0395.1.xml

3. GISTEMP v4 — *GISTEMP Team. GISS Surface Temperature Analysis (GISTEMP)*, version 4. NASA Goddard Institute for Space Studies, https://data.giss.nasa.gov/gistemp/. Lenssen, N. J. L. et al. Improvements in the GISTEMP Uncertainty Model. *Journal of Geophysical Research: Atmospheres* **2019**, 124 (12): 6307–6326, doi: https://doi.org/10.1029/2018JD029522.

References and Data Sources

4. Berkeley Earth – Rohde, R. A. Hausfather, Z. The Berkeley Earth Land/Ocean Temperature Record, *Earth Syst. Sci. Data* **2020**, 12, 3469–3479, https://doi.org/10.5194/essd-12-3469-2020.

5. ERA5 — Hersbach, H. et al. The ERA5 Global Reanalysis. *Quarterly Journal of the Royal Meteorological Society* **2020**, 146 (730): 1999–2049, doi: https://doi.org/10.1002/qj.3803.

6. JRA-55 — Kobayashi, S. et al. The JRA-55 Reanalysis: General Specifications and Basic Characteristics. Journal of the Meteorological Society of Japan **2015**, Ser. II 93 (1): 5–48, doi:10.2151/jmsj.2015-001, https://www.jstage.jst.go.jp/article/jmsj/93/1/93_2015-001/_article.

Two additional data sets are also shown in Figure 7. These are the two data sets which were used in the IPCC Sixth Assessment report but were not at the time updated operationally. Reference is made to them in Figure 7 as NOAA Interim IPCC and Kadow IPCC. (Note that the data set here referred to as 'NOAA Interim IPCC' has superseded NOAAGlobalTemp v5 as the main NOAA operational data set as of January 2023).

NOAA Interim IPCC - Vose, R.S. et al. Implementing Full Spatial Coverage in NOAA's Global Temperature Analysis. *Geophysical Research Letters* **2021**, 48 (4), e2020GL090873, https://doi: 10.1029/2020gl090873.

Kadow IPCC - Kadow, C.; Hall, D. M.; Ulbrich, U. Artificial intelligence reconstructs missing climate information. *Nature Geoscience* **2020**, 13 (6), 408–413. https://doi: 10.1038/s41561-020-0582-5.

MARINE HEATWAVES

The underlying sea surface temperature data used are from version 2.1 of the NOAA Optimum Interpolation Sea Surface Temperature (OISST) data set (https://www.ncei.noaa.gov/products/optimum-interpolation-sst).

Marine heatwaves are defined from the underlying sea surface temperature data using the method of Hobday, A.J. et al.

Hobday, A. J. et al. A hierarchical approach to defining marine heatwaves, *Progress in Oceanography* **2016**, 141, pp. 227-238, https://doi: 10.1016/j.pocean.2015.12.014.

SEA LEVEL

Sea level data are taken from the satellite monitoring product of the Copernicus Climate Change Service: Copernicus Climate Change Service, Climate Data Store, (2018): Sea level gridded data from satellite observations for the global ocean from 1993 to present. Copernicus Climate Change Service (C3S) Climate Data Store (CDS): https://doi:10.24381/cds.4c328c78.

GLACIERS

Mass balance data for reference glaciers are from the World Glacier Monitoring Service (www.wgms.ch). (WGMS, 2021).

WGMS 2021. *Global Glacier Change Bulletin No. 4* (2018-2019). Zemp, M.; Nussbaumer, S. U.; Gärtner-Roer, I. et al., Eds.; ISC(WDS)/IUGG(IACS)/UNEP/UNESCO/WMO, World Glacier Monitoring Service, Zurich, Switzerland, 278 pp. Publication based on database version: doi:10.5904/wgms-fog-2021-05.

References and Data Sources

ICE SHEETS

The Greenland and Antarctic Ice Sheets time-series of mass change is compiled from 50 satellite-based estimates of ice sheet mass balance as part of the Ice Sheet Mass Balance Inter-comparison Exercise (IMBIE) (http://imbie.org/).

The data are freely available at https://data.bas.ac.uk/metadata.php?id=GB/NERC/BAS/PDC/01477.

Shepherd, A.; Ivins, E.; Rignot, E. et al. Mass balance of the Greenland Ice Sheet from 1992 to 2018. *Nature* **2020**, 579 (7798): 233-239.

SEA ICE

Sea ice extent data are from the National Snow and Ice Data Center (NSIDC) (www.nsidc.org).

PERMAFROST

Active layer thickness data reported are from the data set of the Circumpolar Active Layer Monitoring (CALM) Network (https://www2.gwu.edu/~calm/).

MODES OF VARIABILITY

Oceanic Nino Index (ONI), Arctic Oscillation (AO), North Atlantic Oscillation (NAO) and Southern Annular Mode (SAM)/Antarctic Oscillation (AAO) data reported in this section are from the NOAA Climate Prediction Center (https://www.cpc.ncep.noaa.gov/).

PRECIPITATION

Precipitation data are from the monthly data set of the Global Precipitation Climatology Centre (GPCC) (https://www.dwd.de/EN/ourservices/gpcc/gpcc.html).

HIGH-IMPACT AND EXTREME EVENTS

Unless otherwise indicated, statements on the extent to which the likelihood of various types of events have been influenced by anthropogenic climate change draw on papers published in the annual 'Explaining Extreme Events from a Climate Perspective' series in the *Bulletin of the American Meteorological Society* (https://www.ametsoc.org/index.cfm/ams/publications/bulletin-of-the-american-meteorological-society-bams/explaining-extreme-events-from-a-climate-perspective/).

Some impact data are taken from the EM-DAT database, maintained by the Centre for Research on the Epidemiology of Disasters (CRED), University of Louvain, Belgium (www.emdat.be).

MOVING FORWARD: SYNERGISTIC CLIMATE & SDG POLICY

Expert Group on Climate and SDG Synergy. *Synergy Solutions for a World in Crisis: Tackling Climate and SDG Action Together. Report on strengthening the evidence base.* First edition 2023.

For more information, please contact:

World Meteorological Organization

7 bis, avenue de la Paix – P.O. Box 2300 – CH 1211 Geneva 2 – Switzerland

Strategic Communications Office
Cabinet Office of the Secretary-General

Tel: +41 (0) 22 730 83 14 – Fax: +41 (0) 22 730 80 27

Email: communications@wmo.int

public.wmo.int

JN 231335